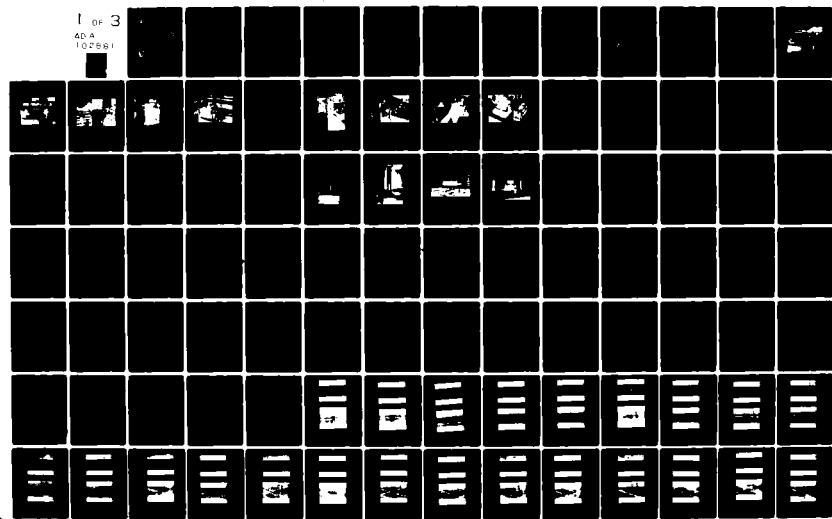


AD-A102 881 ARMY MISSILE COMMAND REDSTONE ARSENAL AL GROUND EQU--ETC F/G 11/4  
QUANTITATIVE ANALYSIS OF IMPACT DAMAGED COMPOSITE TENSION-TORSI--ETC(U)  
SEP 80 J A SCHAEFFEL  
UNCLASSIFIED DRSMI/RL-80-12-TR NL

1 of 3

40-A

102661



DMC FILE COPY

ADA102881

LEVEL II

12  
B S

Technical Report RL-80-12 ✓

QUANTITATIVE ANALYSIS OF IMPACT DAMAGED COMPOSITE  
TENSION-TORSION SPECIMENS USING LASER SPECKLE  
INTERFEROMETRY

John A. Schaeffel  
Ground Equipment and Missile  
Structures Directorate  
US Army Missile Laboratory



September 1980



**U.S. ARMY MISSILE COMMAND**

Redstone Arsenal, Alabama 35809

Approved for public release; distribution unlimited.

#### **DISPOSITION INSTRUCTIONS**

**DESTROY THIS REPORT WHEN IT IS NO LONGER NEEDED. DO NOT  
RETURN IT TO THE ORIGINATOR.**

#### **DISCLAIMER**

**THE FINDINGS IN THIS REPORT ARE NOT TO BE CONSTRUED AS AN  
OFFICIAL DEPARTMENT OF THE ARMY POSITION UNLESS SO DESIG-  
NATED BY OTHER AUTHORIZED DOCUMENTS.**

#### **TRADE NAMES**

**USE OF TRADE NAMES OR MANUFACTURERS IN THIS REPORT DOES  
NOT CONSTITUTE AN OFFICIAL INDORSEMENT OR APPROVAL OF  
THE USE OF SUCH COMMERCIAL HARDWARE OR SOFTWARE.**

14

UNCLASSIFIED

SECURITY CLASSIFICATION OF THIS PAGE (When Data Entered)

DR

1473 REPORT DOCUMENTATION PAGE

READ INSTRUCTIONS  
BEFORE COMPLETING FORM

1. REPORT NUMBER DR-12-7A	2. GOVT ACCESSION NO. AD-A102881	3. RECIPIENT'S CATALOG NUMBER 91
4. TITLE (If classified) Quantitative Analysis of Impact Damaged Composite Tension-Torsion Specimens Using Laser Speckle Interferometry		5. TYPE OF REPORT & PERIOD COVERED Technical Report
6. AUTHOR(s) John A. Schaeffel, Jr.		7. CONTRACT OR GRANT NUMBER(s) DA1162303A214 (17) 1
8. PERFORMING ORGANIZATION NAME AND ADDRESS Commander, US Army Missile Command, ATTN: DRSMI-RL Redstone Arsenal, Alabama 35898		9. PROGRAM ELEMENT, PROJECT, TASK AREA & WORK UNIT NUMBERS AMCMS 6123032140911
10. CONTROLLING OFFICE NAME AND ADDRESS Commander, US Army Missile Command, ATTN: DRSMI-RPT Redstone Arsenal, Alabama 35898		11. REPORT DATE 11 September 1980
12. MONITORING AGENCY NAME & ADDRESS (if different from Controlling Office)		13. NUMBER OF PAGES
14. DISTRIBUTION STATEMENT (of this Report) Approved for public release; distribution unlimited.		15. SECURITY CLASS. (of this report) Unclassified
16. DISTRIBUTION STATEMENT (of the abstract entered in Block 20, if different from Report)		15a. DECLASSIFICATION/DOWNGRADING SCHEDULE
17. SUPPLEMENTARY NOTES		
18. KEY WORDS (Continue on reverse side if necessary and identify by block number) Composites Failure of Composites Impact Damaged Composites Flow Detection Laser Speckle Interferometry Nondestructive Testing Dynamic Impact Loading Young's Fringes		
19. ABSTRACT (Continue on reverse side if necessary and identify by block number) Test specimens in the form of standard tensile coupons were fabricated from XP250 composite laminate material manufactured by the 3M Company. A series of six different wrap angles, measured from and symmetric to the longitudinal specimen axis was used. At each wrap angle eight specimens were fabricated with flaws due to dynamic impact loading. Five unflawed specimens were also fabricated for comparison purposes. Each of the flawed specimens and one unflawed specimen at each wrap angle were individually placed in an apparatus for (continued)		

DD FORM 1 JAN 73 1473 EDITION OF 1 NOV 65 IS OBSOLETE

SECURITY CLASSIFICATION OF THIS PAGE (When Data Entered)

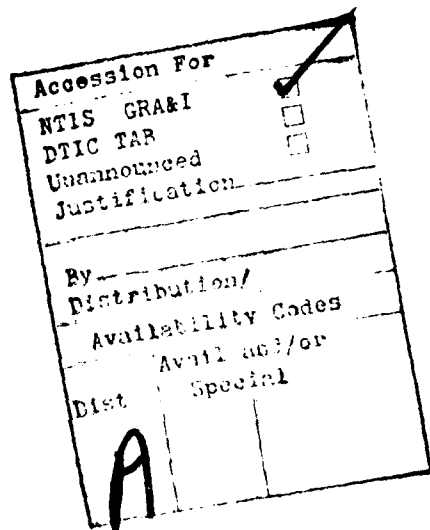
410263

9/14

SECURITY CLASSIFICATION OF THIS PAGE(When Data Entered)

20. ABSTRACT (Cont'd)

generating low load level tension and torsion. Laser speckle interferograms of the specimens were made and analyzed. The ratio of the strain in the flawed region of each specimen was compared to the unflawed specimens at each wrap angle using laser speckle interferometry. These results were correlated with the ultimate strength of each specimen obtained in a simple tension test using an Instron machine. Comparison of results was favorable.



SECURITY CLASSIFICATION OF THIS PAGE(When Data Entered)

#### ACKNOWLEDGEMENT

The author sincerely wishes to thank Mr. Terry L. Vandiver and Ms. Alison S. Dempsey for their assistance in this project.

## CONTENTS

Section	Page
I. INTRODUCTION.....	3
II. THEORETICAL AND EXPERIMENTAL CONSIDERATIONS.....	6
A. Experimental Apparatus.....	6
B. Composite Tensile Specimens.....	12
III. EXPERIMENTATION.....	26
A. Specimens.....	26
B. Dynamic Impact Apparatus.....	26
C. Specimen Preparation.....	31
D. Specimen Properties.....	33
E. Specimen Loading.....	33
F. Optical Specifications.....	34
G. Specimen Rotation Angles.....	34
IV. EXPERIMENTAL RESULTS.....	35
V. CONCLUSIONS.....	39
Appendix A.....	41
Appendix B.....	57
Appendix C.....	59
Appendix D.....	69
Appendix E.....	119
Appendix F.....	139
Appendix G.....	143

CONTENTS (Concluded)

Section	Page
Appendix H.....	147
Appendix I.....	191
Appendix J.....	205
Appendix K.....	211

## I. INTRODUCTION

The behavior of composite materials is a complex phenomena of immense scientific and engineering importance. Since many aircraft and missile structures are currently being fabricated from these materials, it is most advantageous to fully understand and appreciate their behavior under a wide variety of conditions. [1, 2] It is a relatively simple task to obtain material behavior data for the case of static loading. It is harder to apply this data to engineering design. When the loading case becomes one of dynamic loading, the problems associated with obtaining useful data are many orders of magnitude greater.

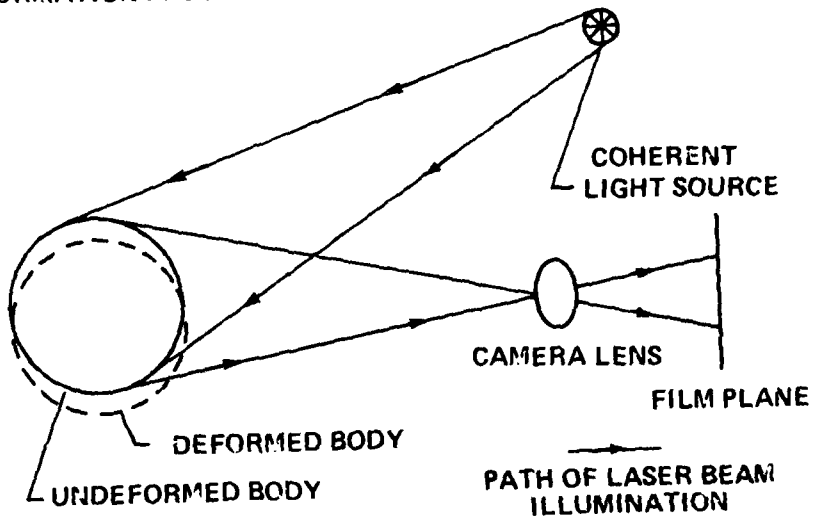
The study presented in this report was conducted to observe how composite tensile specimens deform when subjected to simple tension and torsion loading. [2] The interesting twist to this problem is the fact that the specimens suffered damage prior to loading. The damage was due to fiber breakage and resin crazing from dynamic impact loading.

The dynamic impact loads were introduced in tensile specimens using a drop weight which struck an impactor dart. The impact dart transferred the energy from the drop weight to the specimen in a prescribed manner. This particular type of load configuration might be found in any situation where a composite component is subjected to a blow from another object.

The amount of deformation of the specimen when loaded in tension and torsion was compared with the flaw geometry and ultimate strength data obtained from tensile testing to failure to determine the sensitivity of the structure to the particular flaw type. In the tests, the amount of impact energy, impact dart geometry, specimen wrap angle, and torsion load were all varied for a fixed uniaxial tensile load. The amount of deformation in going from a loaded to an unloaded tensile state was determined for these variables. Since the tensile specimens were damaged in most of the cases, a noncontact method for determining surface deformation had to be utilized. Laser speckle interferometry was chosen since it allowed for variable sensitivity and provided the necessary resolution.

Laser speckle interferograms are most commonly used to make deformation measurements of deformable bodies. Figure 1 illustrates the basic method for

(A) FORMATION PROCESS



(B) RECONSTRUCTION PROCESS

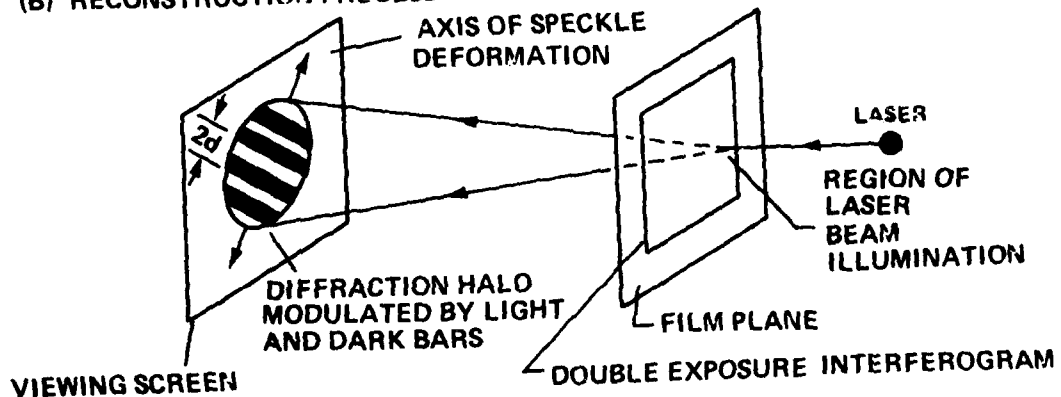


Figure 1. Laser speckle interferometry configuration.

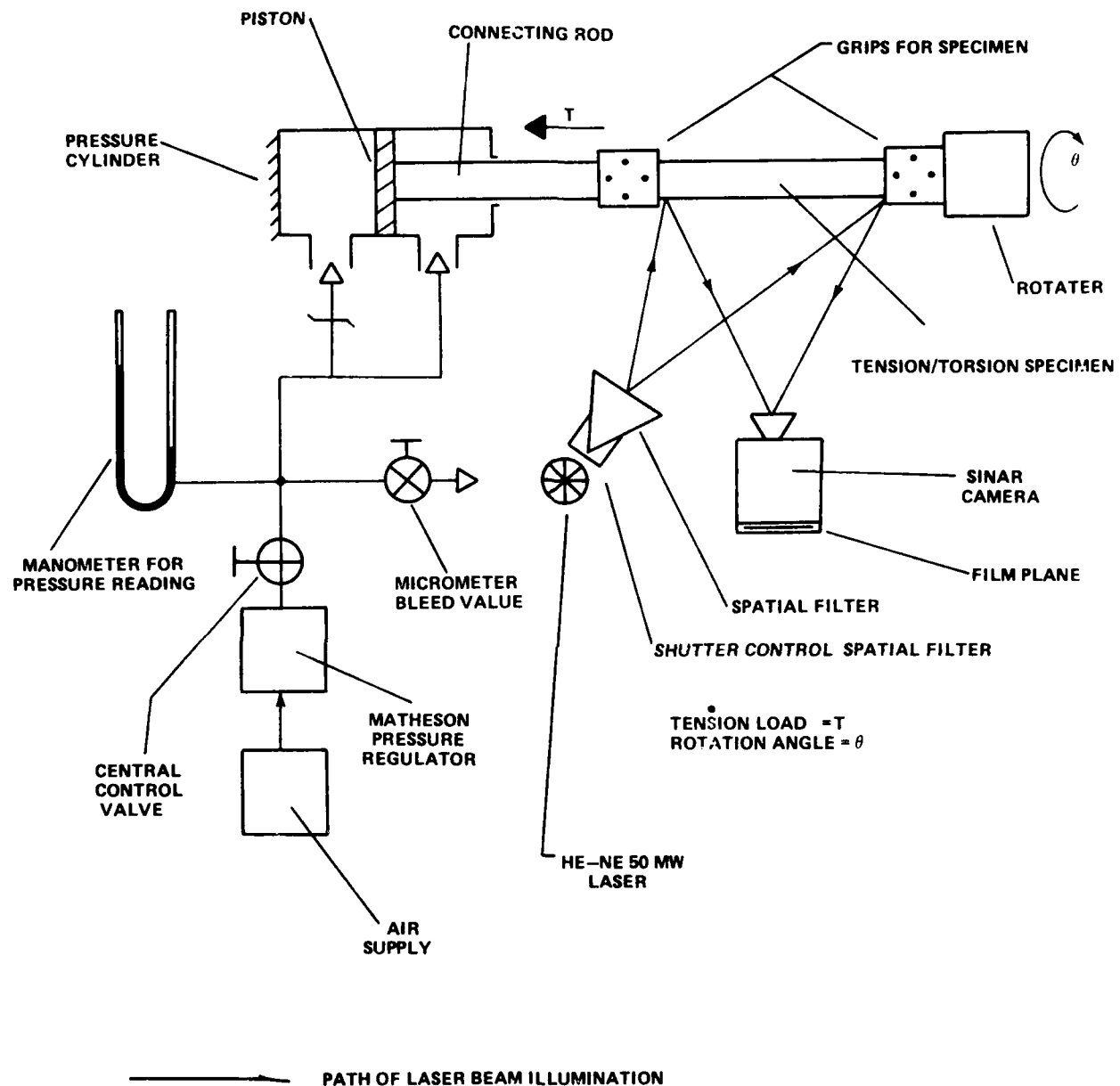


Figure 2. Experimental apparatus used to measure the deformation of tensile specimens loaded with torsion and subjected to dynamic impact damage.

making a laser speckle interferogram. [3] When a diffuse surface of a structure is illuminated with coherent radiation, a grainy speckle effect is imaged by the eye or film plane of a camera due to the interference of light from the structure. This speckle effect is enhanced when the structure has microscopic surface irregularities. If the optical configuration remains fixed, the speckle pattern of the test object may be recorded on the film plane of a camera. Further, if the structure is deformed, the speckle points shift with the deformation and a second exposure of the deformed speckle pattern can be made.

Using a technique of double exposure, speckle interferograms of a structure are normally made by photographing the speckle pattern in a deformed and undeformed configuration. A beam of laser light is then passed through a region of the double exposure where the local deformation is desired. As the beam passes through the film, the deformed and undeformed speckle recorded there diffract the laser light and cause an interference effect on a viewing screen. A diffraction halo modulated by light and dark bars of light is produced where the distance  $2d$  between bars is inversely proportional to the distance between the undeformed and deformed speckle on the film plane. A normal to the light and dark bar pattern indicates the axis of deformation of the speckle.

The work conducted and presented in this report is not intended to be conclusive data for all composites in general. Rather, it is presented to illustrate the methodology of testing composites under a unique load configuration and using an optical non-contact method of measuring surface deformation in going from a loaded to an unloaded state. The results should not be used to generalize composite material behavior when the material properties and geometry differ significantly from those of the host material.

## II. THEORETICAL AND EXPERIMENTAL CONSIDERATIONS

This section documents the experimental apparatus used in the experiments, the composite tensile specimens, their method of manufacture, and the optical method of analysis.

### A. Experimental Apparatus

Figure 2 illustrates the basic apparatus used in the experiment. A combined tension/torsion load machine shown in Figures 3 through 7 was

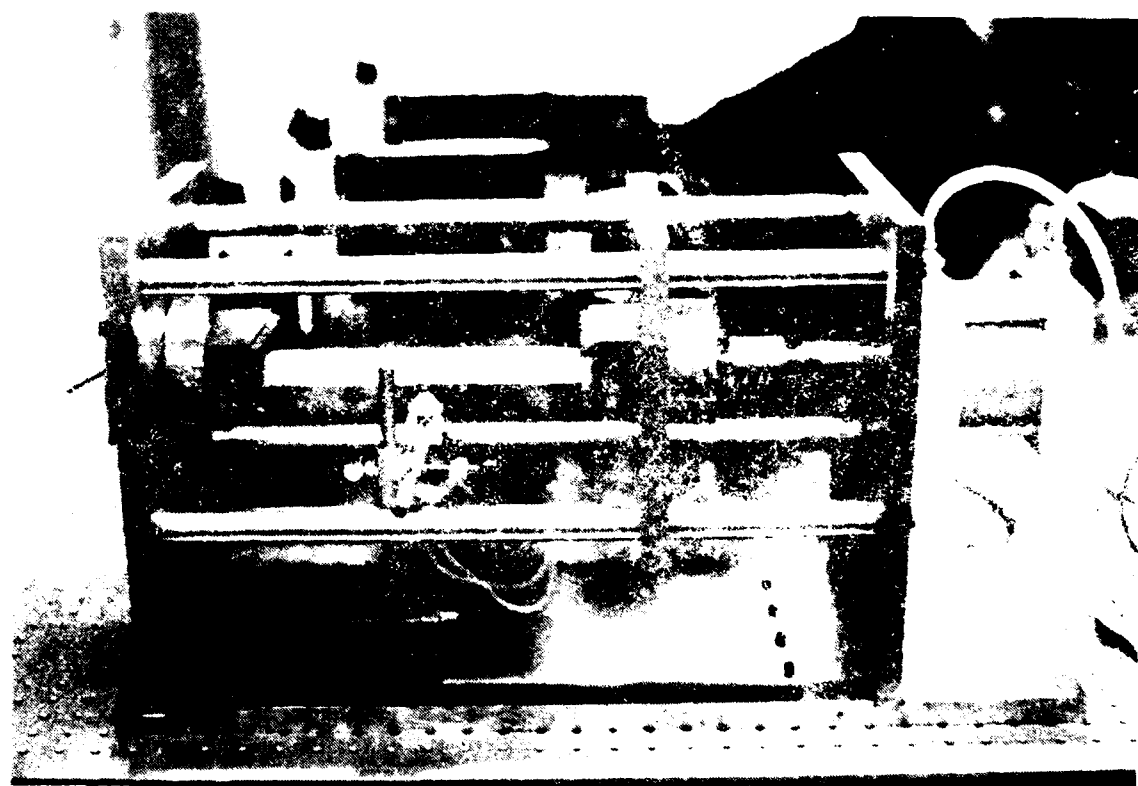


Figure 3. Combined tension and torsion loading machine.

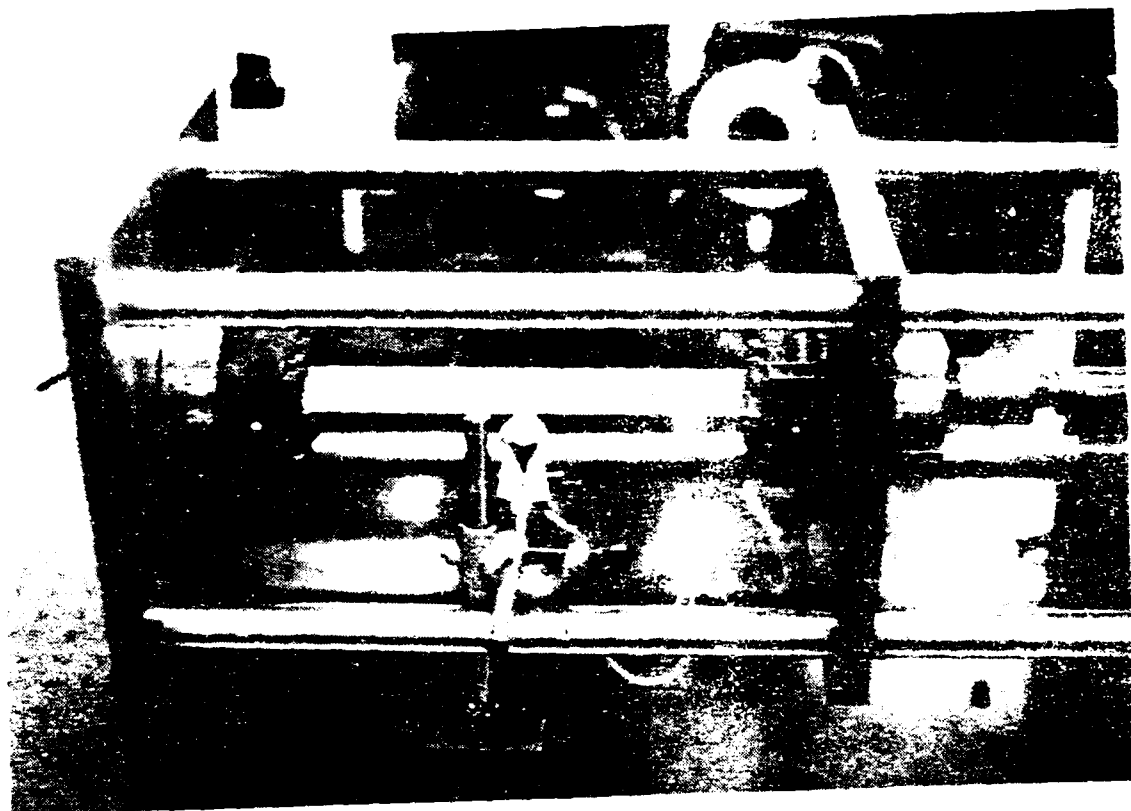


Figure 4. Primary load assembly to tension/torsion load machine.

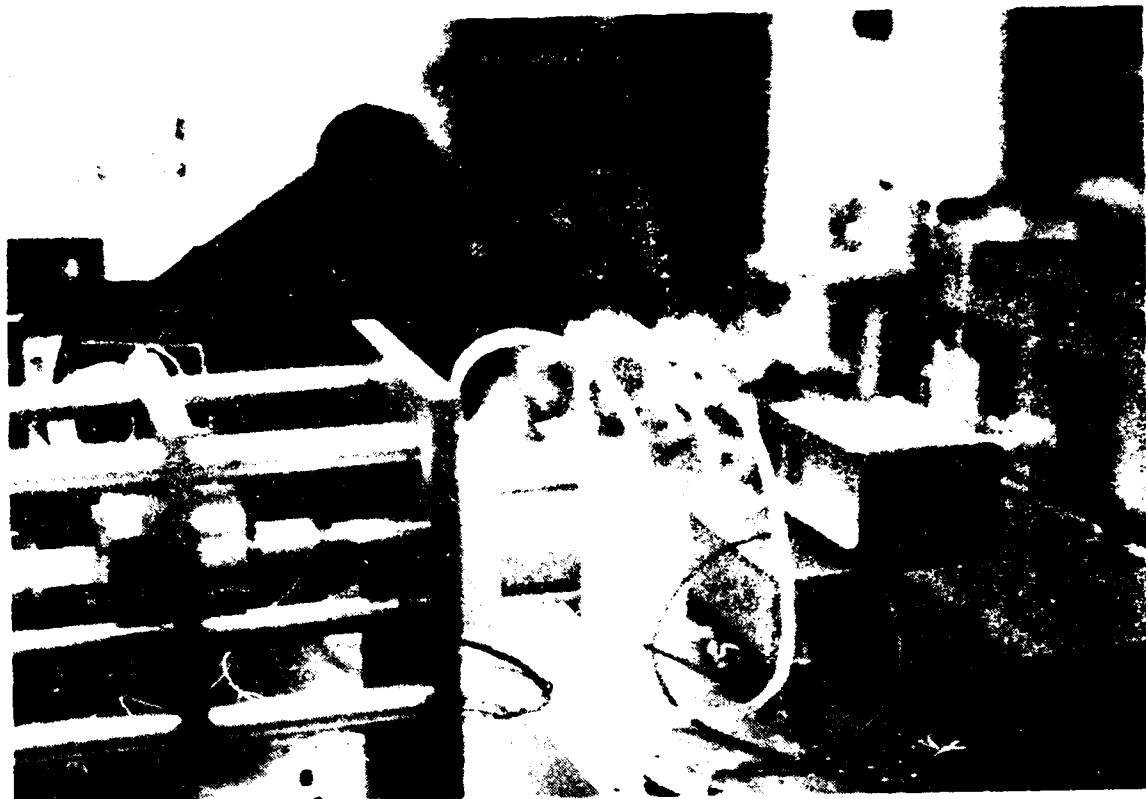


Figure 5. Pneumatic load cylinder for generating a tensile load  $T$  in composite specimens.

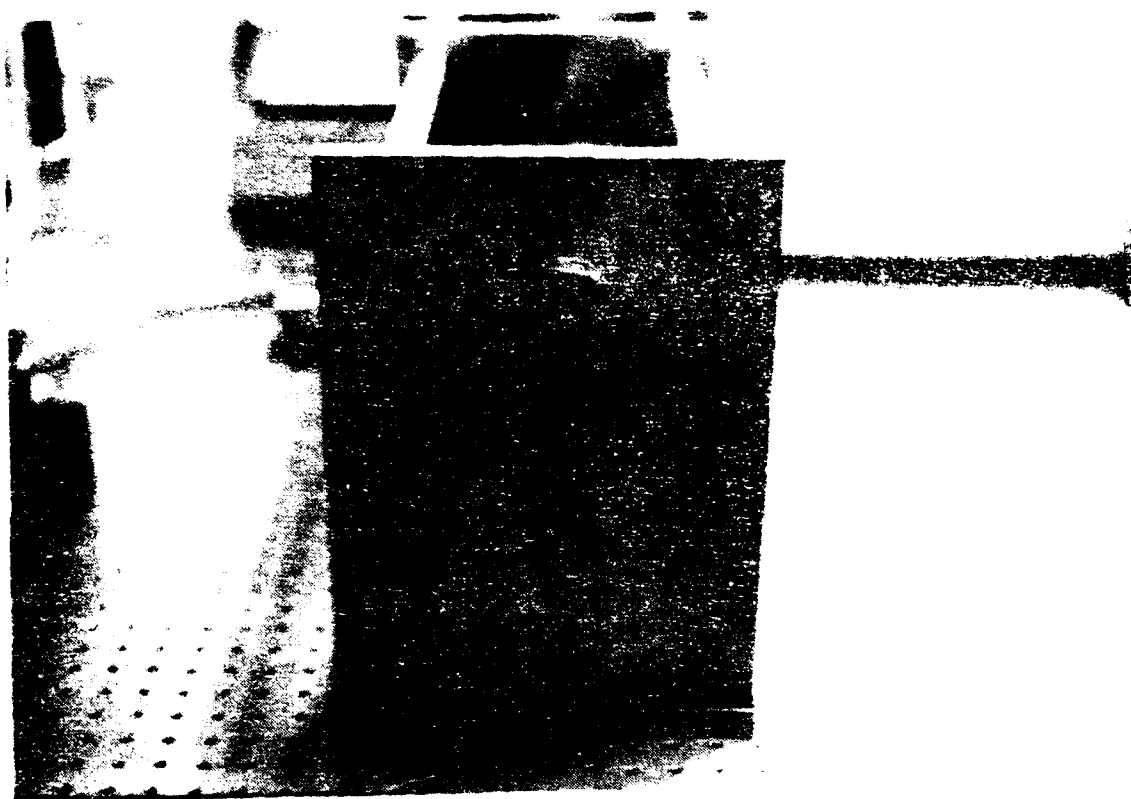


Figure 6. Tensile/torsion load machine A rotator.

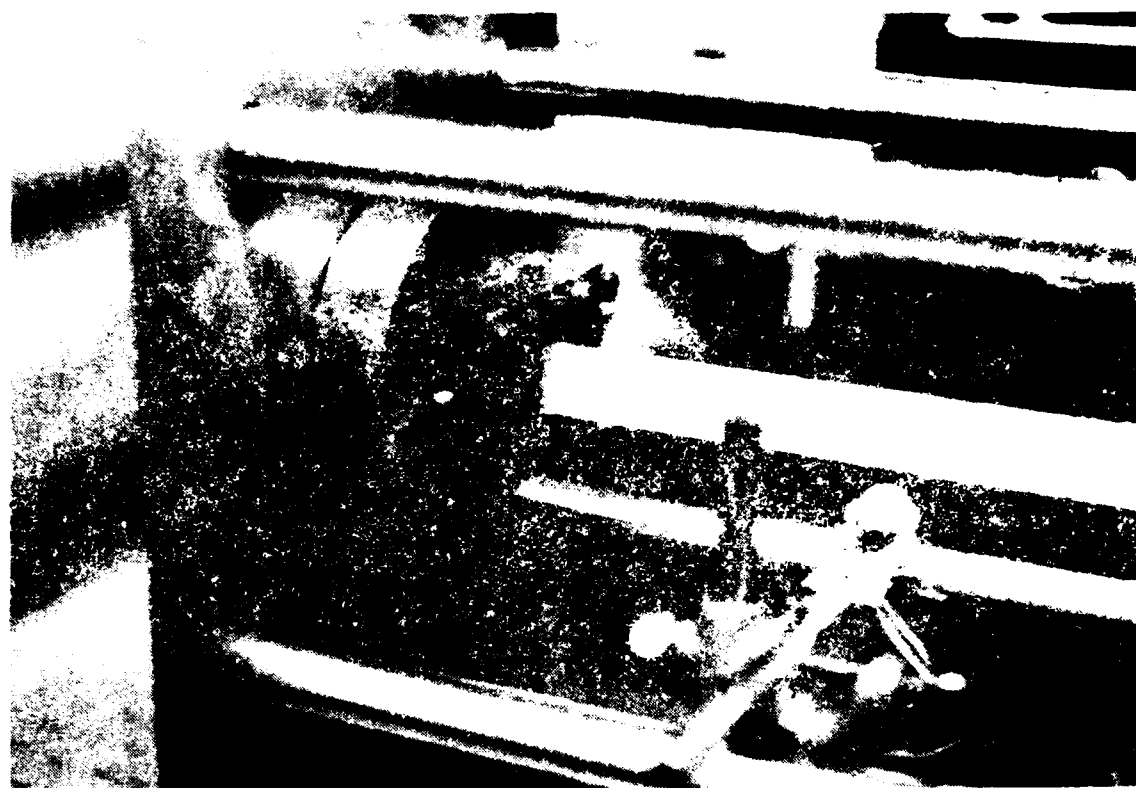


Figure 7. Close-up of rotator head assembly.

fabricated to the drawings shown in Appendix A. This machine was used to introduce a tensile load  $T$  into the specimen which was pre-twisted an amount  $\theta$  over its overall length. The pre-twist angle is a qualitative measure of the degree of torsion loading in the specimen. In a typical test, a specimen (flawed due to impact dynamic loading) was placed between the grips shown in Figure 1. An amount of  $\theta$  pre-twist was applied through the rotator and then the rotator was locked in place. This rotator was capable of rotating a specimen to  $90.0^\circ$  in  $5.0^\circ$  increments. A tensile load  $T$  was then applied to the specimen resulting in a combined tension and torsion load condition. The tensile load was generated using air supplied to a 400 psi rated air cylinder. The air pressure was regulated using a Matheson 0-60 psig model 40-L pressure regulator. Fine control of the air pressure was performed using a Whitey micrometer air valve and the pressure was monitored on a 100 cm Hg manometer. Figures 8 and 9 illustrate the gas supply system.

Once the specimen was loaded, the beam from a Spectra-Physics Model 125 He-Ne gas laser was expanded onto its surface. A Spectra-Physics Model 332 Spatial Filter was used to filter and expand the laser beam. A Uniblitz Model 310B shutter timer control unit was used to control the laser beam exposure time. While in the loaded state, a photograph of the specimen was made. The load was then removed and a second exposure was made. The resulting interferogram was then analyzed and surface displacement data was obtained. Results from the interferograms were then compared to ultimate strength tests obtained from Instron testing the specimens to failure under simple tension loading. Figures 10 and 11 illustrate the experimental lab geometry.

#### B. Composite Tensile Specimens

The uniaxial tensile test specimens were fabricated according to these instructions. One hundred and forty uniaxial composite tensile specimens were prepared.

##### 1. Specific Instructions

a. Material - 3M Scotchply SP250 (also referred to as XP250) prepeg composite sheets in the wrap angles listed in Table 1.

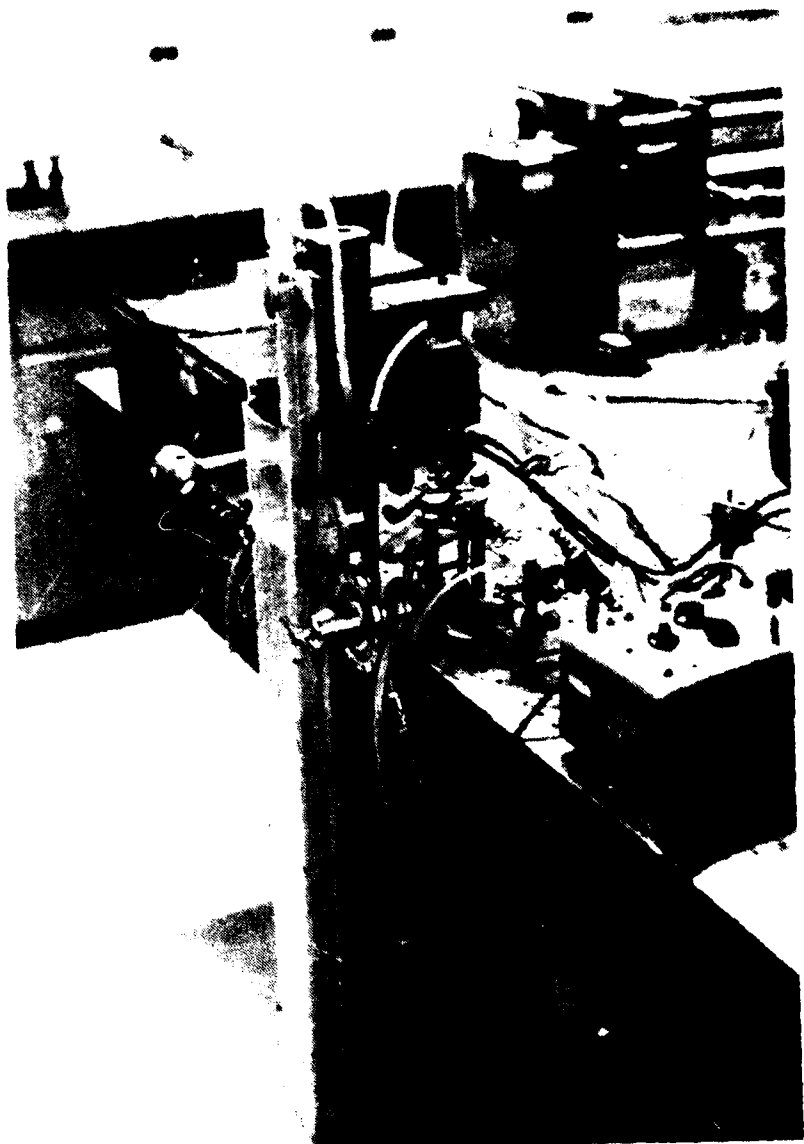


Figure 8. Gas supply system.



Figure 9. Manometer and pressure regulator assembly.

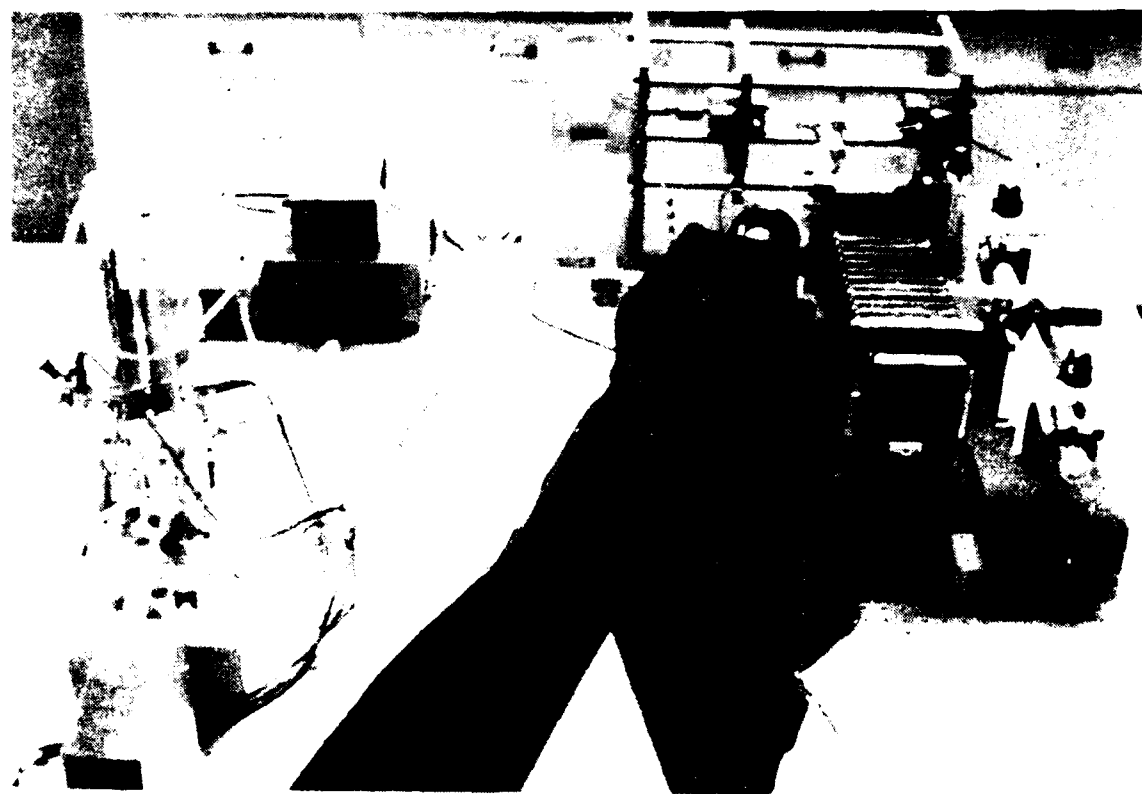


Figure 10. Experimental lab apparatus.

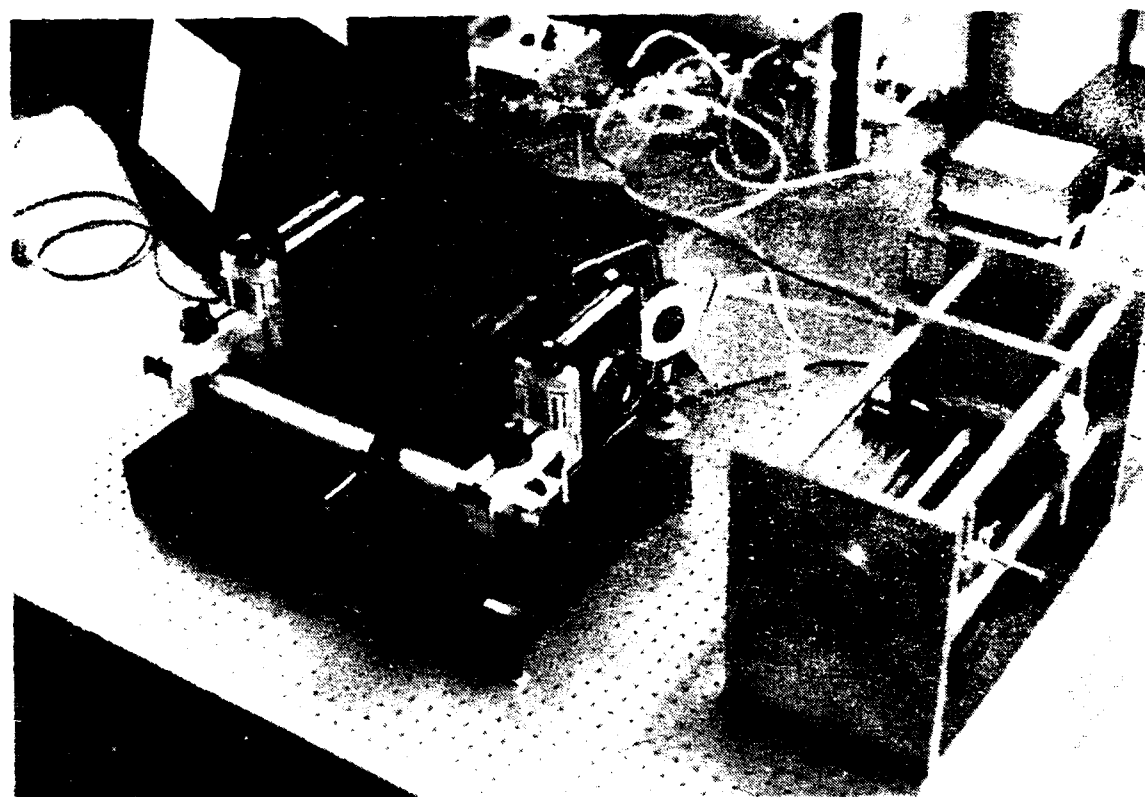


Figure 11. Optical alignment of the laser and camera system.

TABLE 1. COMPOSITE SHEET MATERIAL FOR TENSILE SPECIMENS

8 Ply $\pm 15^\circ$ s	8 Ply $\pm 60^\circ$ s
8 Ply $\pm 20^\circ$ s	8 Ply $0^\circ$
8 Ply $\pm 30^\circ$ s	14 Ply $0^\circ/90^\circ$ s
8 Ply $\pm 45^\circ$ s	8 Ply $0^\circ/\pm 45^\circ/90^\circ$ s

These materials were used to form the composite uniaxial tension specimens. Eight (8) ply  $\pm 60^\circ$  s material is equivalent to 8 ply  $\pm 30^\circ$  s rotated  $90^\circ$ .

b. Endtabs were bonded to the ends of the tensile specimens for gripping in uniaxial tension. Figure 12 shows how each of the four endtabs was placed on a single tensile specimen. The endtab material was 14 Ply  $0^\circ/90^\circ$  s symmetrical 3M Company Scotchply SP250 prepreg composite sheet.

c. Endtabs were bonded to the composite uniaxial tensile specimens using the Eastman 910 adhesive system. Manufacturer's instructions were followed for adhesive bonding of the composite materials.

d. Dimensions for the specimens are given in Table 2 and Figure 13.

e. When bonding endtabs to the uniaxial tensile specimens, all plies adjacent to the adhesive glue-bond joint had the same filament orientation.

f. Endtabs were bonded to each uniaxial tensile specimen before final machining took place.

g. All uniaxial tension specimens and endtabs were cut at least 3 mm oversize and final dimensions were obtained by milling or grinding, or both with water flow.

h. All uniaxial tensile specimens had their respective plies oriented symmetric to the primary axis as given in Figure 1. All ply angles are measured from the primary axis.

i. Specimens did not have any visible delaminations present in either the endtabs or tensile specimens.

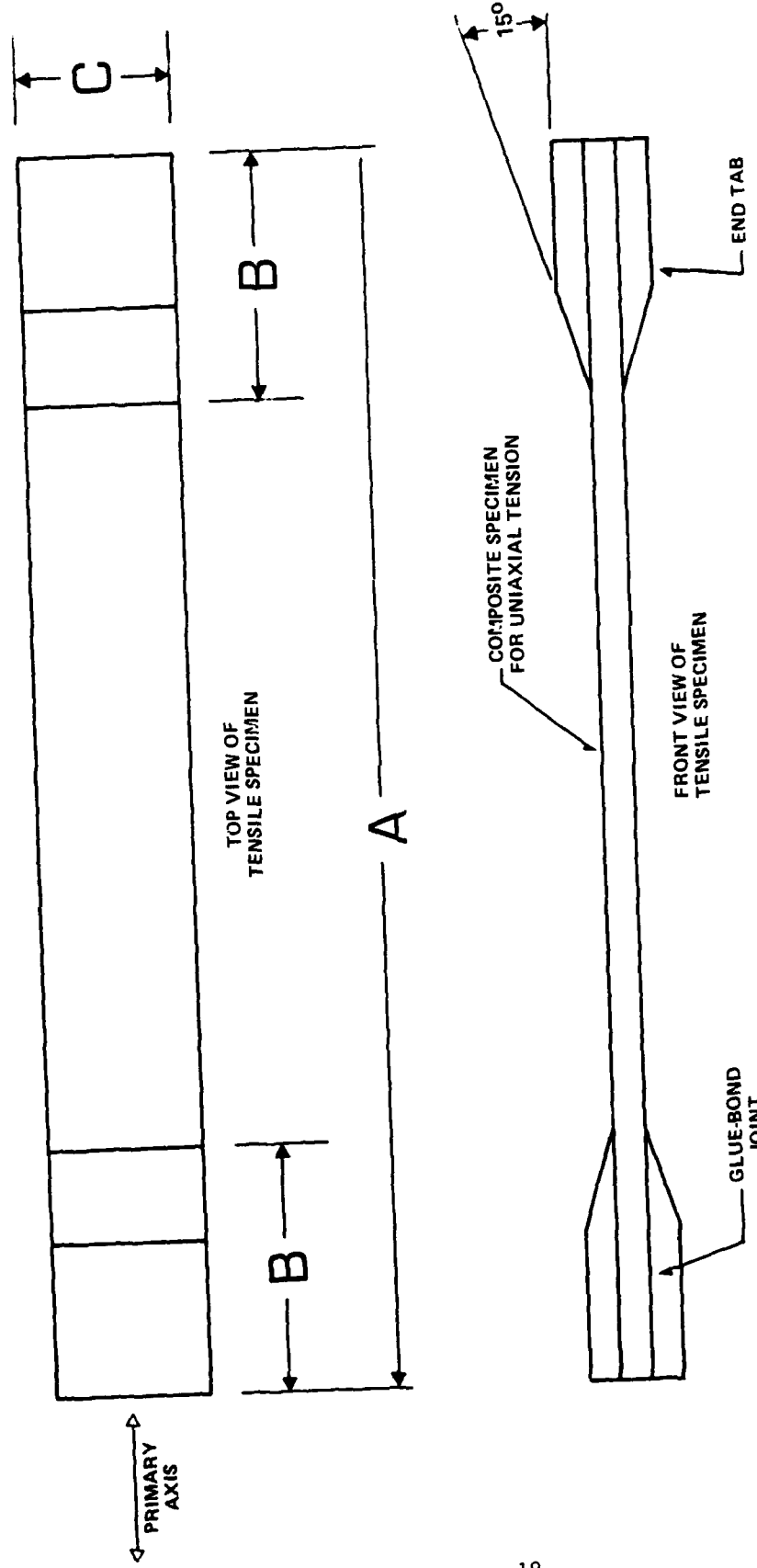


Figure 12. Composite tensile specimen.

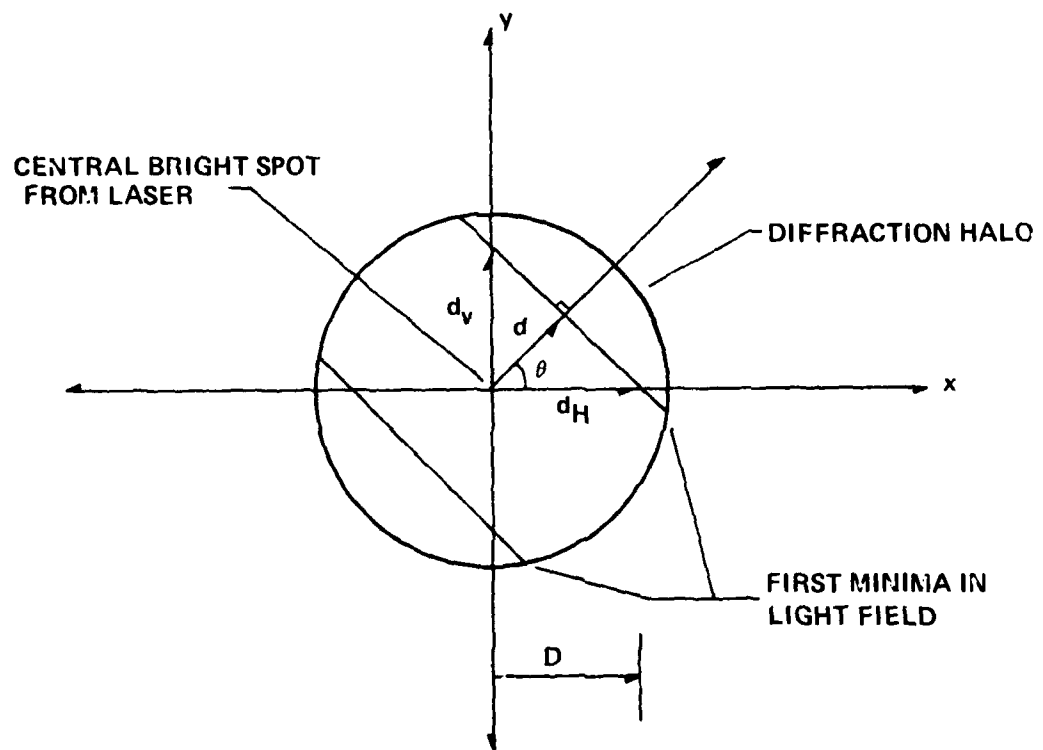


Figure 13. Diffraction halo geometry.

TABLE 2. UNIAXIAL TENSILE SPECIMEN DATA

WRAP ANGLE	DIMENSIONS (mm)			NO. REQUIRED
	A	B	C	
8P $\pm$ 15° <sub>S</sub>	304.8	38.1	25.4	20
8P $\pm$ 20° <sub>S</sub>	304.8	38.1	25.4	20
8P $\pm$ 30° <sub>S</sub>	304.8	38.1	25.4	20
8P $\pm$ 45° <sub>S</sub>	304.8	38.1	25.4	20
8P $\pm$ 60° <sub>S</sub>	304.8	38.1	25.4	20
8P 90° *	304.8	38.1	25.4	20
8P 0°	304.8	38.1	25.4	20

\*8P 90° specimens were too fragile to test.

All specimens were fabricated according to the "Standard Test Method for Tensile Properties of Oriented Fiber Composites" ASTM American National Standard ANSI/ASTM D 3039-76.

where,

S = film scale factor (magnification ratio).

$\lambda$  = wavelength of laser illumination source.

f = distance from interferogram to analyzer screen.

d = distance from central bright spot to first minima.

$U_\theta$  = displacement of the point illuminated by the laser on the object in the  $\theta$  direction.

The vertical,  $U_V$  and horizontal,  $U_H$  components of displacement may be obtained from  $U_\theta$  [6] as:

$$U_H = U_\theta \cos\theta = \frac{S\lambda f}{2d} \cos\theta \quad (2)$$

$$U_V = U_\theta \sin\theta = \frac{S\lambda f}{2d} \sin\theta \quad (3)$$

and from the geometry,

$$\frac{d}{d_H} = \cos\theta \quad (4)$$

$$\frac{d}{d_V} = \sin\theta \quad (5)$$

therefore,

$$u_H = \frac{S\lambda f}{2d_H} \quad (6)$$

$$u_V = \frac{S\lambda f}{2d_V} \quad (7)$$

To speed up the analysis of interferograms, a technique of reading the number of the fringe order at some distance  $D$  (shown in Figure 13) was utilized. In this project, flaws were placed at the centers of the tension/torsion specimens. Displacements at eight locations along the primary axis (through the center of the specimen) and symmetrically centered about the flaw, were taken for each interferogram. This was accomplished by reading the fringe order occurring at some location  $D$  in the analyzer screen plane and along the direction of the primary axis. Thus, deformation around the flawed region and along the primary axis was determined. Figure 14 illustrates a segment of a diffraction halo and how data is obtained from it. In this figure the distance  $D$  is fixed and lies in the analyzer plane along the primary axis direction. The order of the fringe at a distance  $D$  from the central bright spot is recorded as  $n$ .

For the general case,

$$u = \frac{S\lambda f}{ZX} \quad (8)$$

and from Figure 14,

$$X = \frac{D}{2n-1} \quad (9)$$

therefore,

$$u = \frac{S\lambda f}{2D} (2n-1) \quad (10)$$

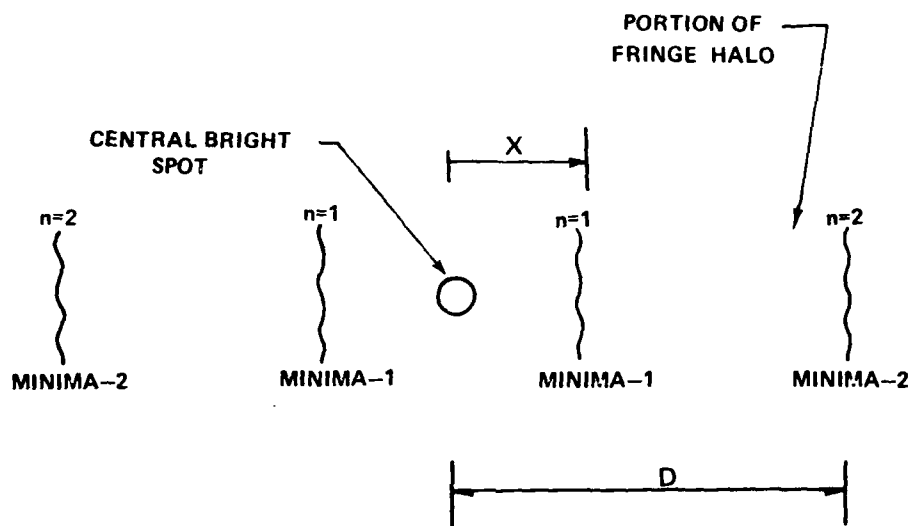


Figure 14. Method of fringe order analysis.

Now the strain  $u^1 = \frac{du}{dx}$  is determined from

$$u^1 = \frac{du}{dx} = \frac{2s\lambda f}{2D} \frac{dn}{dx} = \frac{s\lambda f}{D} n^1 . \quad (11)$$

Define a series of  $N$  locations equally spaced on the interferogram plate (i.e.,  $N = 0, 1, 2, \dots, 6, 7$ ) and let

$$\beta = \frac{dn}{dN} \quad (12)$$

then,

$$n^1 = \frac{dn}{dN} \frac{dN}{dx} \quad (13)$$

$$\epsilon = \frac{s\lambda f}{D} n^1 = \beta \frac{dN}{dx} \frac{s\lambda f}{D} . \quad (14)$$

Therefore, if the fringe order gradient  $\beta$  is known for some location  $N$  on an interferogram and if the gradient of  $N$  with respect to  $X$  is known, then the absolute strain  $\epsilon$  can be determined from Equation 14. In order to accurately predict  $\beta$  at the center of the specimen and in the flawed region of the specimen, a least squares analysis was used.

Suppose  $\bar{N}$  data samples (i.e.,  $\bar{N}_{\max} = 8$ ) of fringe order  $n$  versus plate location  $N$  are taken.  $N_0$  corresponds to  $X_0$  on the interferogram,  $N_1$  to  $X_1$  and so forth.  $\Delta X$  is the distance on the interferogram between the evenly spaced  $X_i$ . Using a quadratic least squares polynomial,

$$y = ux^2 + vx + w . \quad (15)$$

In Equation 15,  $X$  corresponds to  $N_i$  and  $y$  to the fringe order  $n$  at location  $N_i$ .

Forming the difference function yields:

$$\delta = \sum_{i=1}^{\bar{N}} [y_i - (ux_i^2 + vx_i + w)]^2 \quad (16)$$

Differentiating  $\delta$  with respect to  $u$ ,  $v$ ,  $w$  to obtain a minima, yields:

$$\frac{\partial \delta}{\partial u} = 0 = \sum_{i=1}^{\bar{N}} -2 [y_i - (ux_i^2 + vx_i + w)] x_i^2 = 0$$

$$\frac{\partial \delta}{\partial u} = 0 = \sum_{i=1}^N -2[y_i - (ux_i^2 + vx_i + w)] x_i = 0$$

$$\frac{\partial \delta}{\partial w} = 0 = \sum_{i=1}^N -2[y_i - (ux_i^2 + vx_i + w)] = 0 \quad (17)$$

Let,

$\bar{N}$

$$\sum_{i=1} = \sum$$

$$\sum x_i^4 = x_4$$

$$\sum x_i^3 = x_3$$

$$\sum x_i^2 = x_2$$

$$\sum x_i^1 = x_1$$

$$\sum x_i^0 = \bar{N} = x_0$$

$$\sum y_i x_i^2 = y_2$$

$$\sum y_i x_i^1 = y_1$$

$$\sum y_i = y_0 .$$

(18)

Then Equation 17 may be written as

$$\sum y_i x_i^2 = u \sum x_i^4 + v \sum x_i^3 + w \sum x_i^2$$

$$\sum y_i x_i = u \sum x_i^3 + v \sum x_i^2 + w \sum x_i$$

$$\sum y_i = u \sum x_i^2 + v \sum x_i + w \bar{N}$$

(19)

or,

$$y_2 = u x_4 + v x_3 + w x_2$$

$$y_1 = u x_3 + v x_2 + w x_1$$

$$y_0 = u x_2 + v x_1 + w x_0 .$$

(20)

Now let

$$\begin{array}{ll} y_2 = A & x_4 = D \\ y_1 = B & x_3 = E \\ y_0 = C & x_2 = F \\ x_0 = H & x_1 = G \end{array} \quad (21)$$

Then,

$$\begin{bmatrix} D & E & F \\ E & F & G \\ F & G & H \end{bmatrix} \begin{bmatrix} U \\ V \\ W \end{bmatrix} = \begin{bmatrix} A \\ B \\ C \end{bmatrix} \quad (22)$$

Using Crammer's Rule:

$$\begin{aligned} Q &= D \cdot [F \cdot H - G \cdot G] - E \cdot [E \cdot H - G \cdot F] + F \cdot [E \cdot G - F \cdot F] \\ R &= A \cdot [F \cdot H - G \cdot G] - E \cdot [B \cdot H - G \cdot C] + F \cdot [B \cdot G - F \cdot C] \\ S &= D \cdot [B \cdot H - G \cdot C] - A \cdot [E \cdot H - G \cdot F] + F \cdot [E \cdot C - B \cdot F] \\ T &= D \cdot [F \cdot C - B \cdot G] - E \cdot [E \cdot C - B \cdot F] + A \cdot [E \cdot G - F \cdot F] \end{aligned} \quad (23)$$

and,

$$\begin{aligned} U &= \frac{R}{Q} \\ V &= \frac{S}{Q} \\ W &= \frac{T}{Q} \end{aligned} \quad (24)$$

Finally, differentiating Equation 15 yields,

$$\beta = |2UX + V| = Y \quad (25)$$

Appendix B contains a computer program used to compute  $\beta$  at  $x = 3.5$  for  $\bar{N} = 8$  samples of  $n$  fringe orders.

### III. EXPERIMENTATION

This section documents the experimentation conducted on the dynamically impacted composite specimens.

#### A. Specimens

In the testing program, 13 specimens at each of the following wrap angles were used:

TABLE 3. SPECIMEN WRAP ANGLES

Category	Specimen Wrap Angle	No. of Specimens
1	8P 0°	13
2	8P $\pm$ 15° <sub>s</sub>	13
3	8P $\pm$ 20° <sub>s</sub>	13
4	8P $\pm$ 30° <sub>s</sub>	13
5	8P $\pm$ 45° <sub>s</sub>	13
6	8P $\pm$ 60° <sub>s</sub>	13

General data for each specimen includes:

Nominal total length = 12.0 in = 304.8mm

Nominal left-hand tab length = 1.50 in = 38.1mm

Nominal right-hand tab length = 1.50 in = 38.1mm

Nominal specimen length = 9.0 in = 228.6mm

Nominal specimen width = 1.0 in = 25.4mm .

#### B. Dynamic Impact Apparatus

For each wrap angle in the test program, eight of the thirteen specimens were dynamically impacted and five remained unflawed. Figures 15 through 18 illustrate the dynamic impact apparatus modified from a previous project [7] to accommodate the new specimens. In the machine, a 4.76 lb weight is raised to a predetermined height and released. At the bottom of the

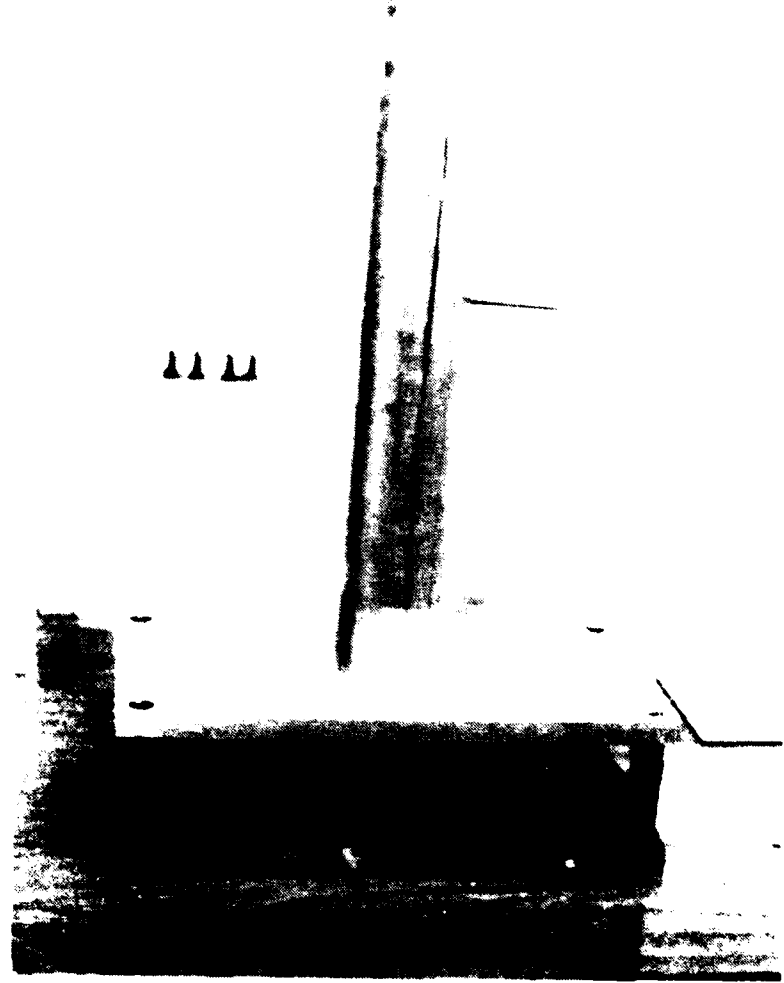


Figure 15. Dynamic impact apparatus.

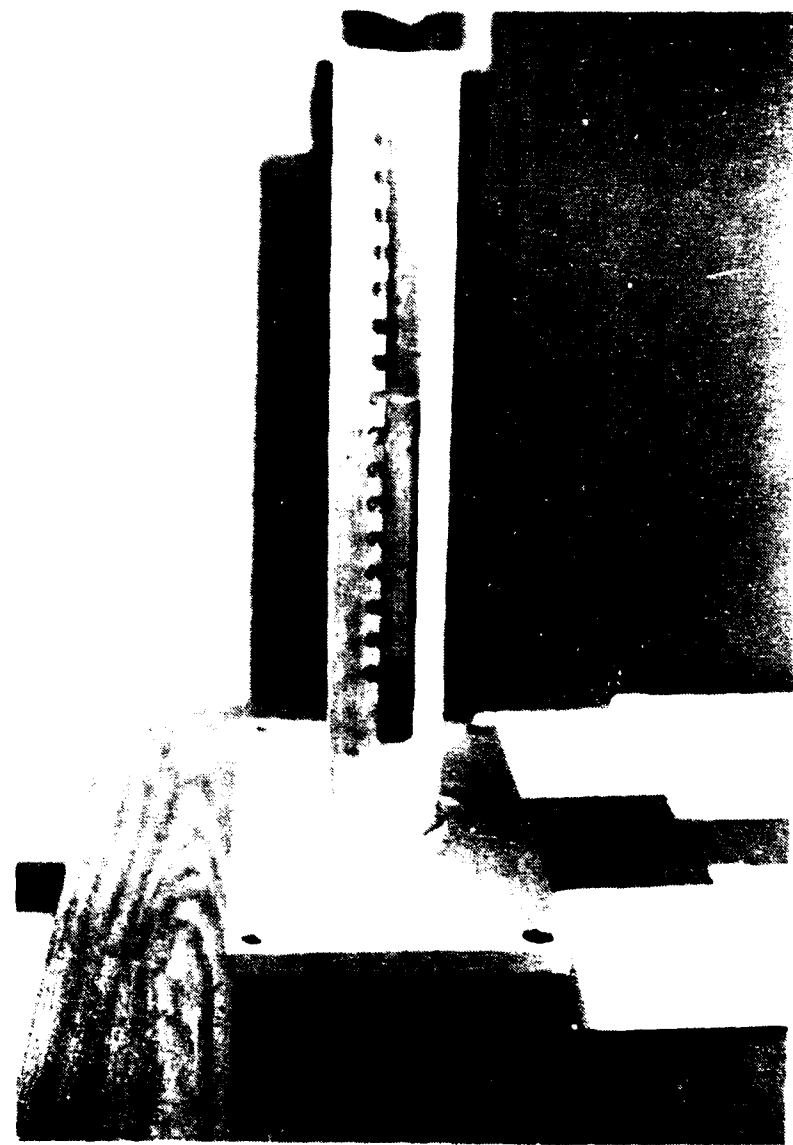


Figure 16. Side view of dynamic impact apparatus.



Figure 17. Dynamic impact darts.

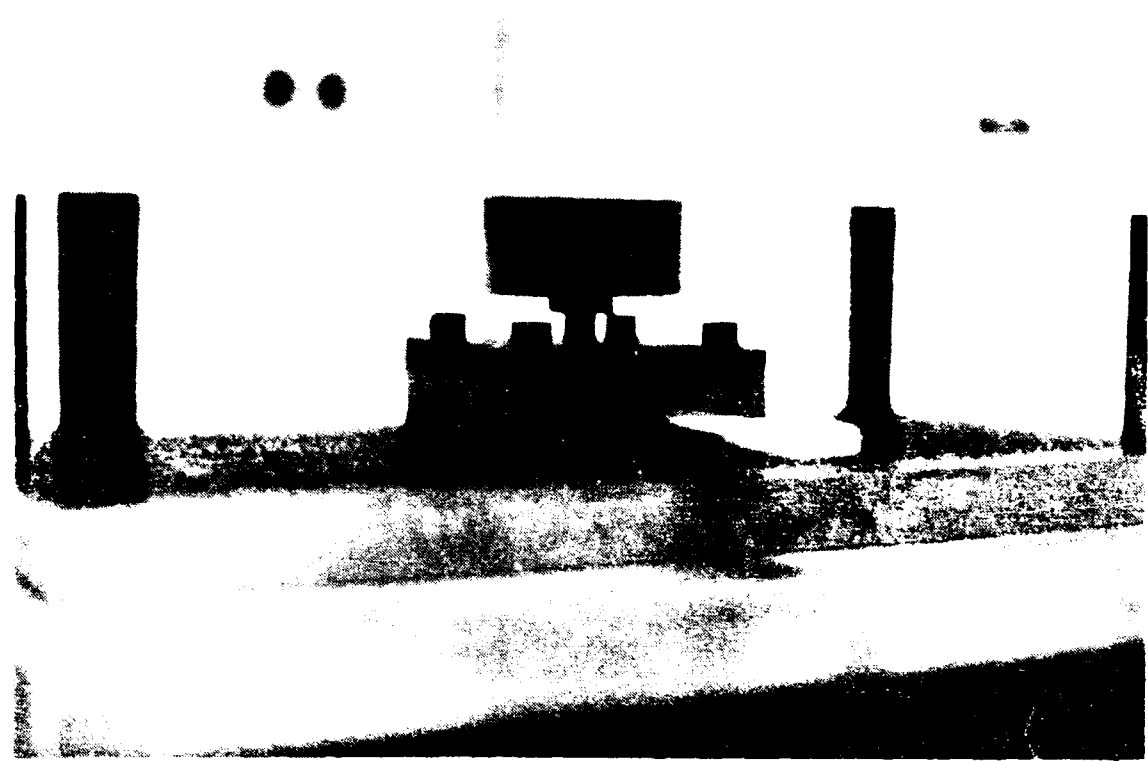


Figure 18. Drop weight transfer of load through the dart to the specimen.

fixture a dart shown in Figure 17, rests on top of a specimen. When the falling weight strikes the dart it transfers its energy to the specimen through the dart. Figure 19 illustrates the operation of the machine. A set of four dynamic impact darts was used in the experiment. These are tabulated in Table 4.

TABLE 4. EXPERIMENTAL DYNAMIC IMPACT DARTS

Impact Dart Size	Nominal Dart Radius	Measured Dart Radius
A	.25 in.	.2497 in.
B	.1875 in.	.1879 in.
C	.125 in.	.1246 in.
D	.09 in.	.0911 in.

In the testing program, thirteen specimens were selected for each wrap angle. Specimens 1 through 8 had flaws created by dynamic impact according to Table 5. Specimens A, B, C, D, and E were unflawed and were used for comparison purposes.

#### C. Specimen Preparation

Before the specimens were dynamically impacted, one side of each specimen was painted with the following material to improve the laser speckle resolution:

Pacific 8010-00-584-3150 Lacquer,  
Nitrocellulose, Type I, TT-L-50G &  
Amend. III, Flat White, No. 37875  
Contract GS-10S-40992, flash point  
-56.6°C (-70°F).

Before the specimens were painted and impacted, their thickness in the pre-flaw region was measured. This information is presented in Appendix C.

Appendix D contains pictures of both sides of each dynamically impacted specimen.

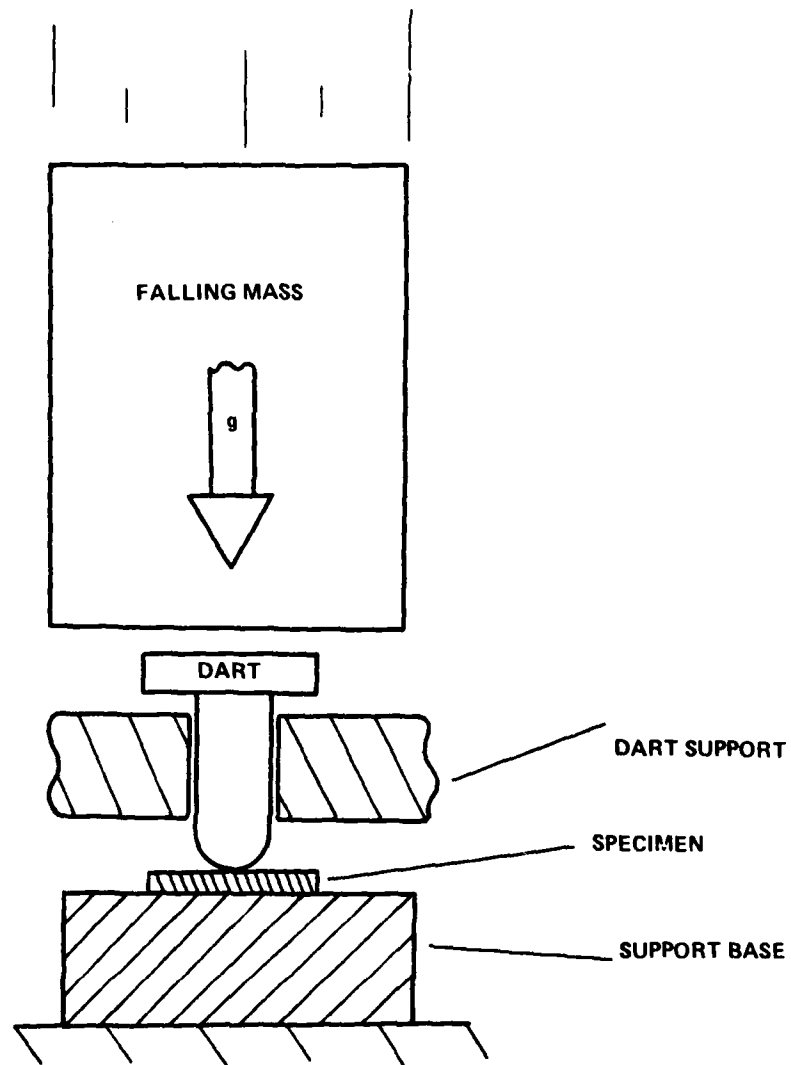


Figure 19. Schematic of dynamic impact apparatus.

#### D. Specimen Properties

The specific material properties of SP250 composite material are included for reference purposes [8]:

$$E_{11}^T = 5.64 \times 10^6 \text{ psi}$$

$$E_{22}^T = 1.74 \times 10^6 \text{ psi}$$

$$v_{12}^T = 0.299$$

$$G_{12} = 0.680 \times 10^6 \text{ psi}$$

$$E_{11}^C = 5.87 \times 10^6 \text{ psi}$$

$$E_{22}^C = 2.12 \times 10^6 \text{ psi}$$

$$v_{12}^C = 0.317$$

$$x_1^T = 134 \text{ KSI}$$

$$x_1^C = 112 \text{ KSI}$$

$$x_2^T = 7.55 \text{ KSI}$$

$$x_2^C = 25.0 \text{ KSI}$$

$$s_{12} = 7.23 \text{ KSI}$$

#### E. Specimen Loading

To make the laser speckle interferograms, a 61.20 cm Hg gage air pressure was supplied to the tension generating air cylinder of the tension/torsion apparatus. In order to move the piston in this cylinder, 11.88 cm Hg gage air pressure had to be supplied. Therefore, the actual cylinder air pressure used to supply tension to the specimen was  $\Delta P = 61.20 \text{ cm Hg} - 11.88 \text{ cm Hg} = 49.32 \text{ cm Hg}$  which is the equivalent of 9.5385 psi. The area of the cylinder used to supply tension to the specimen was  $11.8672 \text{ in}^2$ . Therefore, the tensile load was

$$L = \Delta PA = 9.5385 \text{ psi} (11.8672 \text{ in}^2)$$

$$L = 113.1953 \text{ lb.}$$

When a specimen was clamped in the grips of the tension/torsion apparatus, the grip holder separation was 9.33 inches to allow for end-tab slope requirements. Appendix C indicates the average load stress over an unflawed section of each specimen for the load  $L = 113.1953$  lb. It was computed by dividing the load  $L$  by the cross sectional area of each specimen in tension.

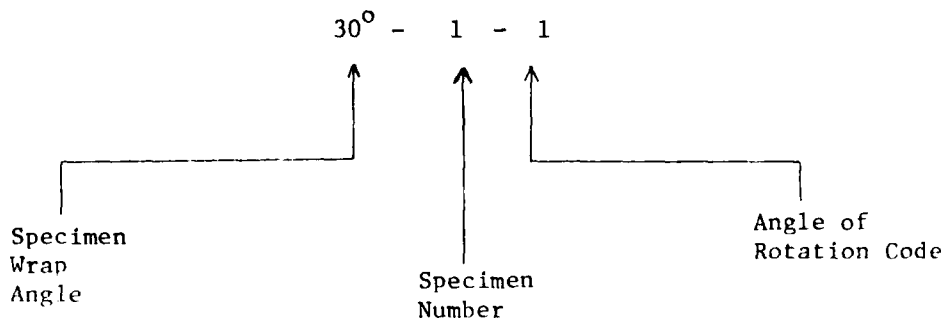
#### F. Optical Specifications

The following optical specifications were used in the testing program:

1. The double exposure interferograms were made using two 18 second exposures on AGFA-GEVAERT 10E75 Holotest 4" x 5" glass plate film.
2. 50 milliwatts of output laser beam power was used.
3. The nominal lense to specimen distance was 15.0 inch.
4. A Sinar Camera at F5.6 was used.
5. The nominal spatial filter to specimen distance was 19.0 inchs.

#### G. Specimen Rotation Angles

For each of the six wrap angles tested, a set of nine specimens from each was tested interferometrically. These tests included specimens 1 through 8 which were flawed and specimen A which had no flaw present. For each specimen tested at each wrap angle a set of four interferograms was made. Each specimen had one of four pre-rotation angles shown in Table 6 introduced into it. The specimen was then loaded and a laser exposure was made. The load was removed and a second exposure was made. Each of the interferograms in the test program was coded as in the following example.



A total of 216 interferograms was analyzed.

TABLE 6. SPECIMEN TORSION ANGLES

Angle of Rotation Code	Total Rotation Angle	Rotation in degrees Per inch of specimen (over 9.0 inch)	Rotation in Rad. Per inch of specimen (over 9.0 inch)
1	0°	0.0000 °/in	0.0000 rad/in.
2	10°	1.1111 °/in	0.0387 rad/in.
3	20°	2.2222 °/in	0.0775 rad/in.
4	30°	3.3333 °/in	0.1163 rad/in.

#### IV. EXPERIMENTAL RESULTS

After the experimental apparatus was constructed and assembled onto an optical vibration-isolation table, the experimental work was ready to begin. First, all the specimens were checked for delaminations and rejected if any proved of any significance. They were then cleaned using and air dried. Next, each specimen was individually measured for thickness values in their center. In flawed specimens, this was the pre-flaw region. Based on the tensile load  $T$  in Section F, the working stress levels for the specimens were computed. The thickness measurements and stress levels are tabulated in Appendix C.

Upon completion of all thickness measurements and stress calculations, the specimens were painted according to Section C and allowed to air dry. Dynamic impact flaws were then placed in Specimens 1 through 8 for each of the six wrap angles according to Section B and Table 5. Appendix D contains the results of this particular effort.

The next step was to make laser speckle interferograms of Specimens 1 through 8 and A for each of the six wrap angles. A total of four interferograms was made of each specimen according to Table 6 and Section G. For each specimen, the rotator was set at one of the angles: 0°, 10°, 20°, or 30°. The specimen was then loaded to 113 lbs, a laser photograph was taken, the load removed and a second (double exposure) photograph taken according to Section E. The interferograms were processed in Kodak HRP Developer, Stop Bath and Rapid Fixer. They were then dried and stored for analysis.

TABLE 5. FLAWED SPECIMEN BREAK-OUT

SPECIMEN NUMBER	INDENTER DART SIZE	IMPACT WEIGHT	IMPACT HEIGHT	IMPACT ENERGY
1	A	5.76 lb	7.15 in.	41.184 in-lb
2	A	5.76 lb	15.15 in.	87.264 in-lb
3	B	5.76 lb	7.15 in.	41.184 in-lb
4	B	5.76 lb	15.15 in.	87.264 in-lb
5	C	5.76 lb	7.15 in.	41.184 in-lb
6	C	5.76 lb	15.15 in.	87.264 in-lb
7	D	5.76 lb	7.15 in.	41.184 in-lb
8	D	5.76 lb	15.15 in.	87.264 in-lb

Analysis of the interferograms was as follows:

1. The scale factor  $S = (1.14)^{-1}$  in Equation 14. Also  $\lambda = 2.4913 \times 10^{-5}$  in,  $f = 64.25$  in.,  $D = 2.90$  in., and  $\Delta x = .5$  inch.  $dN/dx = 2.0$ .
2. Figure 20 illustrates the locations on each interferogram where the fringe order  $n$  was obtained as a function of  $r$ .

For this case  $r$  is the equivalent to  $N$ .

Appendix E contains tables of  $n$  values versus  $r$  for all the interferograms. The data was obtained according to Section 2.3. The next step was to use the information contained in Appendix E and Section 2.3 to generate the  $\beta$  values for each interferogram given in Appendix F.  $\beta$  was computed for  $r = 3.5$  for each interferogram. This corresponded to the center of each specimen flaw region.

Now from Equation 14:

$$E = \frac{S\lambda f}{D} \beta \frac{dN}{dx}$$

For a flawed specimen i:

$$E_i = \frac{S\lambda f}{D} \beta_i \frac{dN}{dx} \quad (26)$$

And for the unflawed specimen A:

$$E_A = \frac{S\lambda f}{D} \beta_A \frac{dN}{dx} \quad (27)$$

To compute the percent change in strain in a flawed specimen i as compared to the unflawed specimen A in the region  $r = 3.5$  yields

$$PCS = \text{Percent Change in Strain} = \left| \frac{E_i - E_A}{E_A} \right| \times 100\% = \left| \frac{\beta_i - \beta_A}{\beta_A} \right| \times 100\% \quad (28)$$

This information is shown tabulated in Appendix G.

After the interferometric data was analyzed, the specimens were placed in a 10,000 pound capacity Instron Machine and tested to failure. The specimens were loaded at .1 inch/min load rate. Appendix H contains photographs of the specimens tested to failure. Appendix I contains tables giving the ultimate load for each specimen and at each wrap angle. The five unflawed

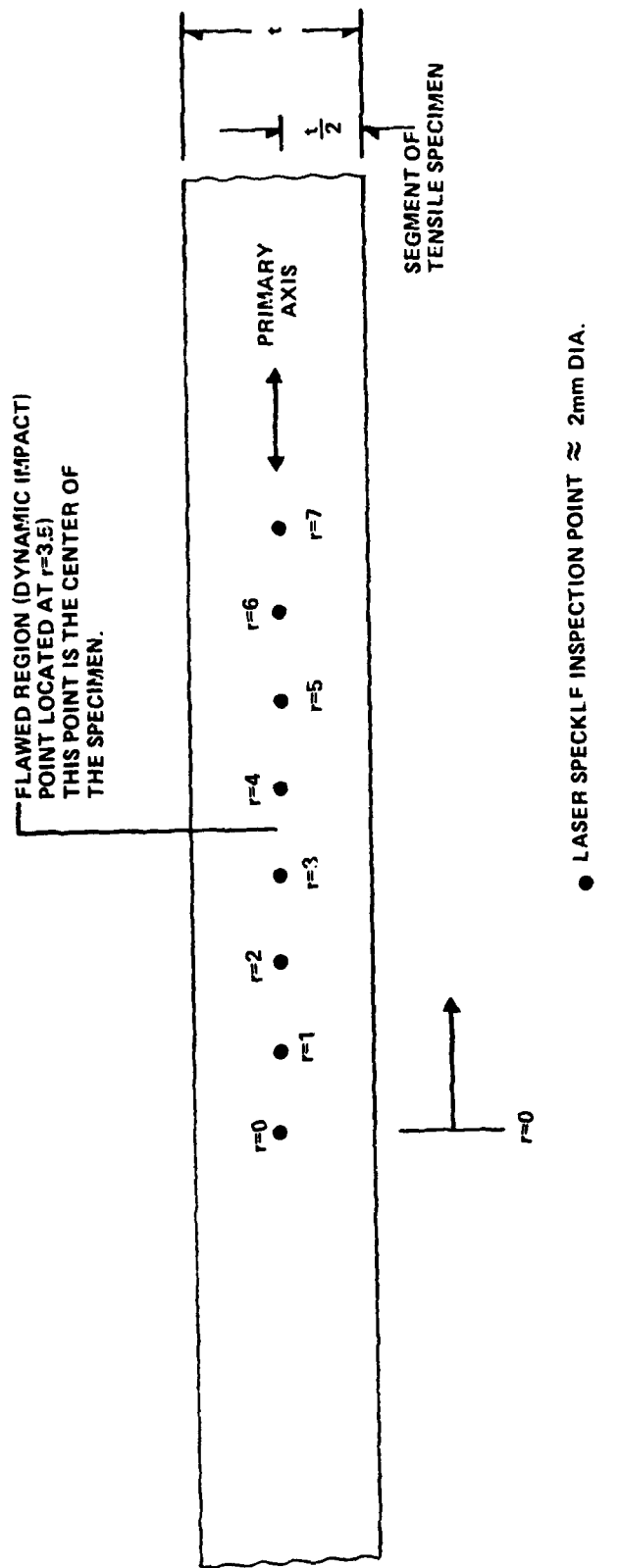


Figure 20. Location of laser speckle data inspection points on interferograms.

specimens were used at each wrap angle to obtain an average unflawed ultimate load value and to check the variation in the ultimate failure load for the unflawed specimens. Appendix J contains a summary of the ultimate failure load data for the test specimens. Appendix K contains a complete summary of all the experimental results.

#### V. CONCLUSIONS

Figures D-1 through D-48 of Appendix D illustrate the flawed regions of each specimen following impact loading. As observed from these figures, fiber-matrix delamination occurs parallel to the wrap angle and the amount of delamination increases with the impact energy. Wrap angle specimens of  $0^\circ$  and  $60^\circ$  are particularly susceptible to impact damage.  $15^\circ$  to  $30^\circ$  specimens appear to resist impact damage the best. These results are further substantiated in Appendices I and J which contain the ultimate load strength data for each specimen. Figure J-1 illustrates that as the wrap angle increases the ultimate load strength of the unflawed specimens decreases. Tables J-3 and J-4 of Appendix J illustrate that the ultimate load strength of a tensile specimen is particularly "flaw sensitive" at  $0^\circ$  and above  $45^\circ$  wrap angle.  $15^\circ$  to  $30^\circ$  wrap angle specimens show the least flaw sensitivity. Table J-5 illustrates that  $0^\circ$  specimens and  $45^\circ$  and above wrap angle specimens are particularly sensitive to an increase in dynamic impact energy.

Tables G-1 through G-6 in Appendix G illustrate the percent change in strain over the flawed region of a specimen as compared to an unflawed specimen. The results tend to have a rather random nature independent of flaw site and geometry. However, at  $60^\circ$  wrap angles, Table G-6 illustrates that the probability of detecting a flaw significantly increases. The detectability of a flawed region appears to be largely independent of the specimen rotation angle (torsional angle). Tables G-1 through G-6 were individually averaged together to obtain an average percent change in strain at each wrap angle. This number takes into account all loading energies, specimen rotation angles and possible indenter dart sites. This information is listed at the bottom of each table. From these results it is seen that  $0^\circ$  and  $60^\circ$  specimens are ideally detectable and for some reason the  $30^\circ$  specimens show unusual sensitivity. Again, as indicated by the tensile testing program, the  $15^\circ$  and  $20^\circ$  specimens show the least detectability and have the least decrease in ultimate failure load.

Appendix K contains a summary of the laser speckle interferometry data. Table K-1 was computed by averaging  $\beta$  for all the flawed specimen conditions at each wrap and rotation angle. These values are referred to as  $\beta_1$ . Note that  $\beta_1$  increases with wrap angle and generally has a minimum value between  $10^\circ$  and  $20^\circ$  rotation angle. Table K-2 is identical to Table K-1 except that only specimen A is recorded at each wrap and rotation angle. Values in Table K-1 are referred to as  $\beta_2$  values. Figure K-1 is a graph of  $\beta_2$  versus wrap angle. The data at  $45^\circ$  wrap angle is suspicious and is shown for reference. Curves both including and not including data at  $45^\circ$  were graphed. From this figure the correct value of  $\beta_2$  is believed to be about .272 but is very questionable. It is possible that there is some unusual material behavior around  $45^\circ$  wrap angle. Table K-3 contains a summary of the ultimate failure loads of the specimens.  $L_1$  is the average failure load for specimens 1-8 at each wrap angle.  $L_2$  is the average failure load for the unflawed specimens A-E.

Table K-4 contains a summary of all the data in Appendix K.  $\Delta\beta$  is the ratio of the average strain in the flawed region of the specimens to that of an unflawed specimens.  $\psi$  is a measure of the sensitivity of the interferometric analysis process and is the ratio of  $\Delta\beta$  to  $\Delta L$ . Figure K-2 illustrates the variation of  $\psi$  with wrap angle. Above  $45^\circ$  wrap angle the sensitivity becomes very large. Ideally  $\Delta\beta$  indicates the sensitivity of the laser speckle interferometric flaw detection process. The more that  $\Delta\beta$  deviates from 1.0 the greater the sensitivity.  $\Delta L$  indicates how critical the set of flaw conditions was to the specimens. The smaller values of  $\Delta L$  ( $<1.0$ ) indicate greater dynamic impact sensitivity. From this information,  $60^\circ$  wrap angle specimen flaws are the easiest to detect and exert the greatest influence on the strength of the specimens. However,  $20^\circ$  wrap angle specimen flaws are the hardest to detect and exert the least influence on the strength of the specimens.

In conclusion, the results of the tensile test program agree fairly well with those of the interferometric testing program. Results indicate that, although some scatter exists in the interferometric data, it proves to be a viable solution to flaw detection.

#### APPENDIX A

These drawings were used to build the combined tension and torsion loading machine used in this experiment.

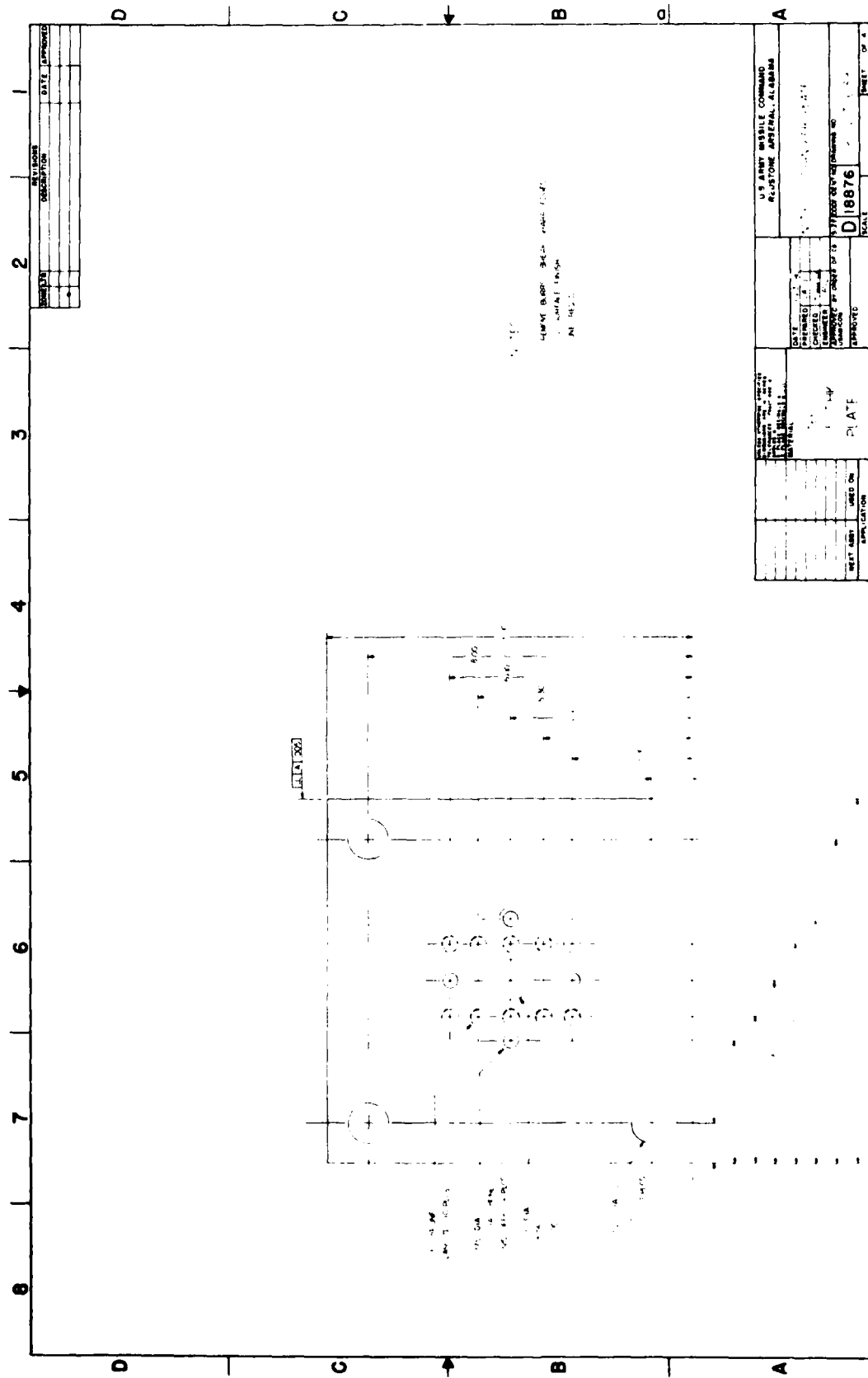


Figure A-1

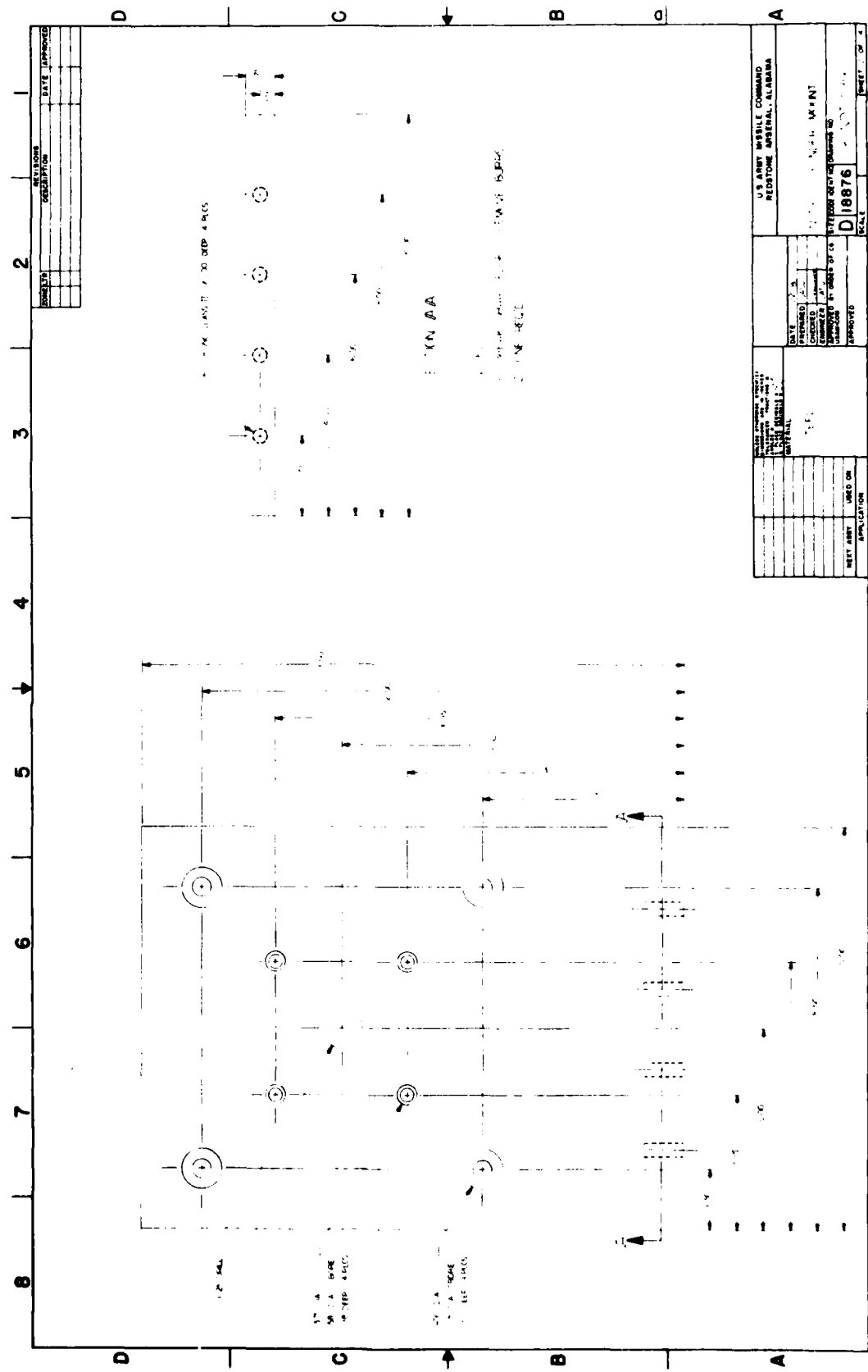


Figure A-2

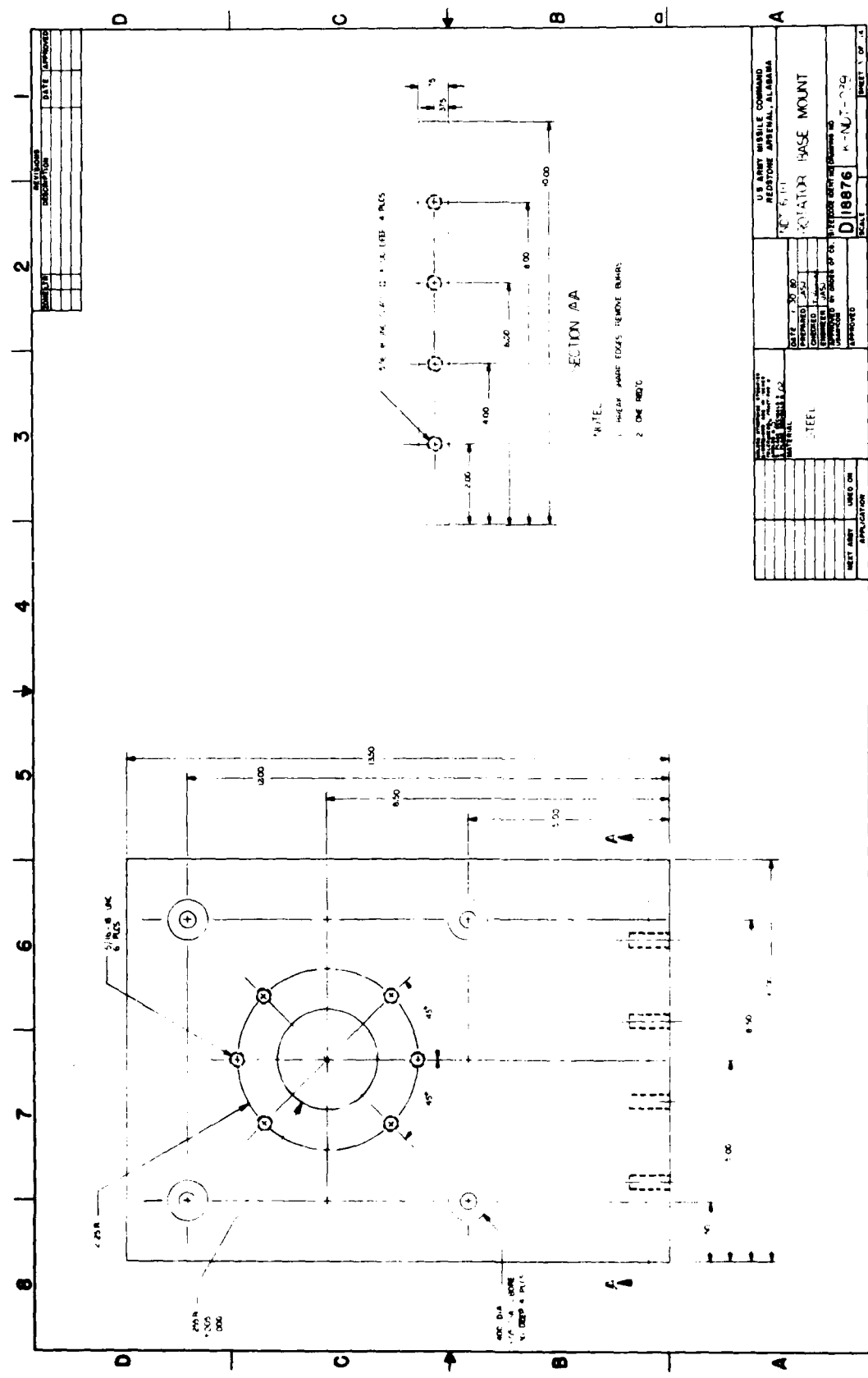


Figure A-3

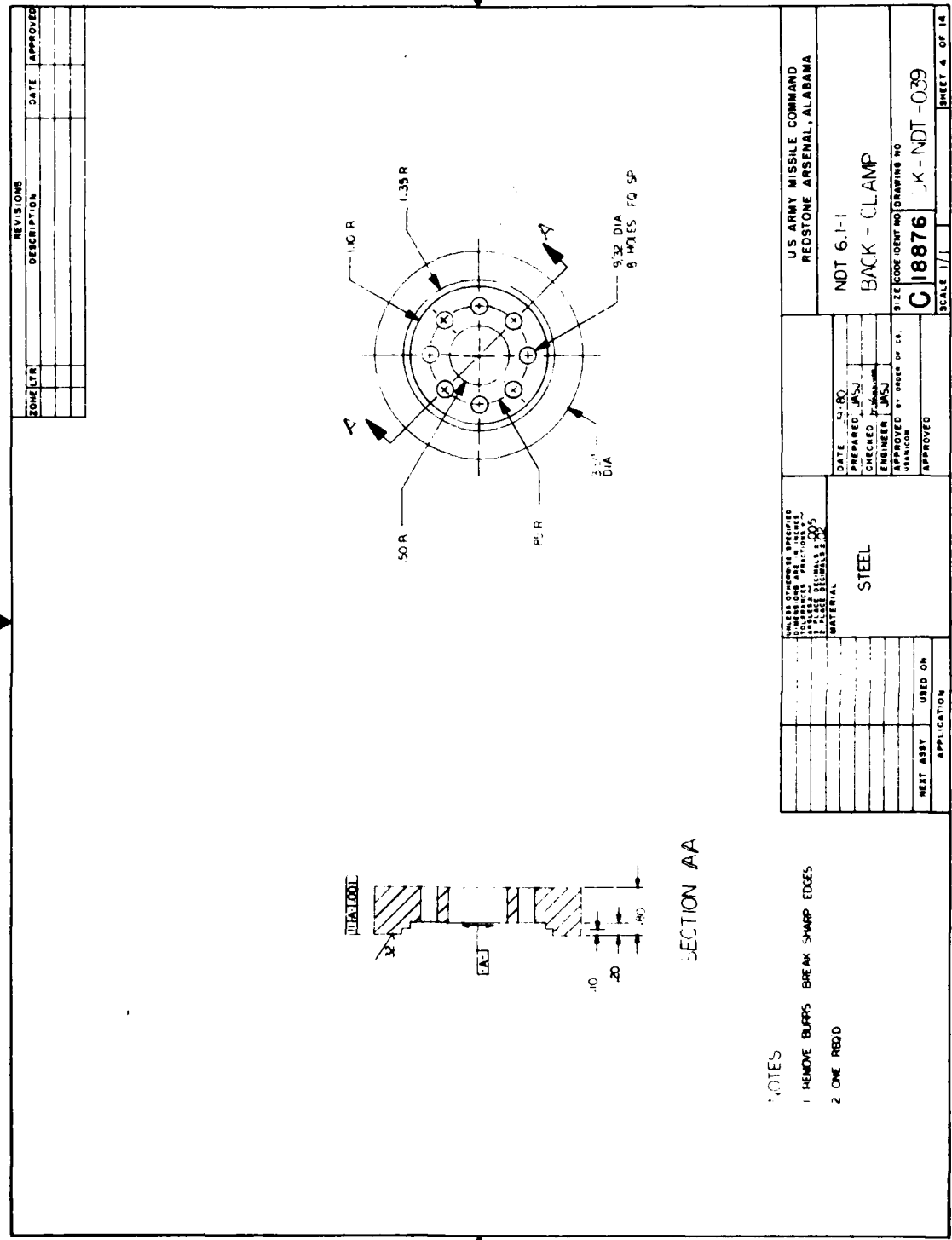


Figure A-4

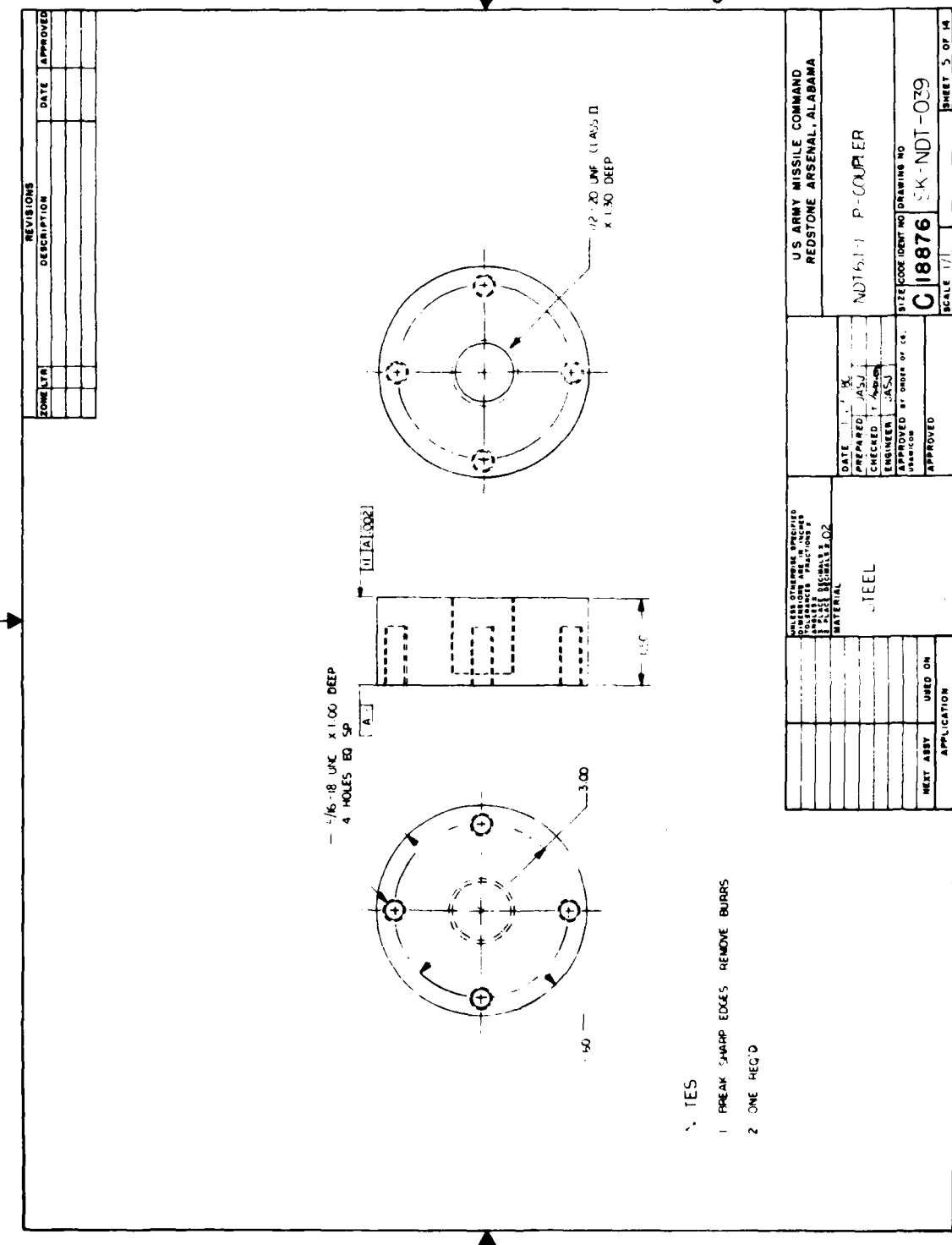


Figure A-5

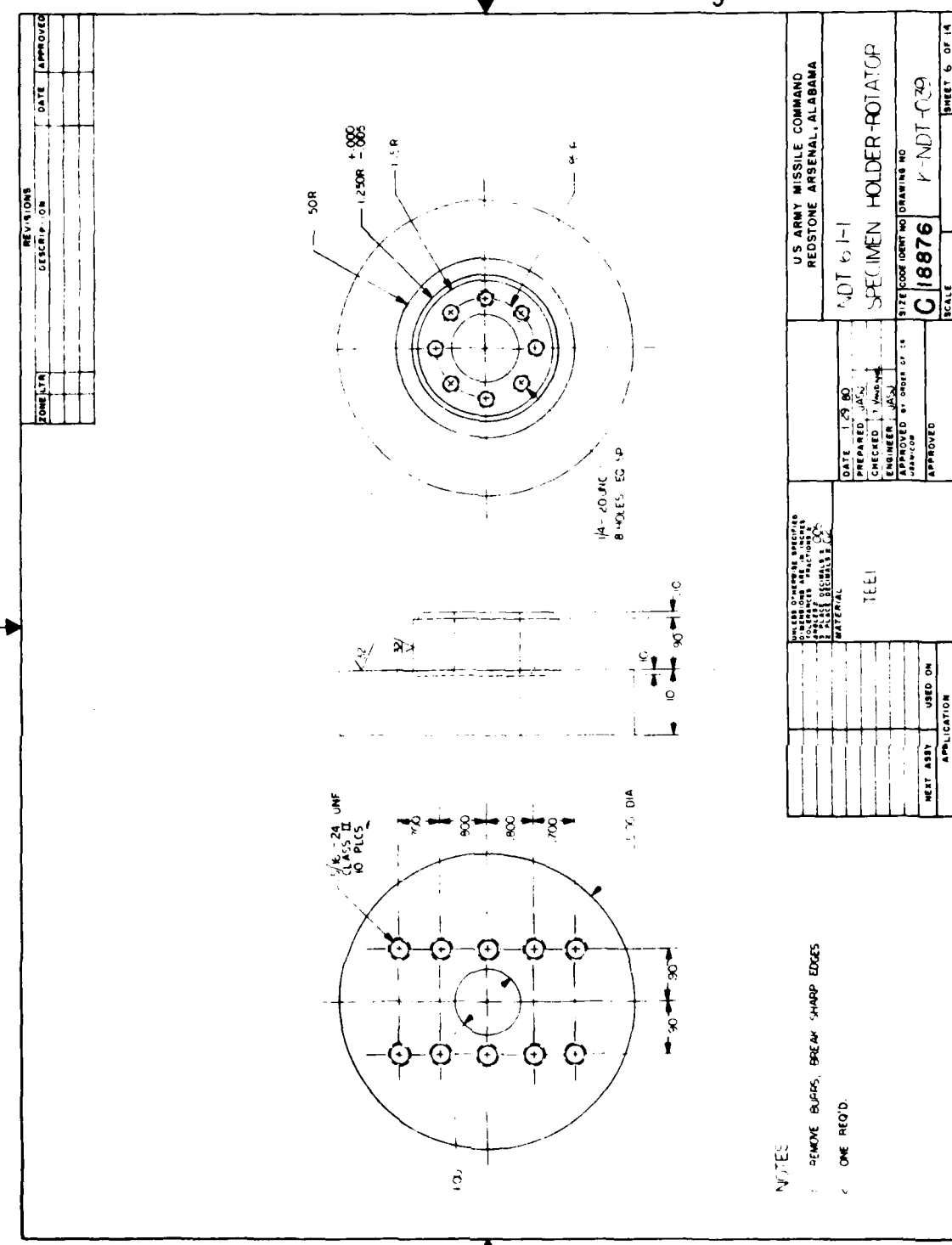


Figure A-6

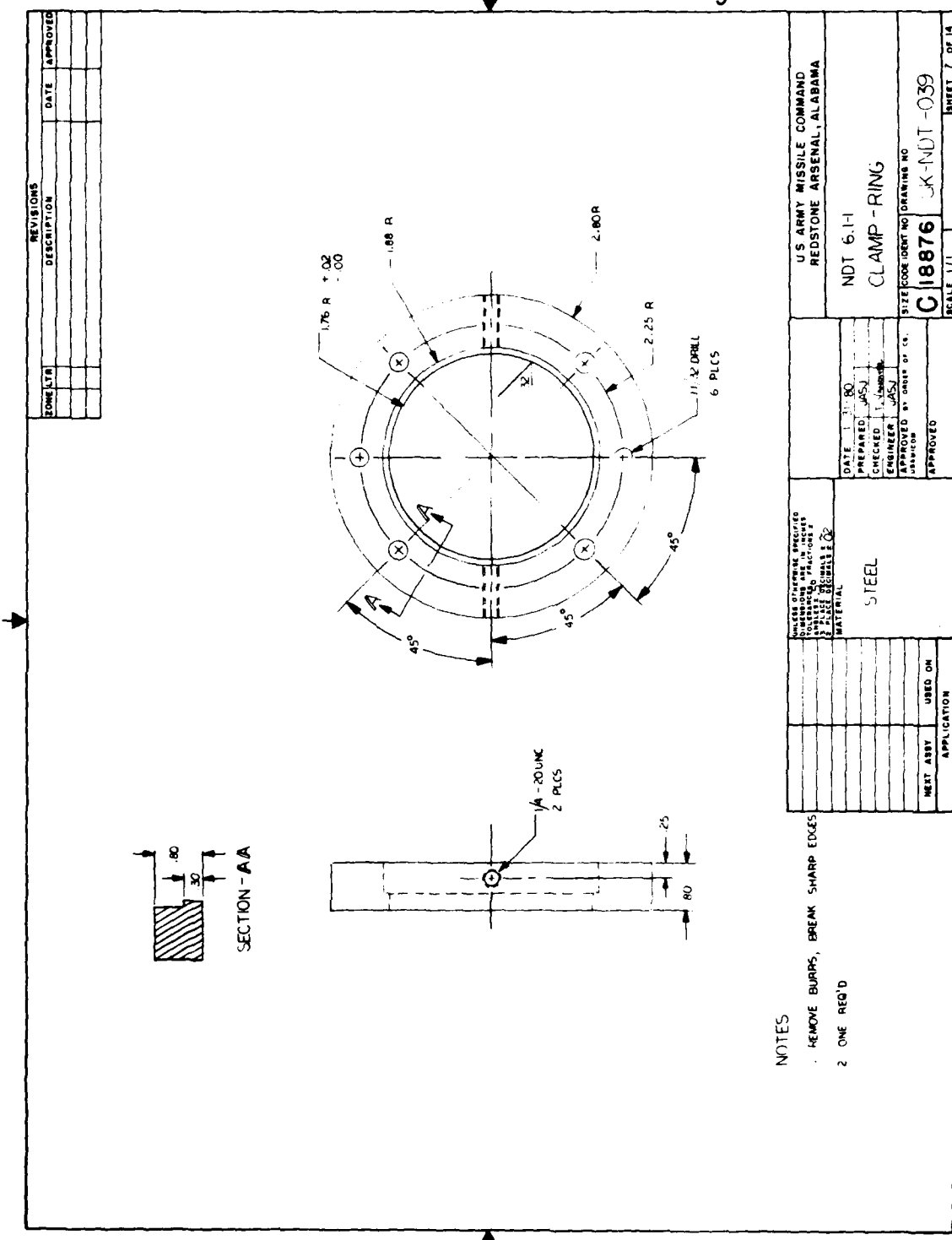


Figure A-7

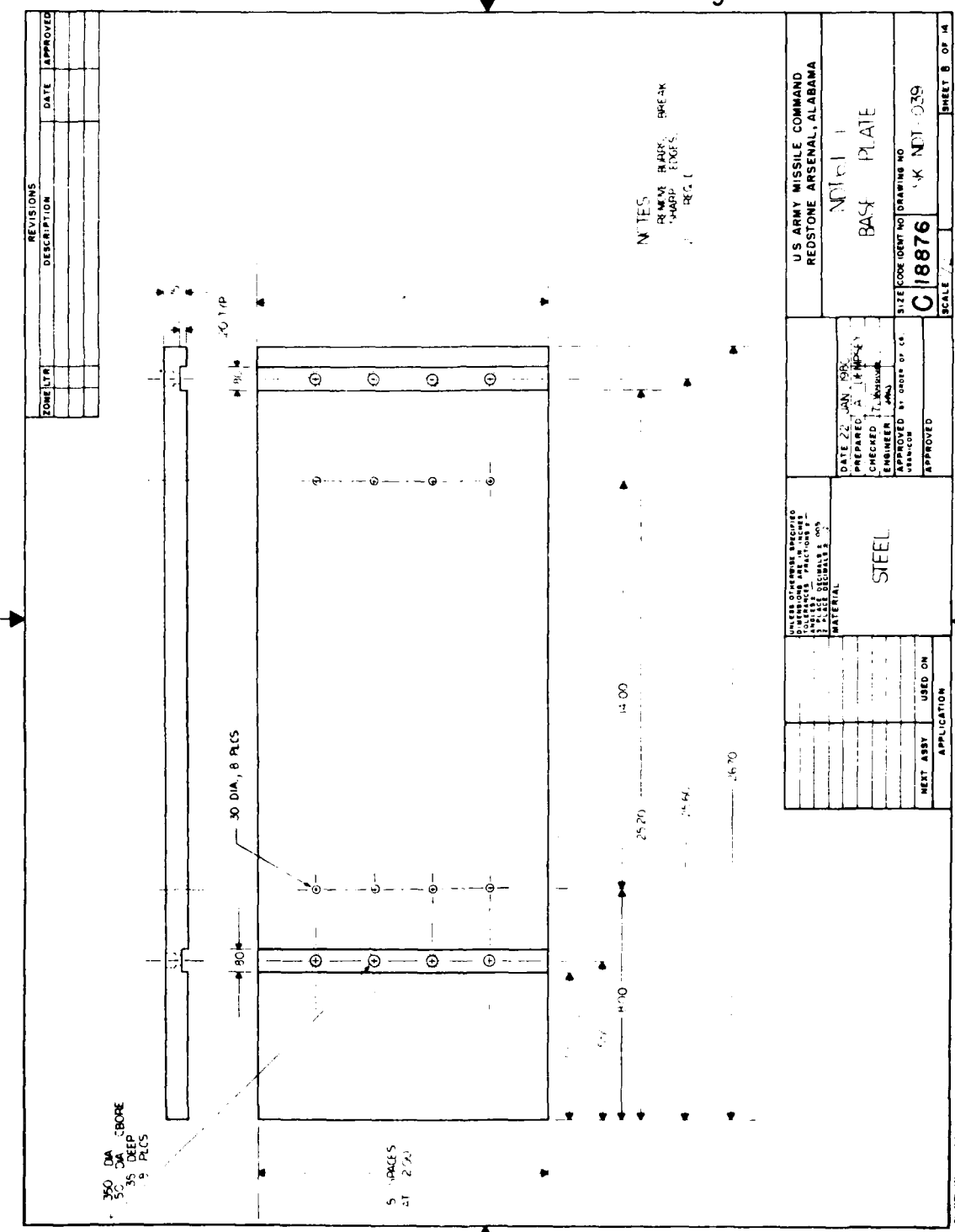


Figure A-8

Figure A-9

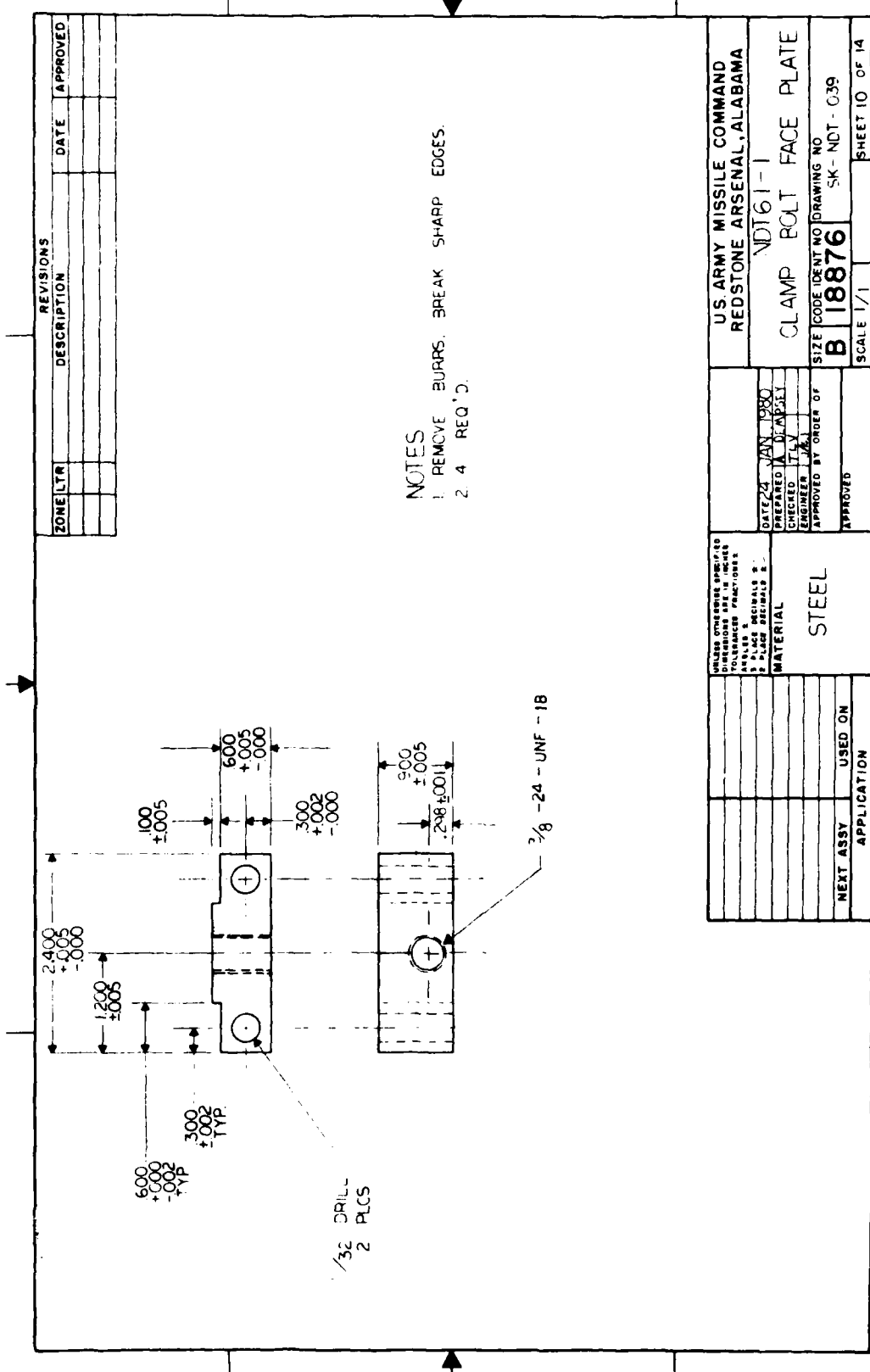


Figure A-10

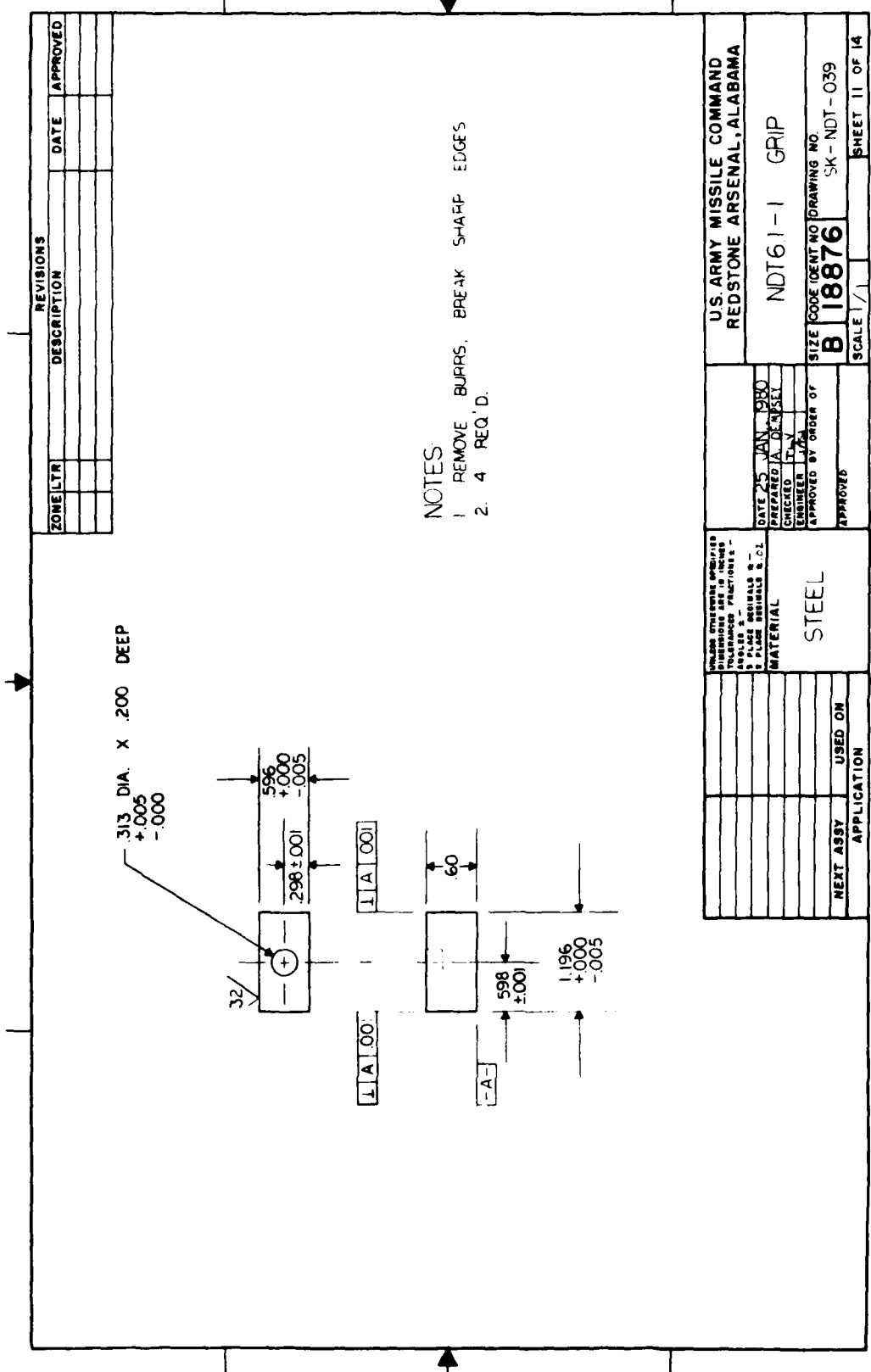


Figure A-11

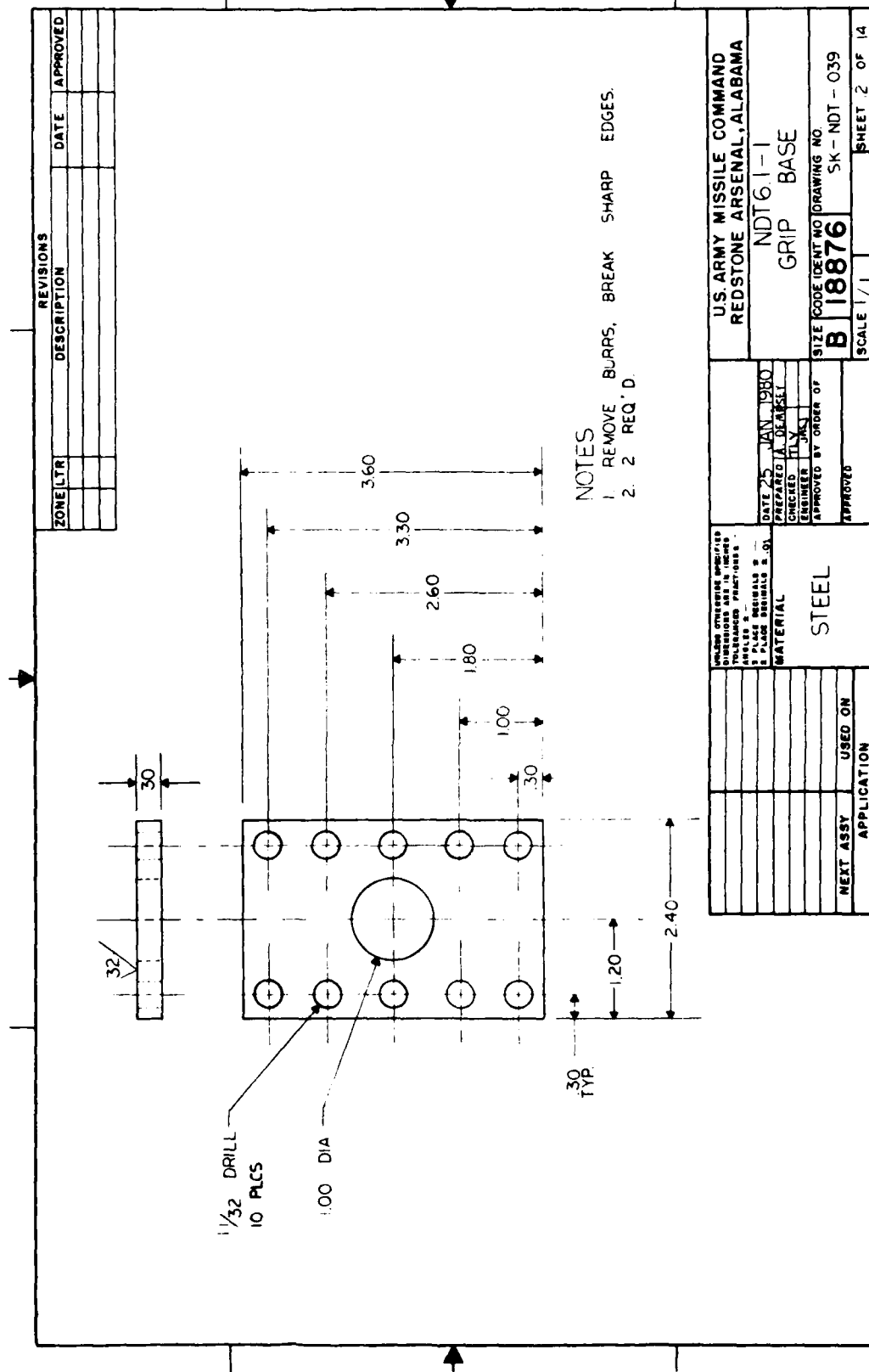


Figure A-12

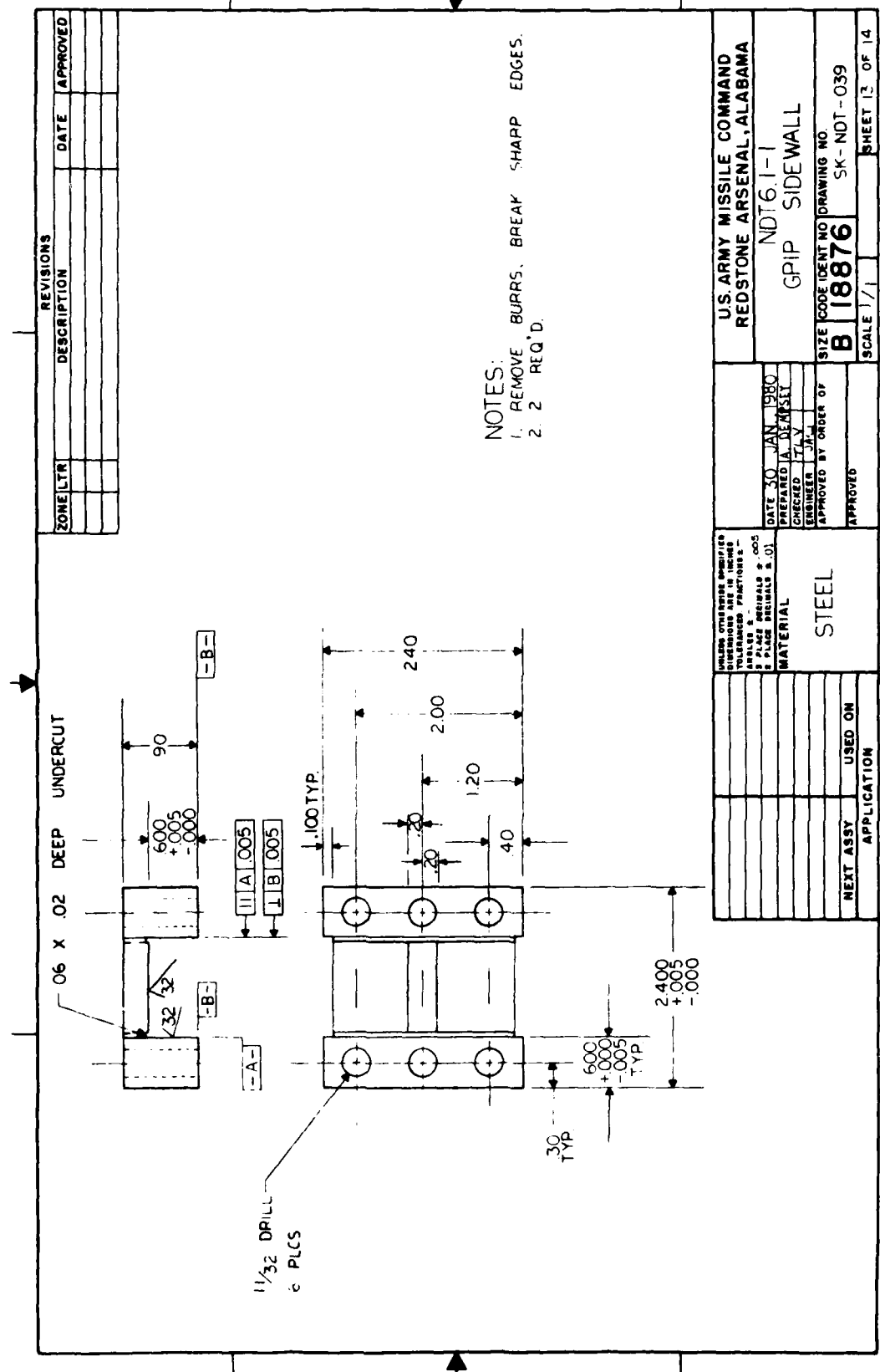


Figure A-13

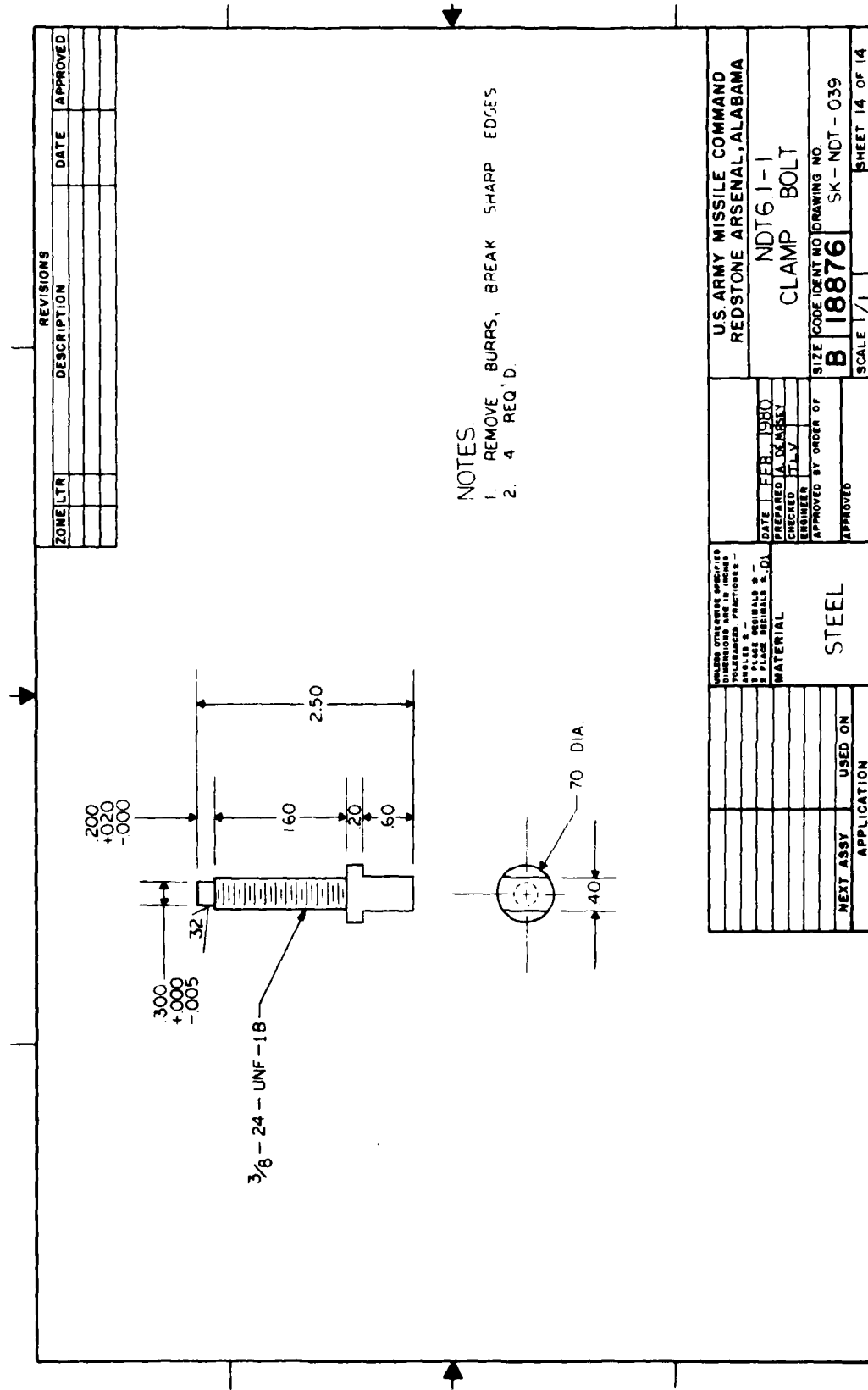


Figure A-14

APPENDIX B

Computer code used to compute the variable quantities of  
Section 2.3.

TABLE B-1

FORTRAN IV      V01C-03A

```

0001      DIMENSION O(8)
0002  1      CONTINUE
0003      A=0.
0004      B=0.
0005      C=0.
0006      D=0.
0007      E=0.
0008      F=0.
0009      G=0.
0010      H=0.
0011      READ(5,2) 0(1),0(2),0(3),0(4),0(5),0(6),0(7),0(8)
0012  2      FORMAT(8F5.0)
0013      DO 3 I=1,8,1
0014      IF(O(I).EQ.0.) GOTO 3
0015      P=O(I)
0016      X=FLOAT(I-1)
0017      A=A+(P*X*X)
0018      B=B+(P*X)
0019      C=C+P
0020      D=D+(X*X*X*X)
0021      E=E+(X*X*X)
0022      F=F+(X*X)
0023      G=G+X
0024      H=H+1.
0025
0026  3      CONTINUE
0027      Q=D*(F*X-G*X)-E*(E*X-H*X)+F*(E*X-G*X)
0028      R=A*(F*X-H*X)-E*(B*X-H*X)+F*(B*X-G*X)
0029      S=D*(B*X-H*X)-A*(E*X-H*X)+F*(E*X-C*B*X)
0030      T=D*(F*C-B*X)-E*(E*X-C*B*X)+A*(E*X-G*X)
0031      U=R/Q
0032      V=S/Q
0033      W=T/Q
0034      Y=ABS(7.*U+V)
0035      WRITE(5,4) U,V,W,Y
0036  4      FORMAT(' U=',F12.6,' V=',F12.6,' W=',F12.6,
15X,' Y=',F12.6)
0037      GOTO 1
0038      END

```

#### APPENDIX C

This appendix contains thickness data and working stress levels for the flawed and unflawed specimens when loaded in the tension/torsion fixture.

$$\% D \equiv \frac{\sigma_w(\max) - \sigma_w(\min)}{\sigma_w(\text{avg})} \times 100\%$$

$$\% D^* \equiv 2 \cdot \frac{\sigma_w(\max) - \sigma_w(\min)}{\sigma_w(\max) + \sigma_w(\min)} \times 100\%$$

$\sigma_w$   $\equiv$  Specimen Stress Level

TABLE C-1    0° WRAP ANGLE SPECIMEN THICKNESS MEASUREMENTS AND  
WORKING STRESS LEVELS

SPECIMEN NUMBER	SPECIMEN THICKNESS	SPECIMEN STRESS LEVEL
1	.0652 in.	1736.1 psi
2	.0658 in.	1720.2 psi
3	.0652 in.	1736.1 psi
4	.0652 in.	1736.1 psi
5	.0661 in.	1712.4 psi
6	.0652 in.	1736.1 psi
7	.0669 in.	1692.0 psi
8	.0658 in.	1720.2 psi

% D = 2.55%  
% D\* = 2.57%

TABLE C-2 + 15° WRAP ANGLE SPECIMEN THICKNESS MEASUREMENTS  
AND WORKING STRESS LEVELS

SPECIMEN NUMBER	SPECIMEN THICKNESS	SPECIMEN STRESS LEVEL
1	.0660 in.	1715.0 psi
2	.0658 in.	1720.2 psi
3	.0658 in.	1720.2 psi
4	.0654 in.	1730.8 psi
5	.0656 in.	1725.5 psi
6	.0662 in.	1709.8 psi
7	.0661 in.	1712.4 psi
8	.0648 in.	1746.8 psi

% D = 2.14%  
% D\* = 2.14%

TABLE C-3 + 20° WRAP ANGLE SPECIMEN THICKNESS MEASUREMENTS  
AND WORKING STRESS LEVELS

SPECIMEN NUMBER	SPECIMEN THICKNESS	SPECIMEN STRESS LEVEL
1	.0664 in.	1704.7 psi
2	.0642 in.	1763.1 psi
3	.0643 in.	1760.4 psi
4	.0656 in.	1725.5 psi
5	.0643 in.	1760.4 psi
6	.0666 in.	1699.6 psi
7	.0651 in.	1738.7 psi
8	.0645 in.	1754.9 psi

% D = 3.65%  
% D\* = 3.66%

TABLE C-4 + 30° WRAP ANGLE SPECIMEN THICKNESS AND WORKING STRESS LEVELS.

SPECIMEN NUMBER	SPECIMEN THICKNESS	SPECIMEN STRESS LEVEL
1	.0668 in.	1694.5 psi
2	.0649 in.	1744.1 psi
3	.0648 in.	1746.8 psi
4	.0639 in.	1771.4 psi
5	.0660 in.	1715.0 psi
6	.0657 in.	1722.9 psi
7	.0640 in.	1768.6 psi
8	.0651 in.	1738.7 psi

% D = 4.42%

% D\* = 4.43%

TABLE C-5 + 45<sup>0</sup> WRAP ANGLE SPECIMEN THICKNESS MEASUREMENTS  
AND WORKING STRESS LEVELS

SPECIMEN NUMBER	SPECIMEN THICKNESS	SPECIMEN STRESS LEVEL
1	.0646 in.	1752.2 psi
2	.0662 in.	1709.8 psi
3	.0656 in.	1725.5 psi
4	.0658 in.	1720.2 psi
5	.0647 in.	1749.5 psi
6	.0638 in.	1774.2 psi
7	.0672 in.	1684.4 psi
8	.0670 in.	1689.4 psi

% D = 5.20%  
% D\* = 5.19%

TABLE C-6 + 60° WRAP ANGLE SPECIMEN THICKNESS MEASUREMENTS  
AND WORKING STRESS LEVELS

SPECIMEN NUMBER	SPECIMEN THICKNESS	SPECIMEN STRESS LEVEL
1	.0637 in.	1770.0 psi
2	.0639 in.	1771.4 psi
3	.0645 in.	1754.9 psi
4	.0623 in.	1816.9 psi
5	.0632 in.	1791.0 psi
6	.0629 in.	1799.6 psi
7	.0597 in.	1896.0 psi
8	.0629 in.	1799.6 psi

% D = 7.83%  
% D\* = 7.72%

TABLE C-7  $0^{\circ}$  WRAP ANGLE UNFLAWED SPECIMEN THICKNESS MEASUREMENTS

SPECIMEN NUMBER	SPECIMEN THICKNESS
A	.0660 in.
B	.0668 in.
C	.0668 in.
D	.0663 in.
E	.0672 in.

TABLE C-8  $\pm 15^{\circ}$  WRAP ANGLE UNFLAWED SPECIMEN THICKNESS MEASUREMENTS

SPECIMEN NUMBER	SPECIMEN THICKNESS
A	.0652 in.
B	.0650 in.
C	.0649 in.
D	.0651 in.
E	.0653 in.

TABLE C-9  $\pm 20^{\circ}$  WRAP ANGLE UNFLAWED SPECIMEN THICKNESS MEASUREMENTS

SPECIMEN NUMBER	SPECIMEN THICKNESS
A	.0668 in.
B	.0645 in.
C	.0666 in.
D	.0655 in.
E	.0651 in.

TABLE C-10  $\pm 30^{\circ}$  WRAP ANGLE UNFLAWED SPECIMEN THICKNESS MEASUREMENTS

SPECIMEN NUMBER	SPECIMEN THICKNESS
A	.0640 in.
B	.0653 in.
C	.0643 in.
D	.0644 in.
E	.0640 in.

TABLE C-11  $\pm 45^{\circ}$  WRAP ANGLE UNFLAWED SPECIMEN THICKNESS MEASUREMENTS

SPECIMEN NUMBER	SPECIMEN THICKNESS
A	.0652 in.
B	.0668 in.
C	.0658 in.
D	.0643 in.
E	.0649 in.

TABLE C-12  $\pm 60^{\circ}$  WRAP ANGLE UNFLAWED SPECIMEN THICKNESS MEASUREMENTS

SPECIMEN NUMBER	SPECIMEN THICKNESS
A	.0632 in.
B	.0619 in.
C	.0648 in.
D	.0609 in.
E	.0633 in.

#### APPENDIX D

This appendix contains photographs of the flawed regions of all the dynamically impacted specimens used in this effort. Both the painted and unpainted sides of each specimen are shown.



Figure D-1.  $n^{\prime}2$  specimen.

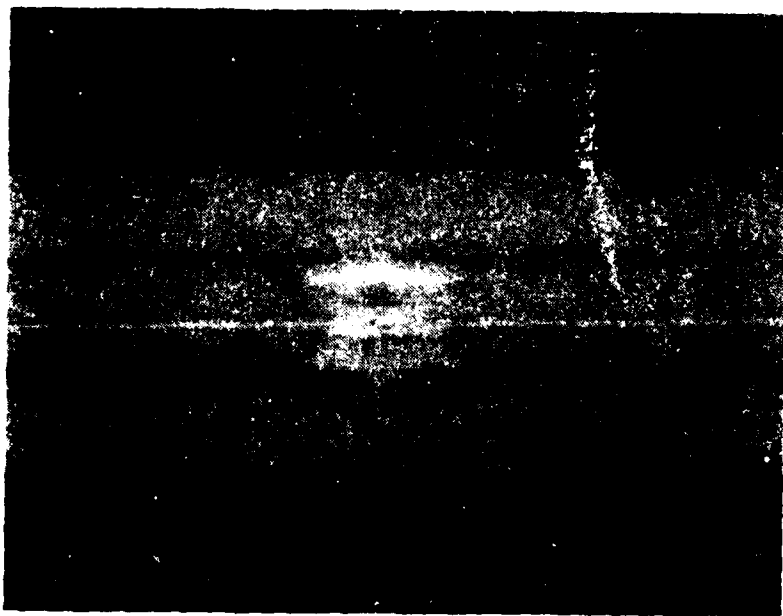


Figure D.1. (Continued)

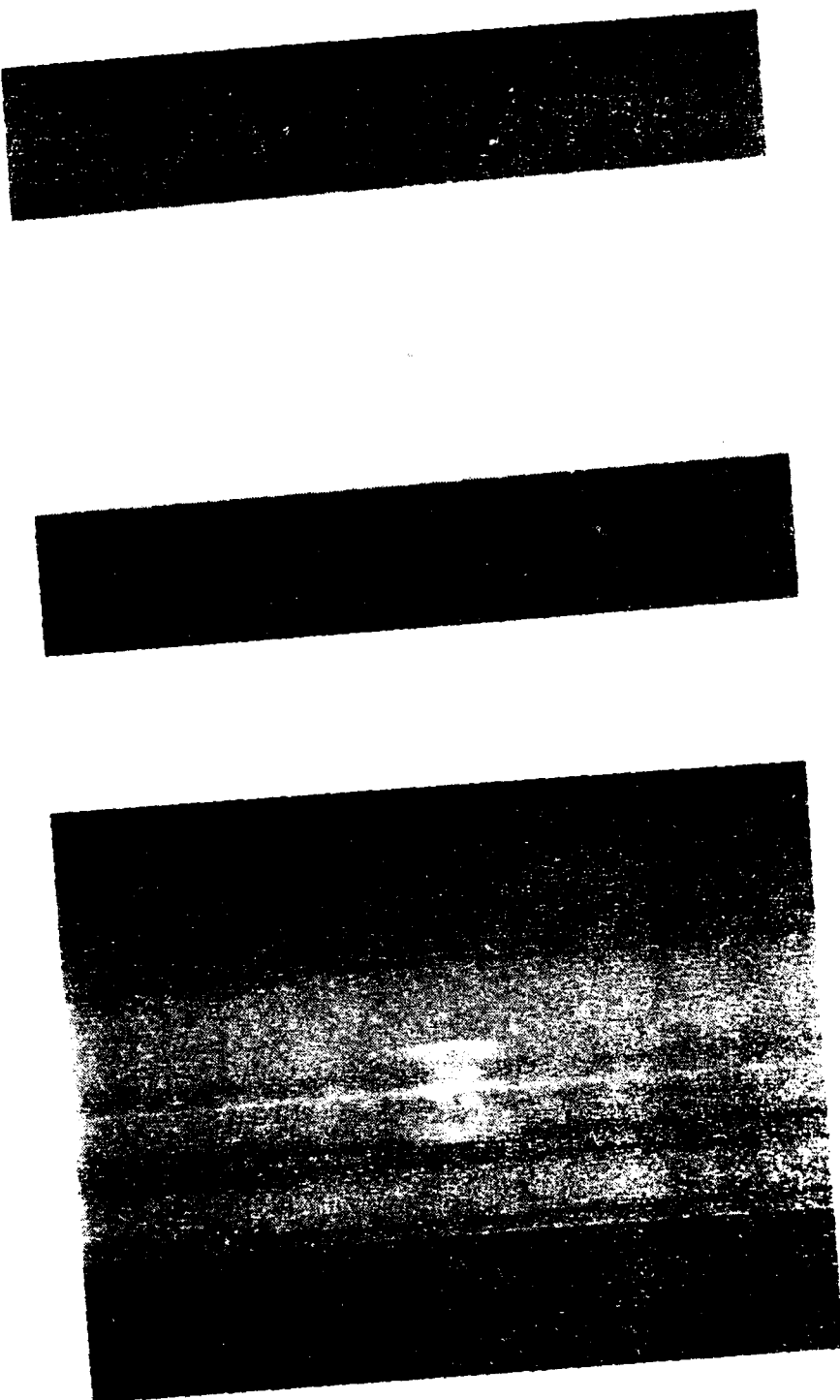


Figure 11-3. *Redacted image*

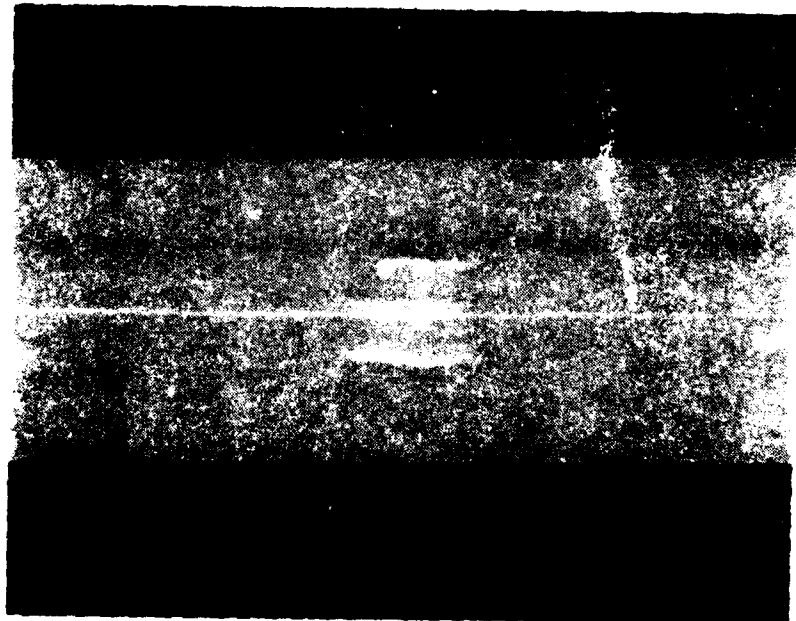


Figure D-4.  $^{106}\text{Ru}$  source from

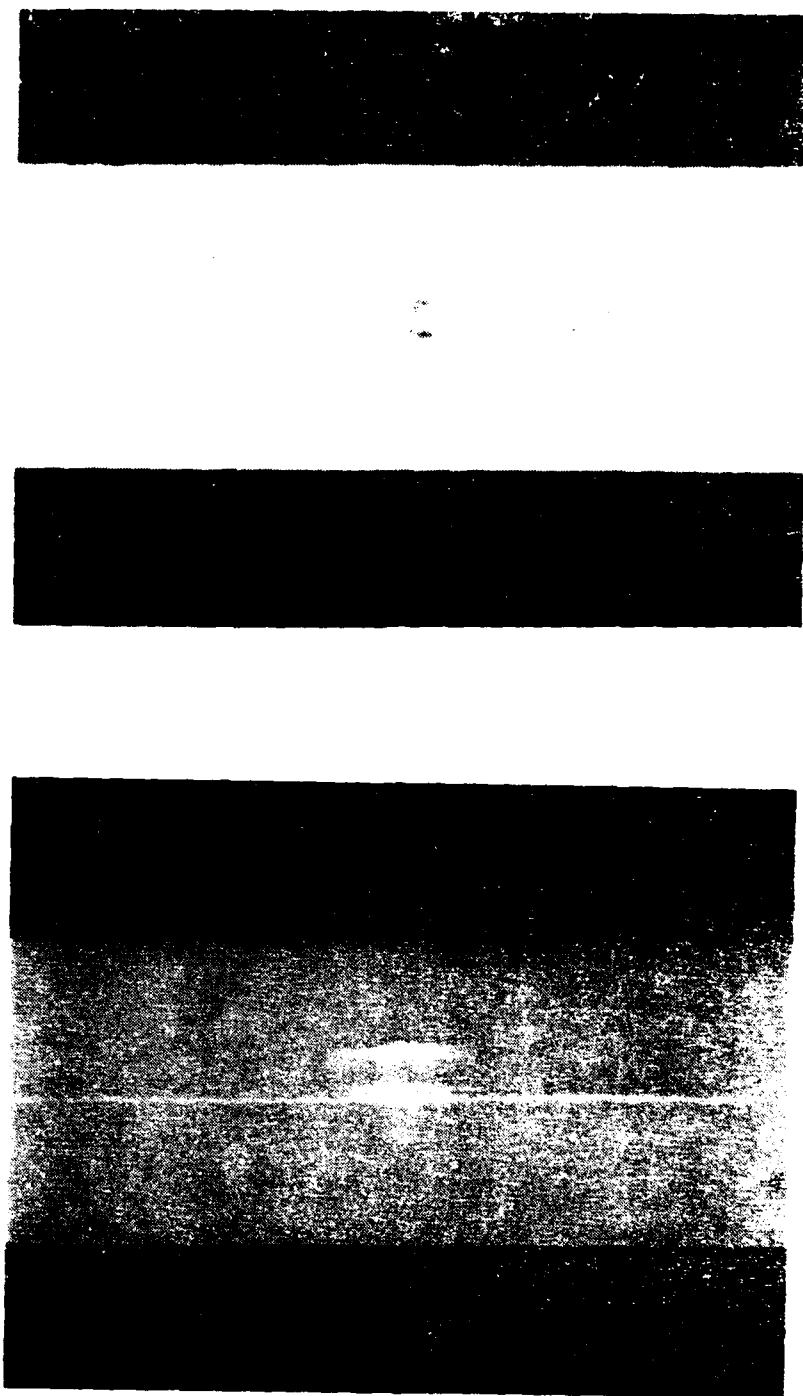


Figure 10.3:  $\psi_{\text{L}}^{(0)}$  spectrum.

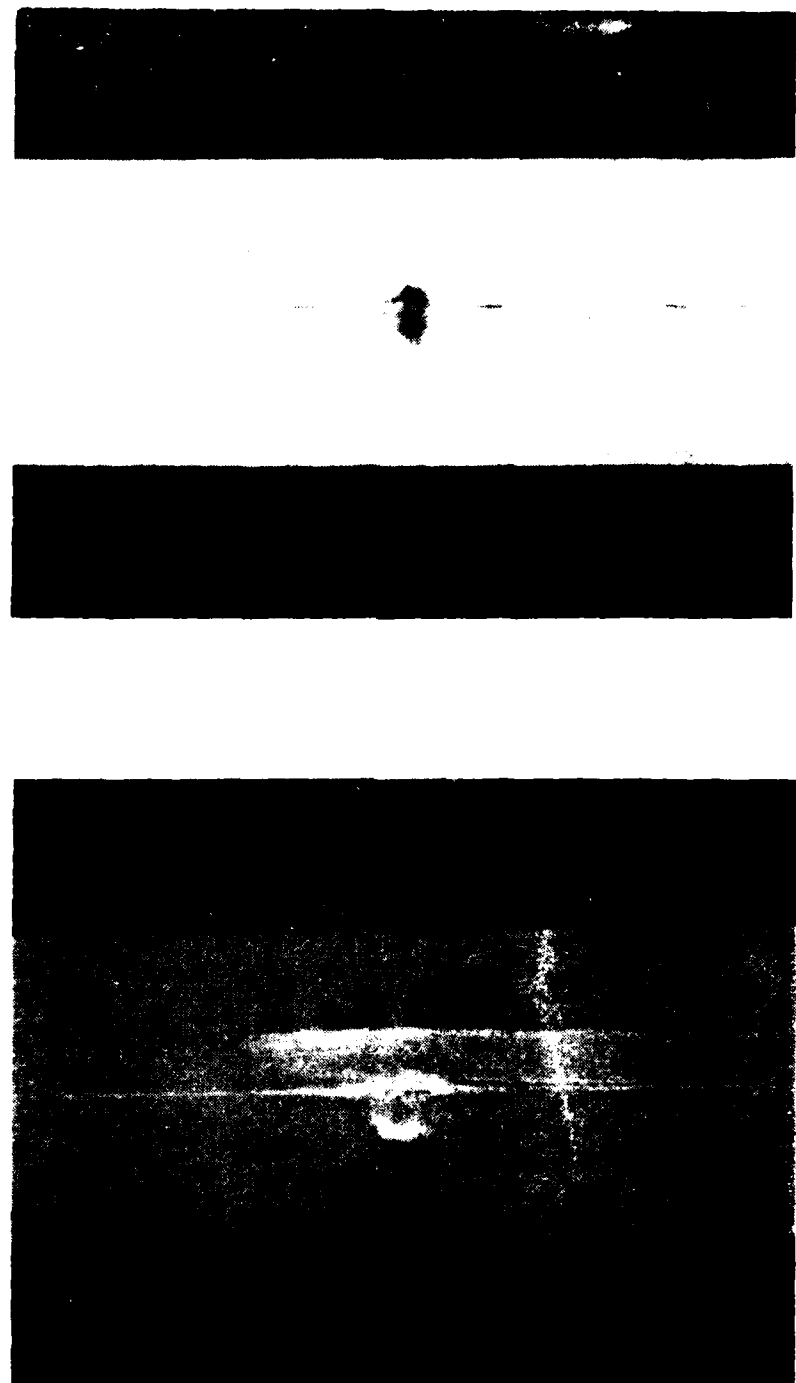


Figure D-6 D<sup>0</sup>-6 specimen.

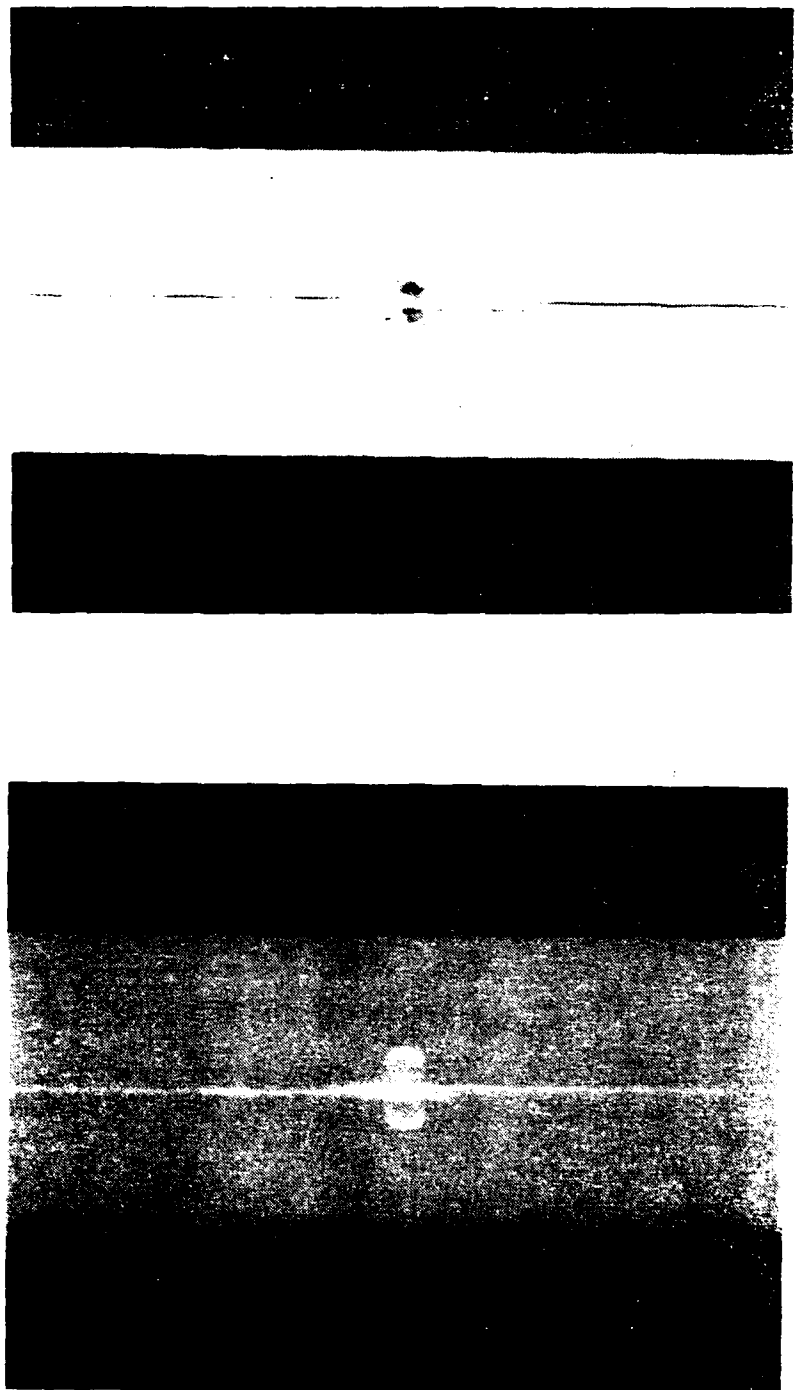


Figure D-1. Sample book.



—

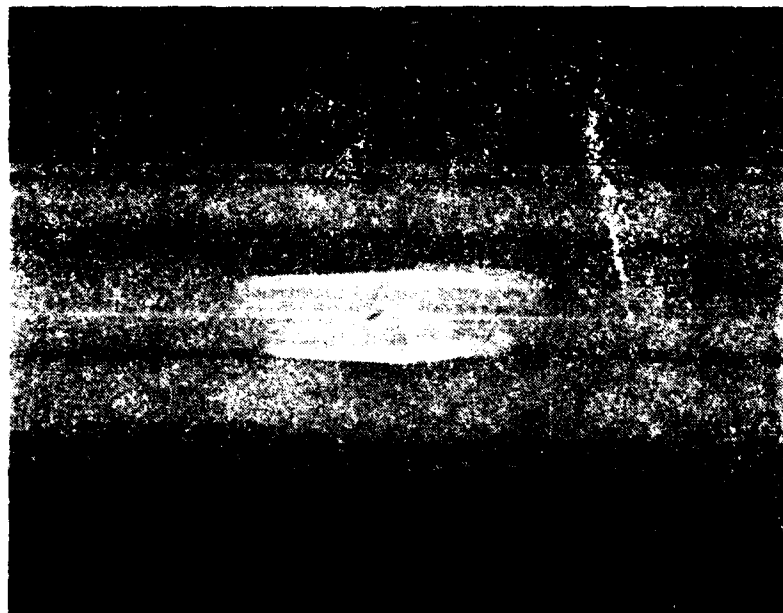


Figure D-8.  $\eta^D_{\text{L}}$  specimen.

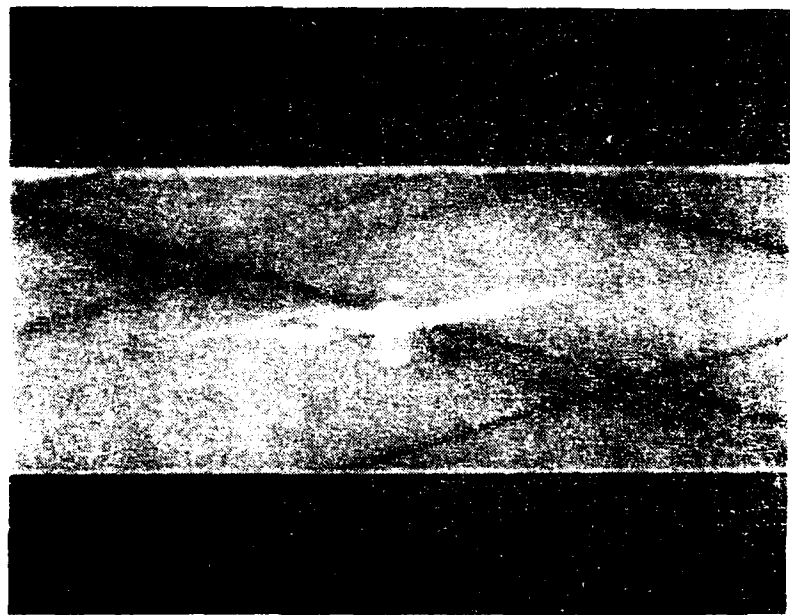
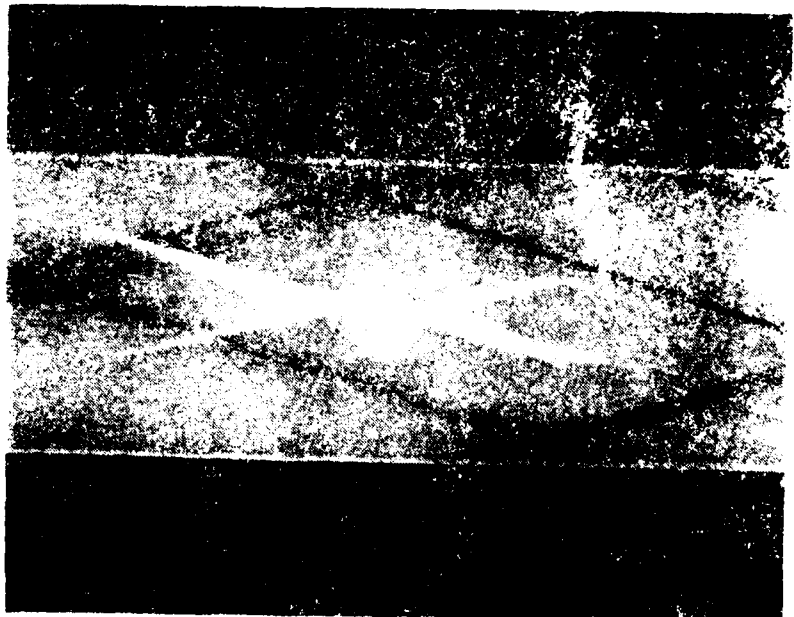


Figure 9-9. (a) A specimen.



Page 1 of 1



Figure 1-11. A gamma ray.

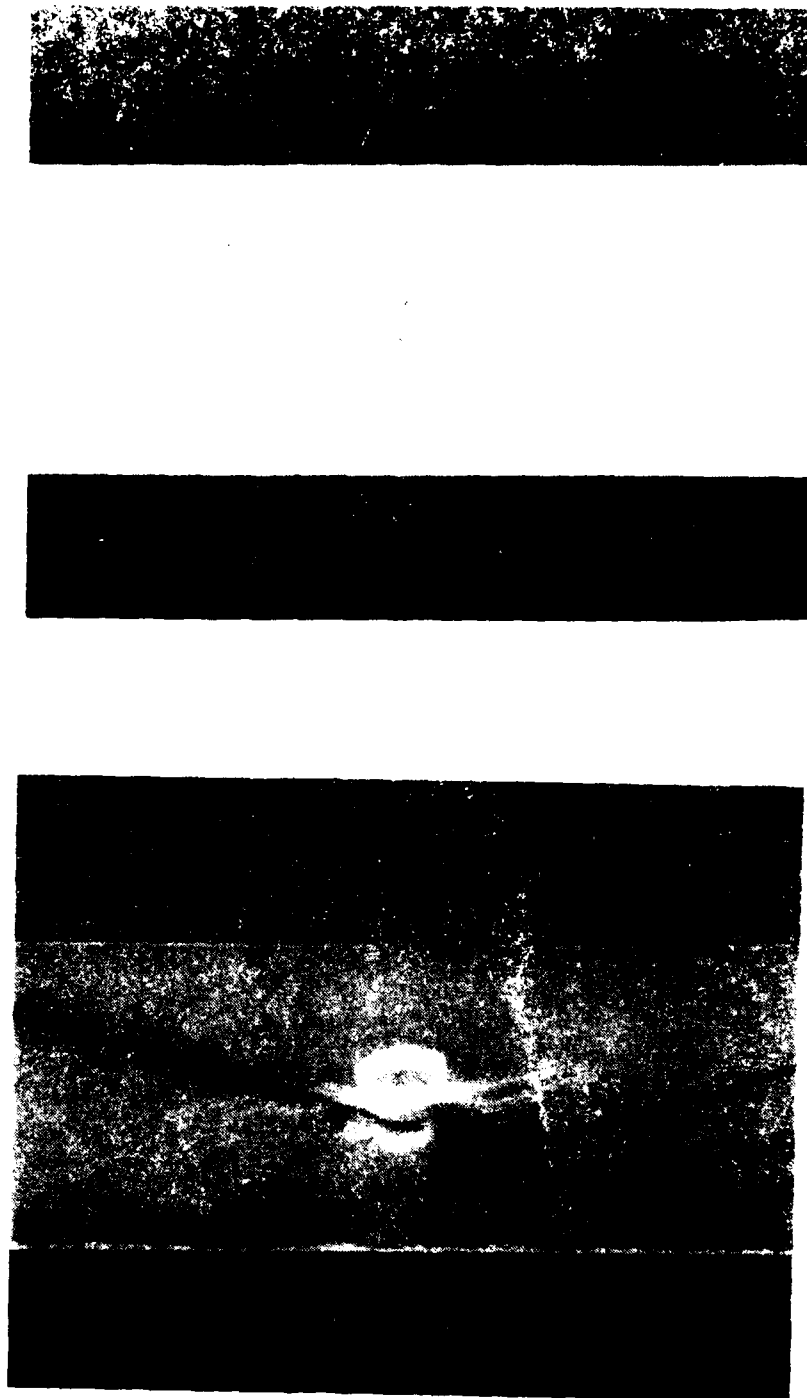
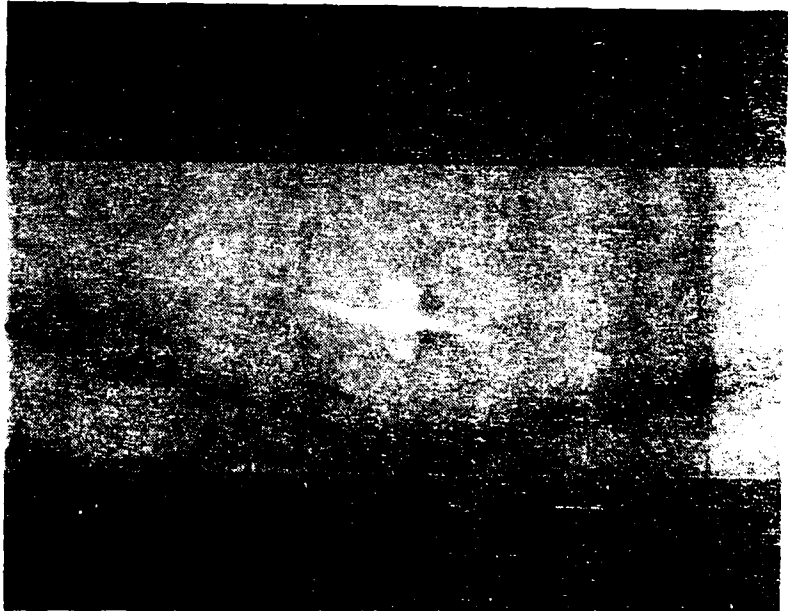


Figure D-12.  $\text{Fe}^{2+}\text{3}$  specimen.



Copyright 2013 by the author.

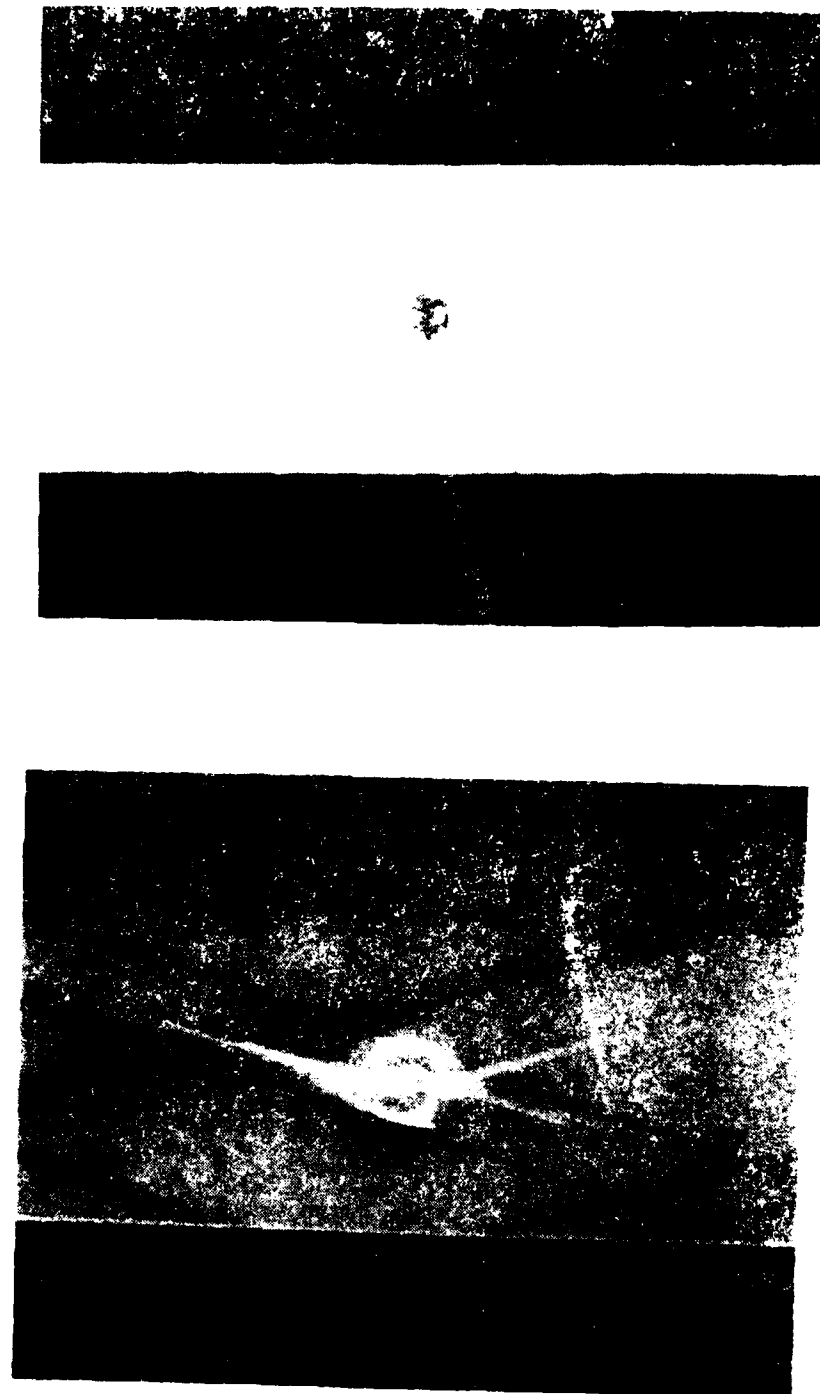


Figure D-11 (b) (5) (D)(1)(B)(i).



•



Figure 11. Redaction boxes.

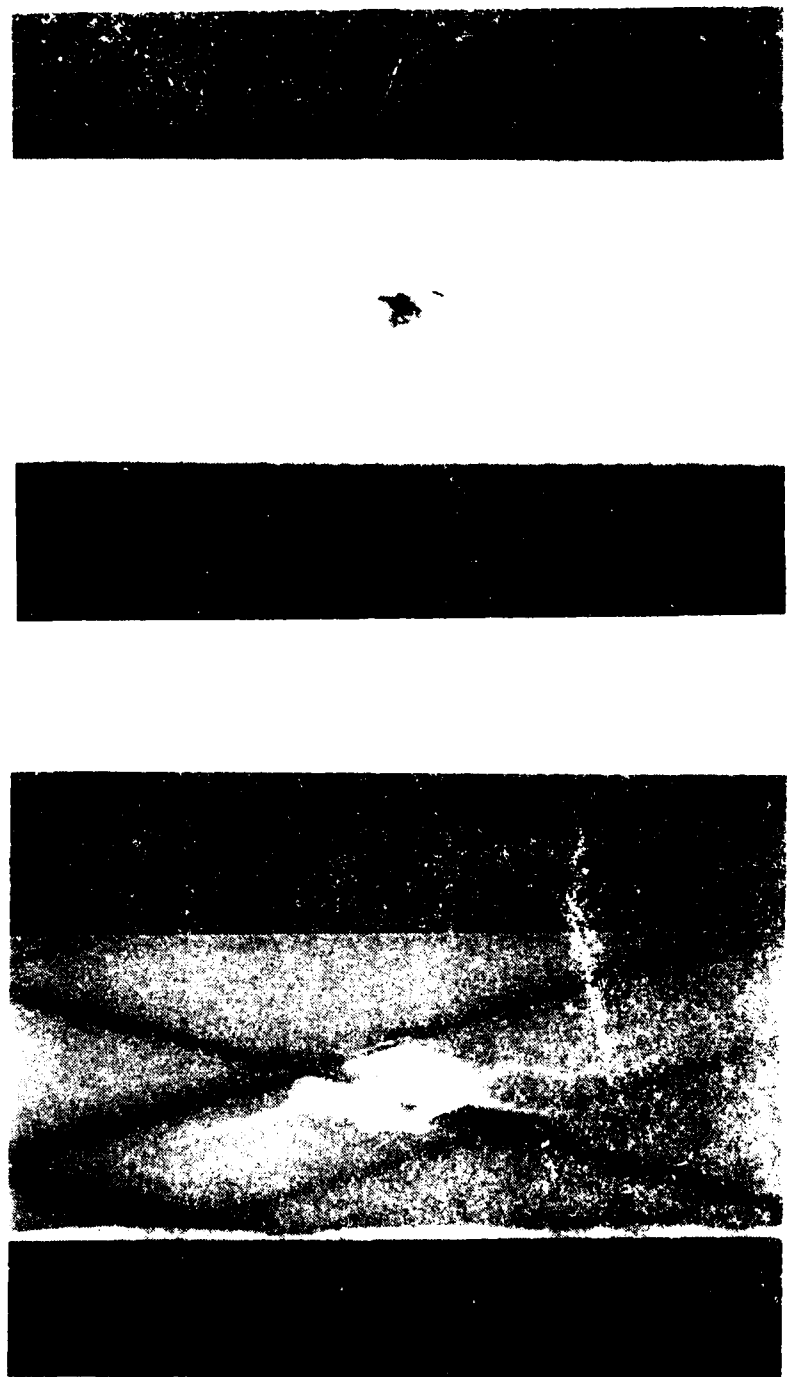


Figure D-10.  $\mu$ CT image of the book.

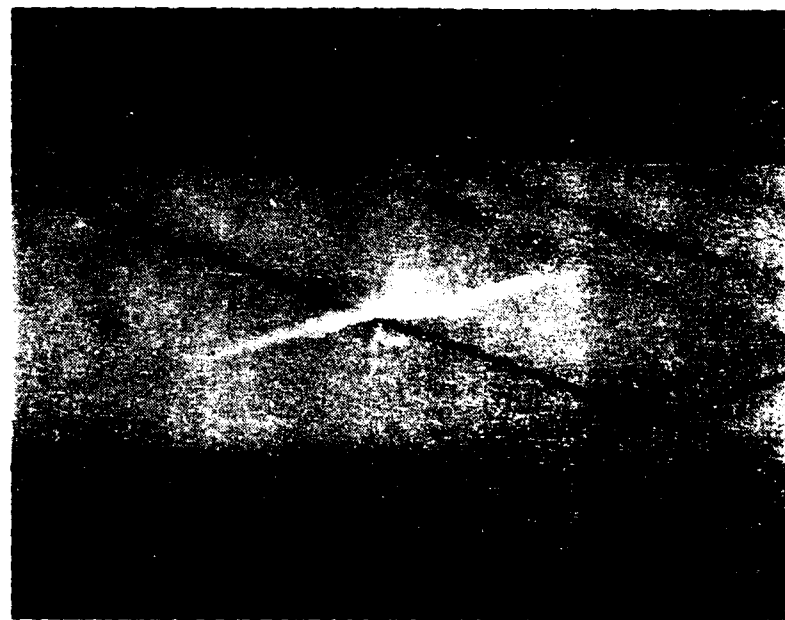


Figure 17. (Continued)



Figure 1.1.1.1. A sprig from

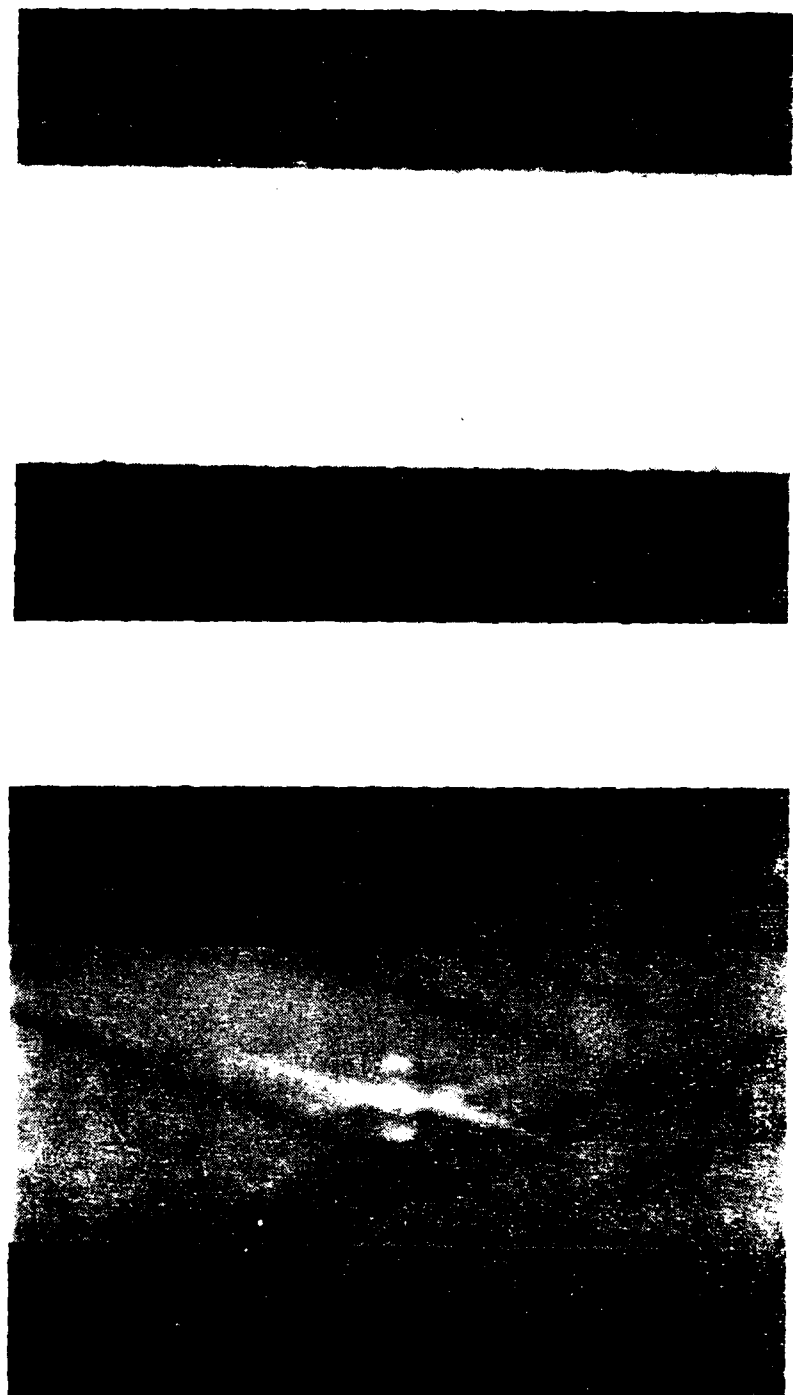


Figure 11. The same image as in Fig. 10.

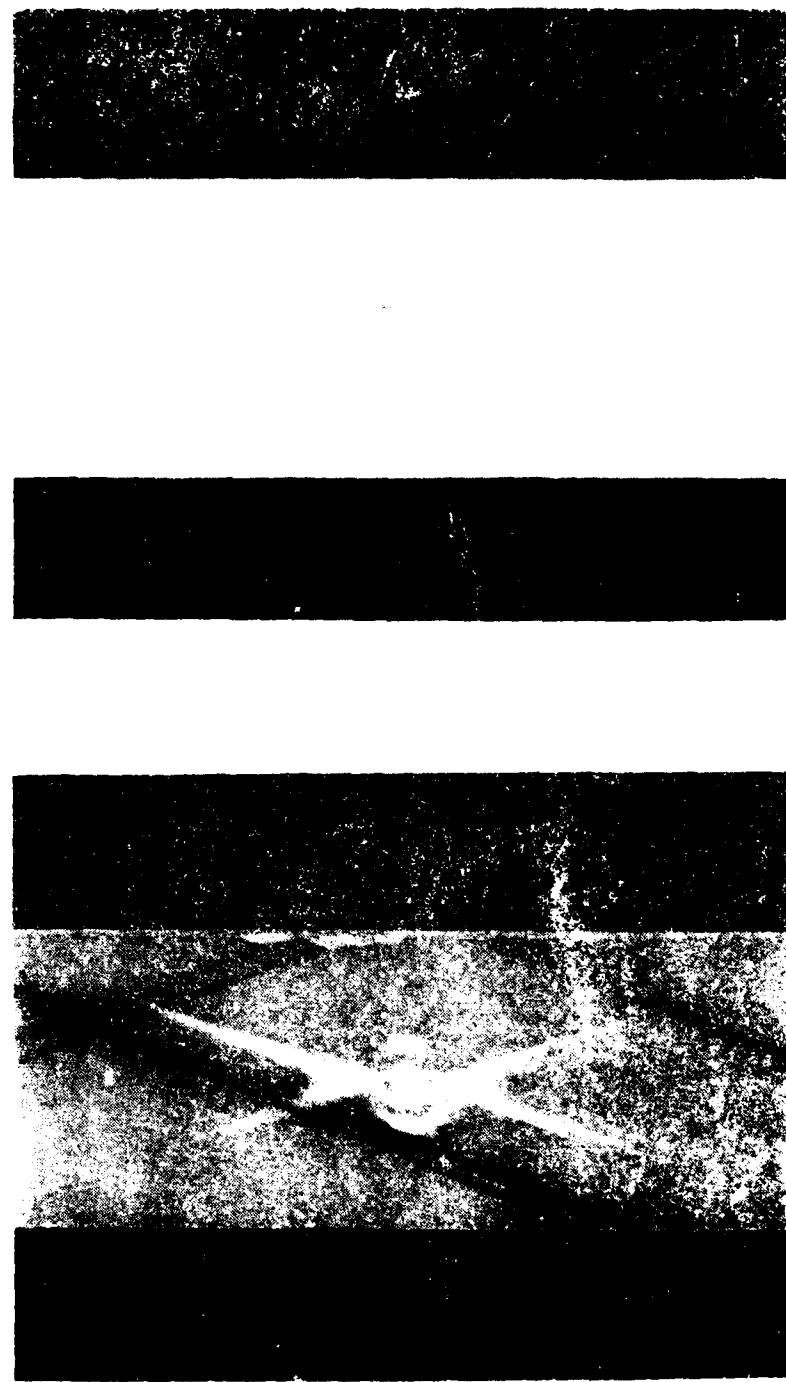


Figure 10. (a) (b) (c)

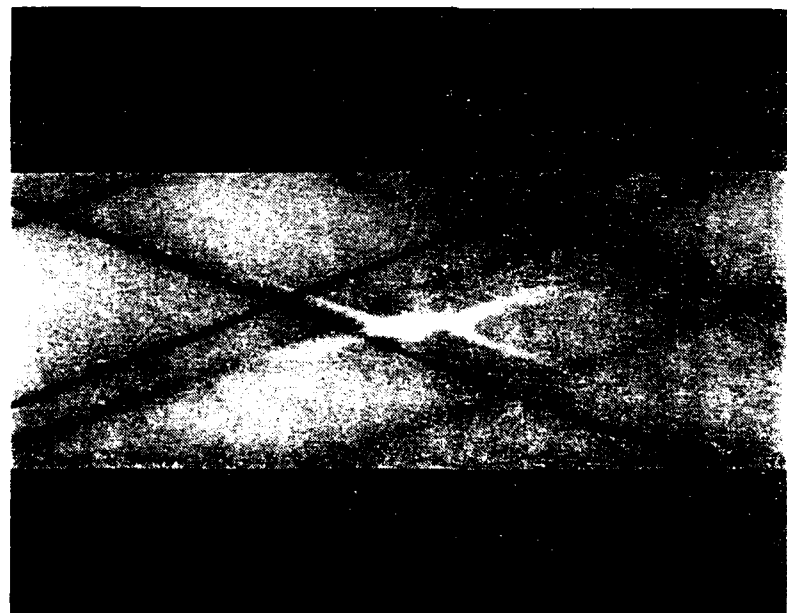
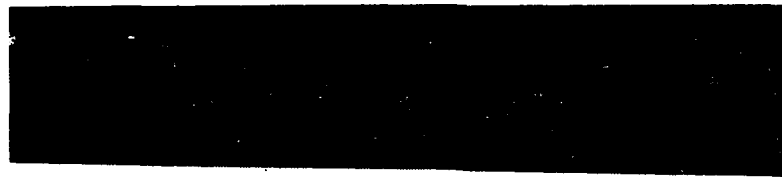


Figure 1. (Top) A redacted page.

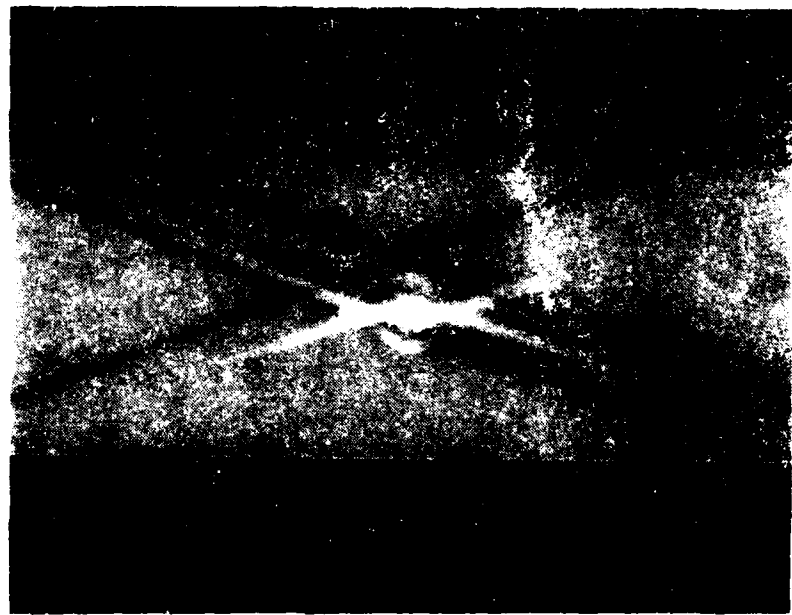


Figure 14.23. The same scene.



1

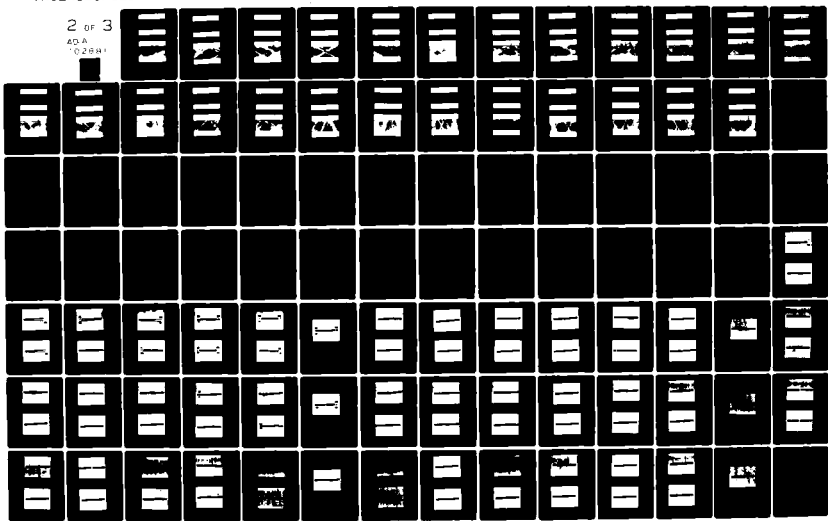


1. *Suppose that*  $\alpha$  *is a*  $\beta$

AD-A102 881 ARMY MISSILE COMMAND REDSTONE ARSENAL AL GROUND EQU--ETC F/G 11/4  
QUANTITATIVE ANALYSIS OF IMPACT DAMAGED COMPOSITE TENSION-TORSI--ETC(U)  
SEP 80 J A SCHAEFFEL  
UNCLASSIFIED DRSMI/RL-80-12-TR

NL

2 of 3  
40A  
02641



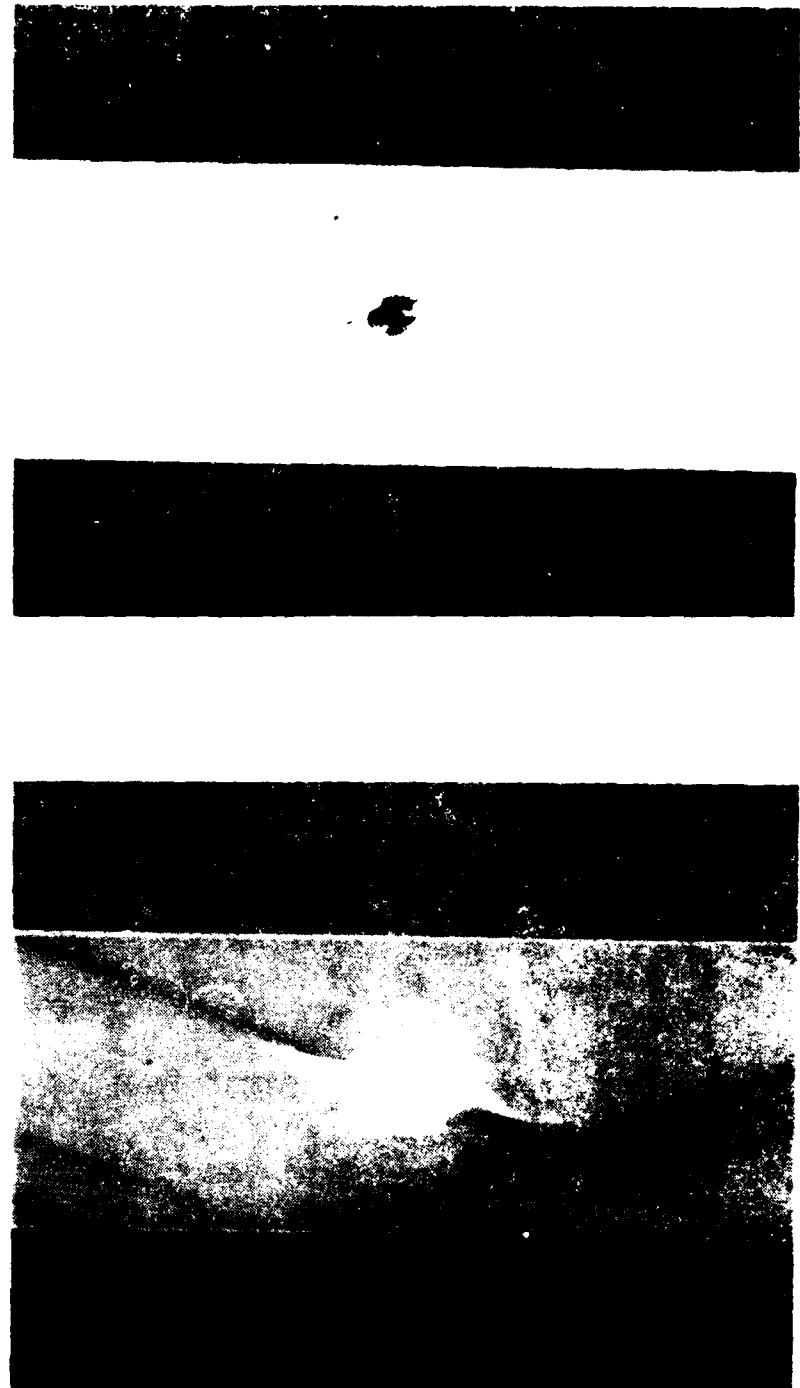


Figure D-24 -  $\alpha\beta\gamma$  specimen.



Figure 11.20.  $\Delta^2$  vs.  $\Delta$  for  $\alpha = 0.5$ .

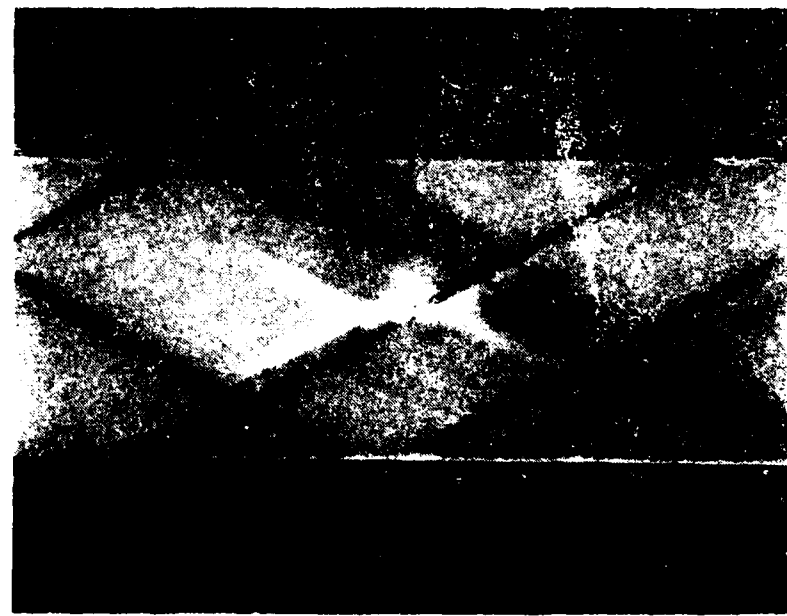


Figure 9-26. A redacted photograph.



Figure 10.  $\delta^{34}\text{S}$  ( $\text{ppm}$ ) vs.  $\delta^{34}\text{S}$  ( $\text{ppm}$ )



Figure D-28.  $\beta_1^{(0)} = 1.0 \text{ cm}.$

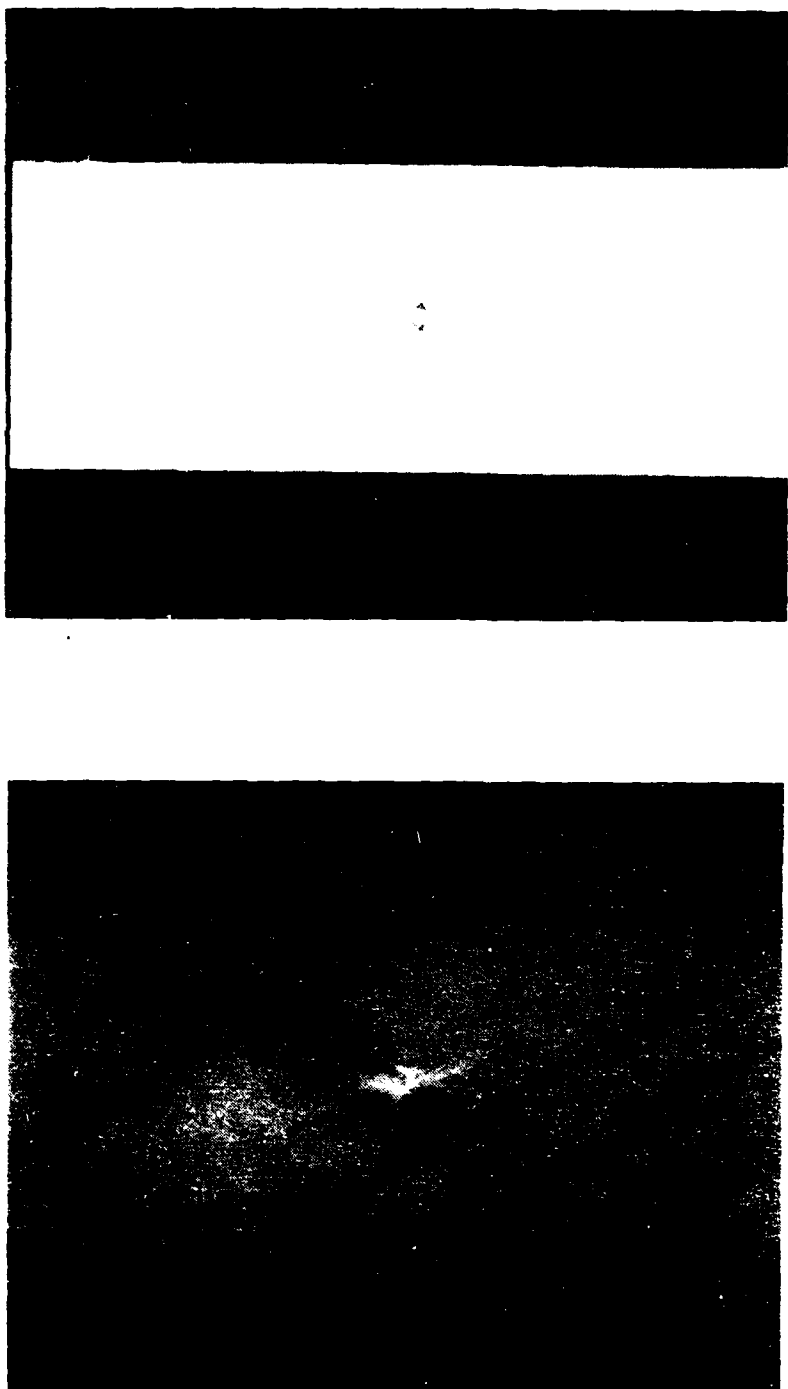


Figure 10.  $\text{D}_{\text{100}}$  of the  $\text{PVC}/\text{C}_6\text{H}_5\text{NO}_2$  blend.

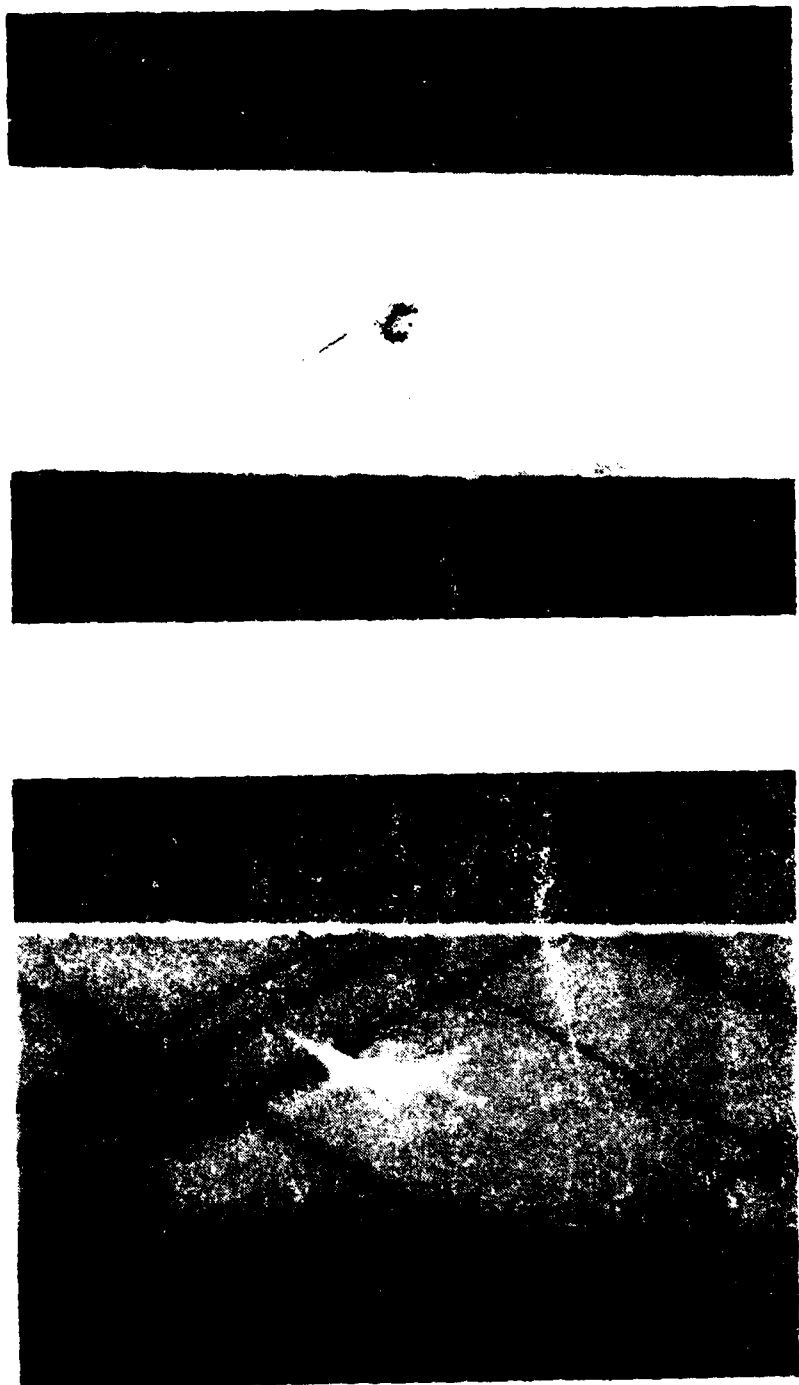


Figure D-30 -  $\text{MgO}$  specimen.

aq



2

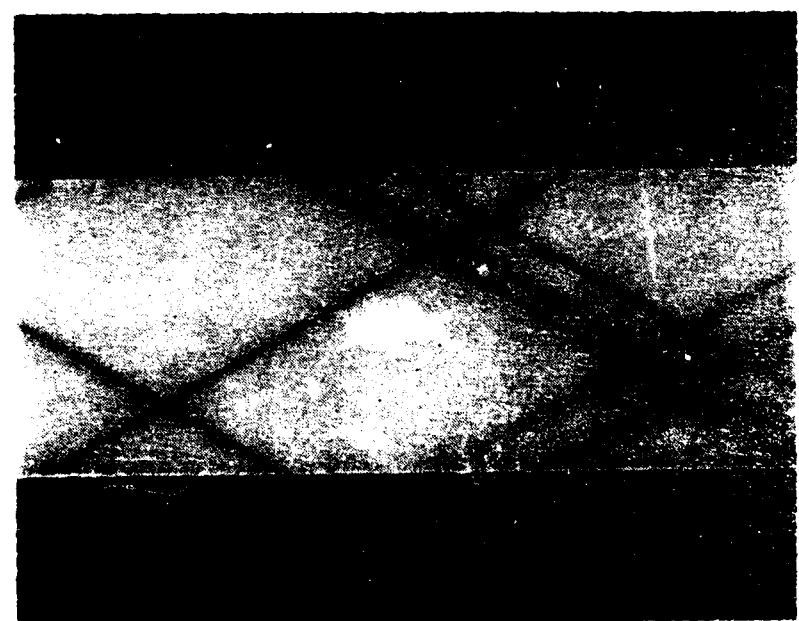


Figure 3-31. Redacted photograph.

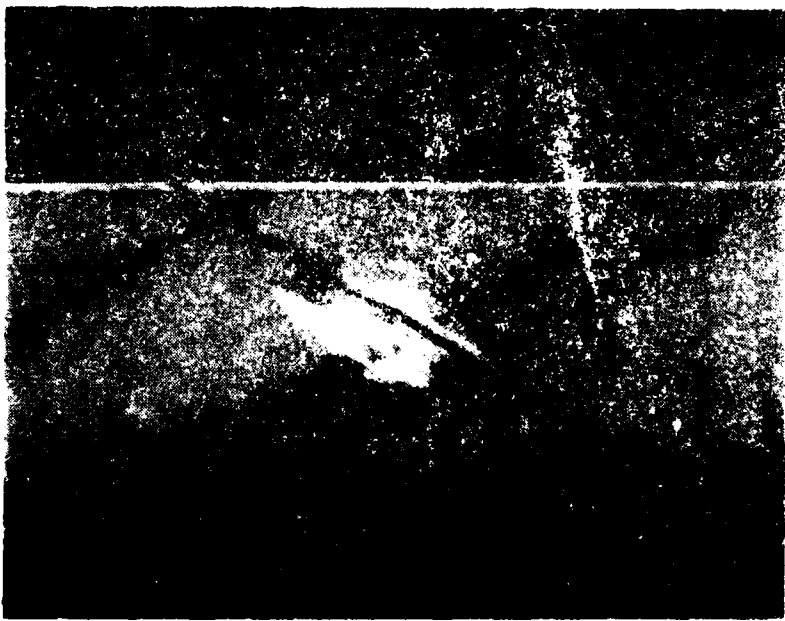


Figure D-32. 40° Specimen.

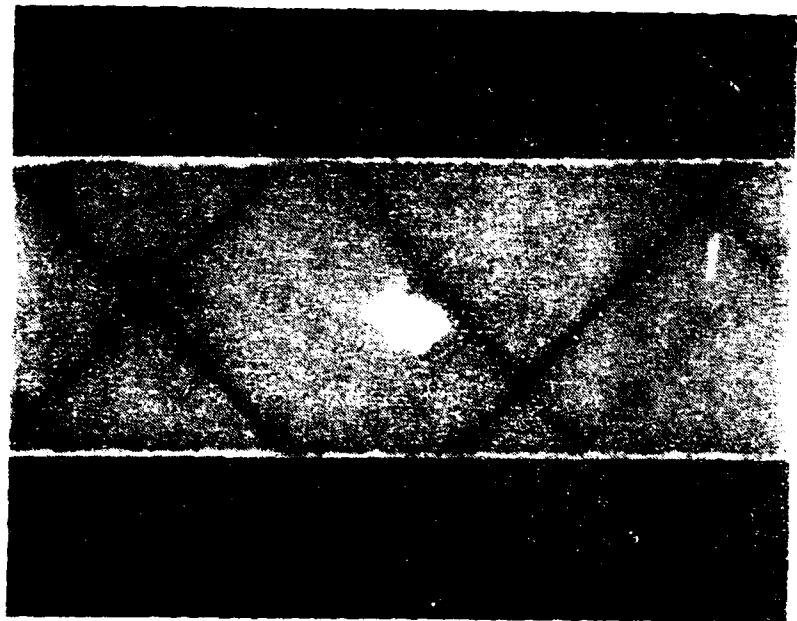


Figure 10.22. Duct tape repair.

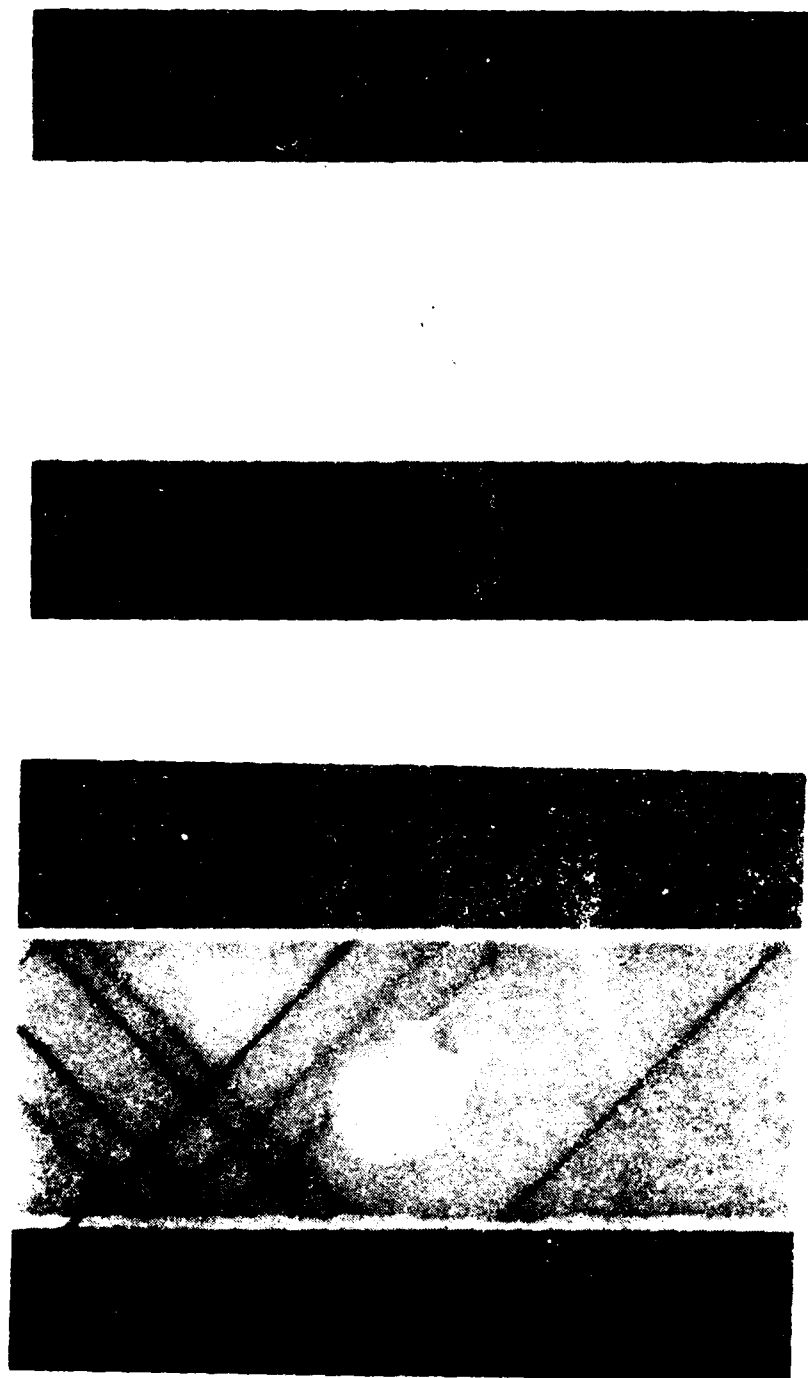
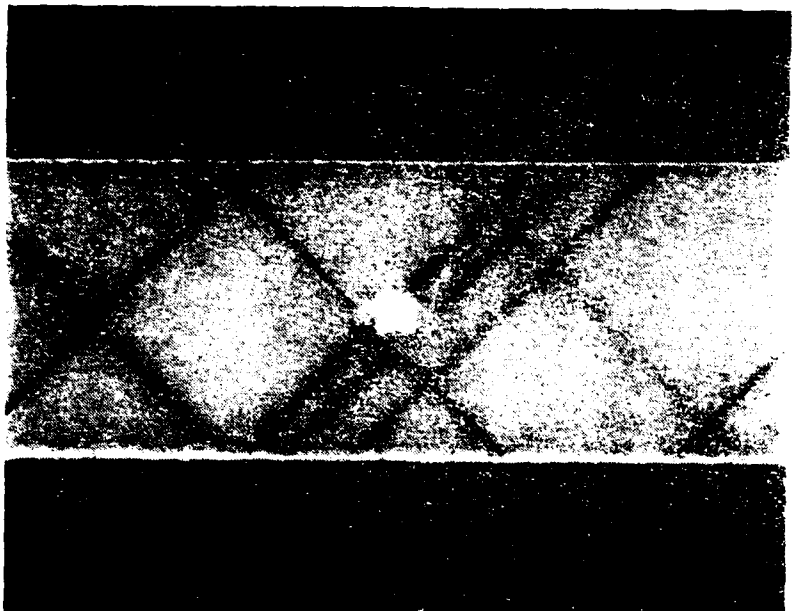
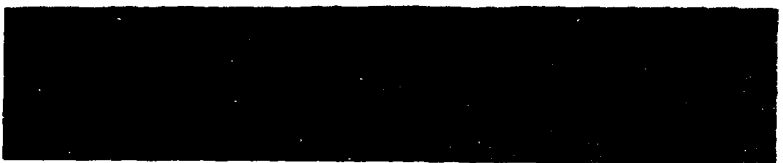


Figure D-33-46% of area.



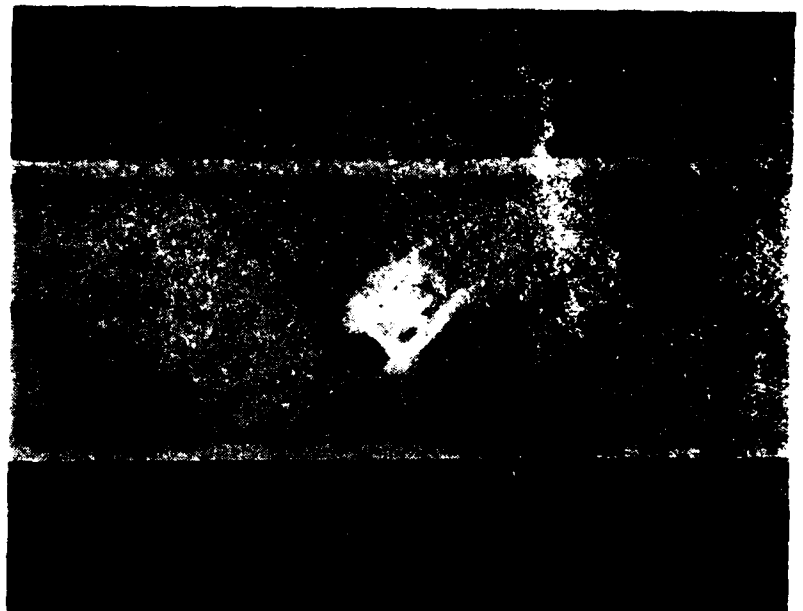


Figure D-36. Redacted image.



2

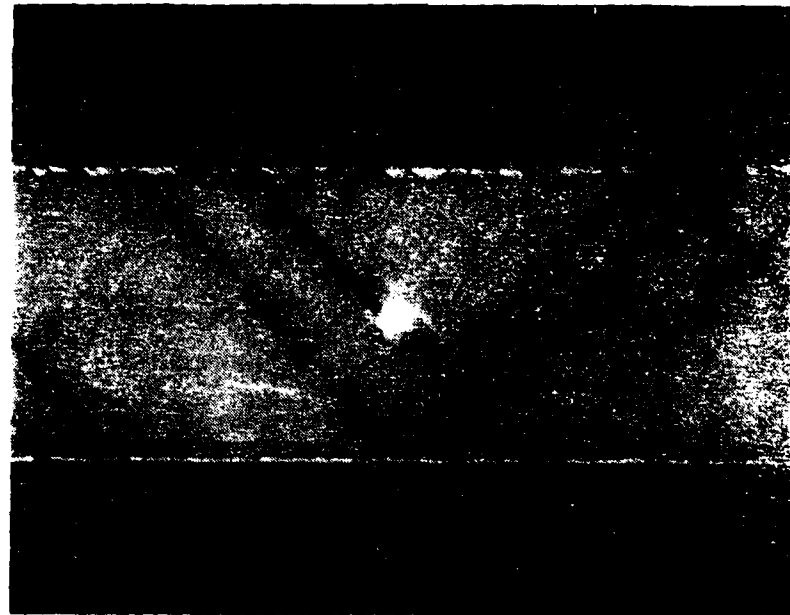


Figure 18.31. *Redacted* images.

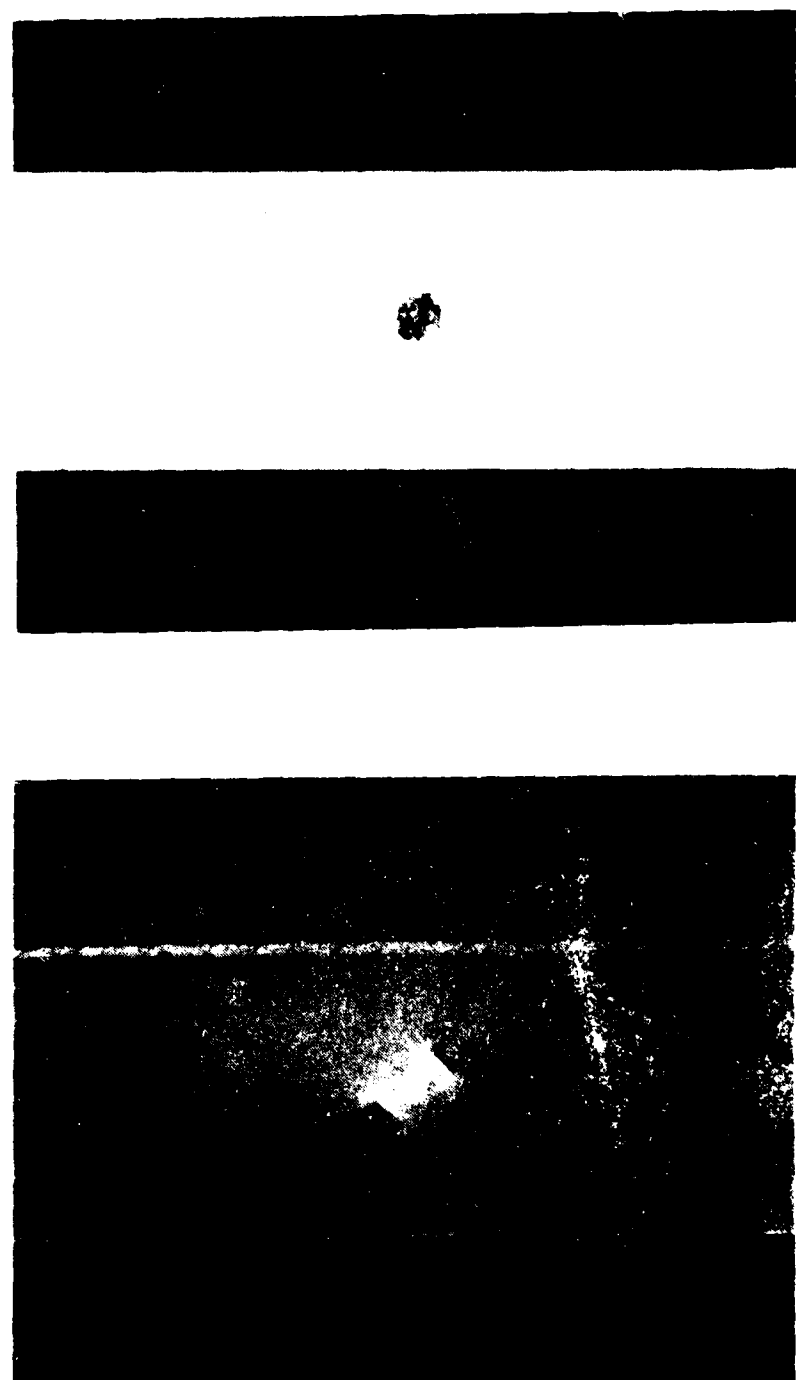


Figure 13.  $10^3$   $\mu$  polymer.

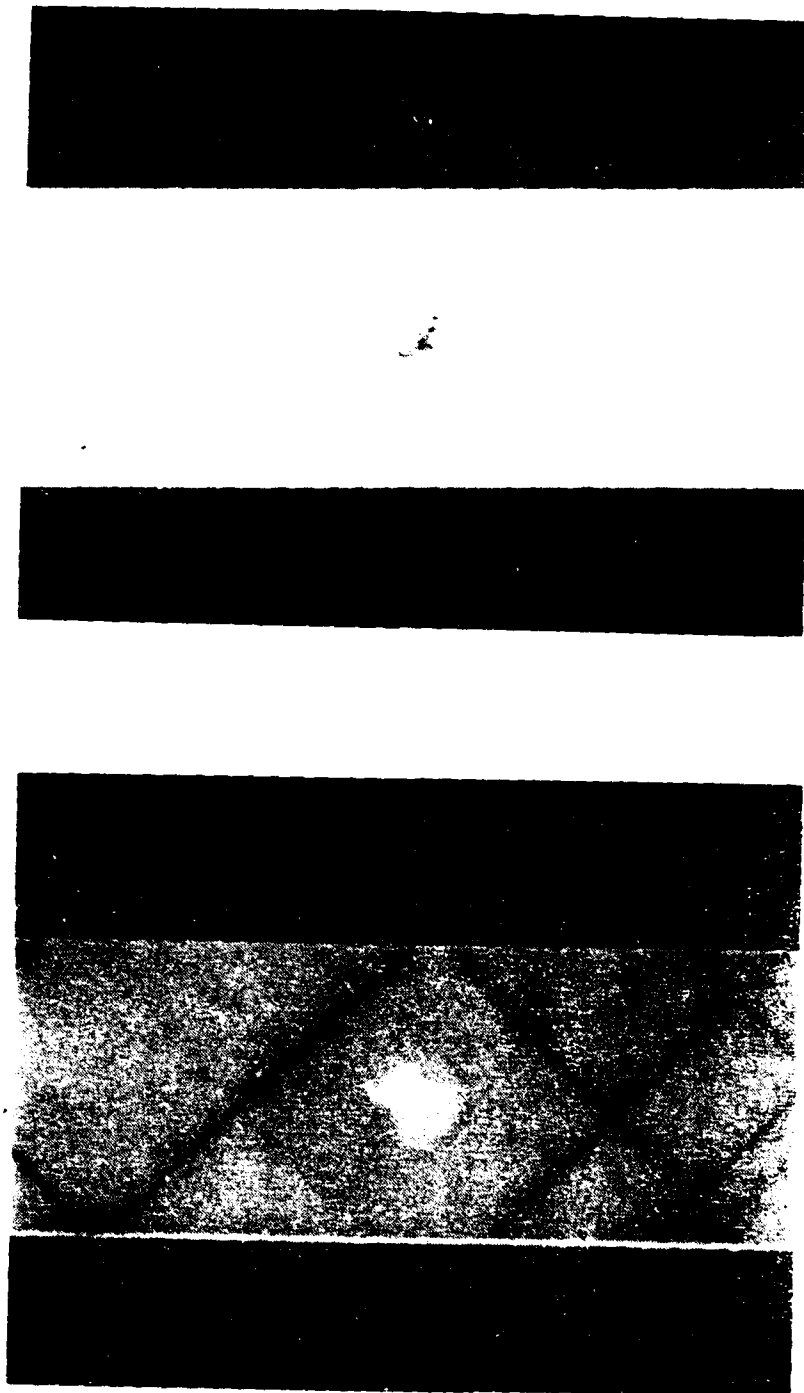


Figure D-39. VLT spectra (cont.)

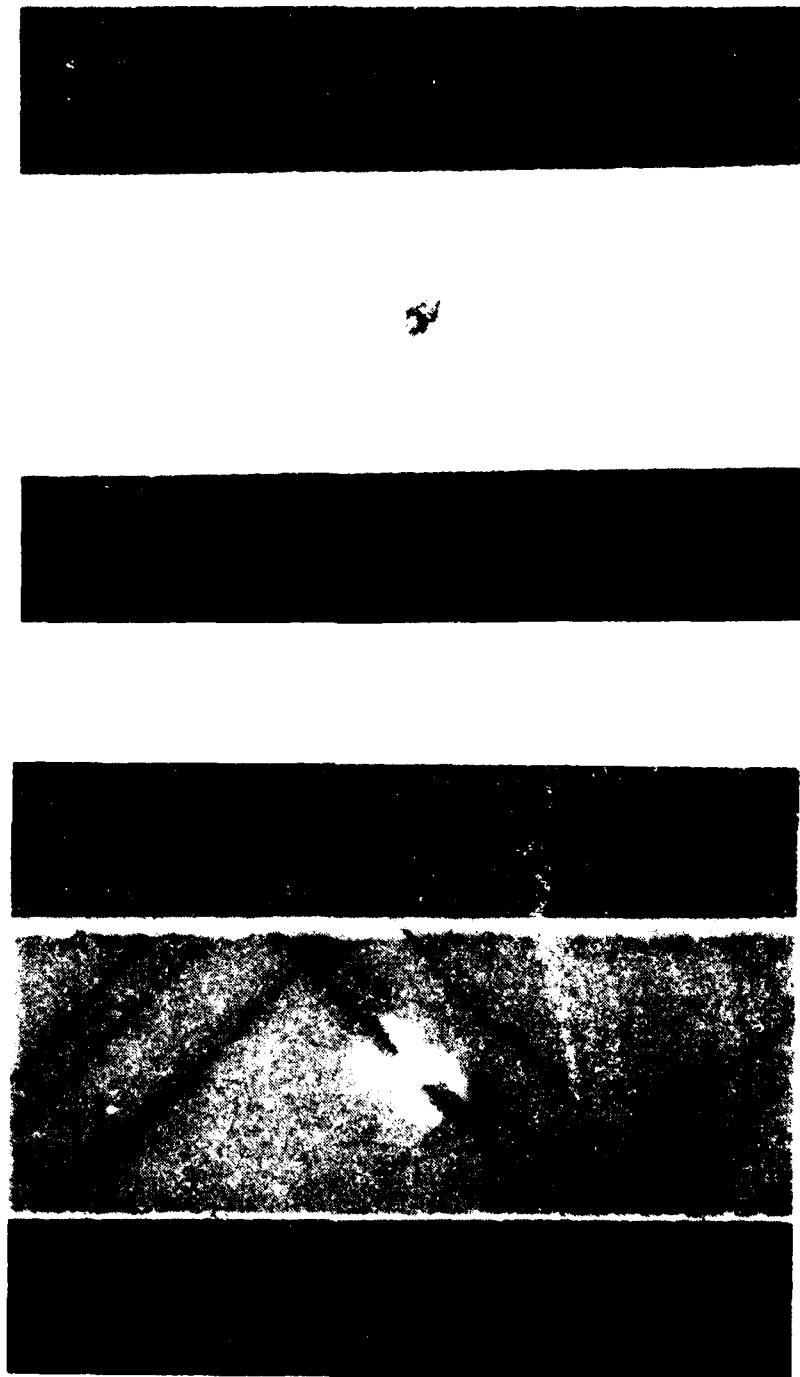


Figure D-40.  $24^{\prime \prime} \times 36^{\prime \prime}$  (continued).

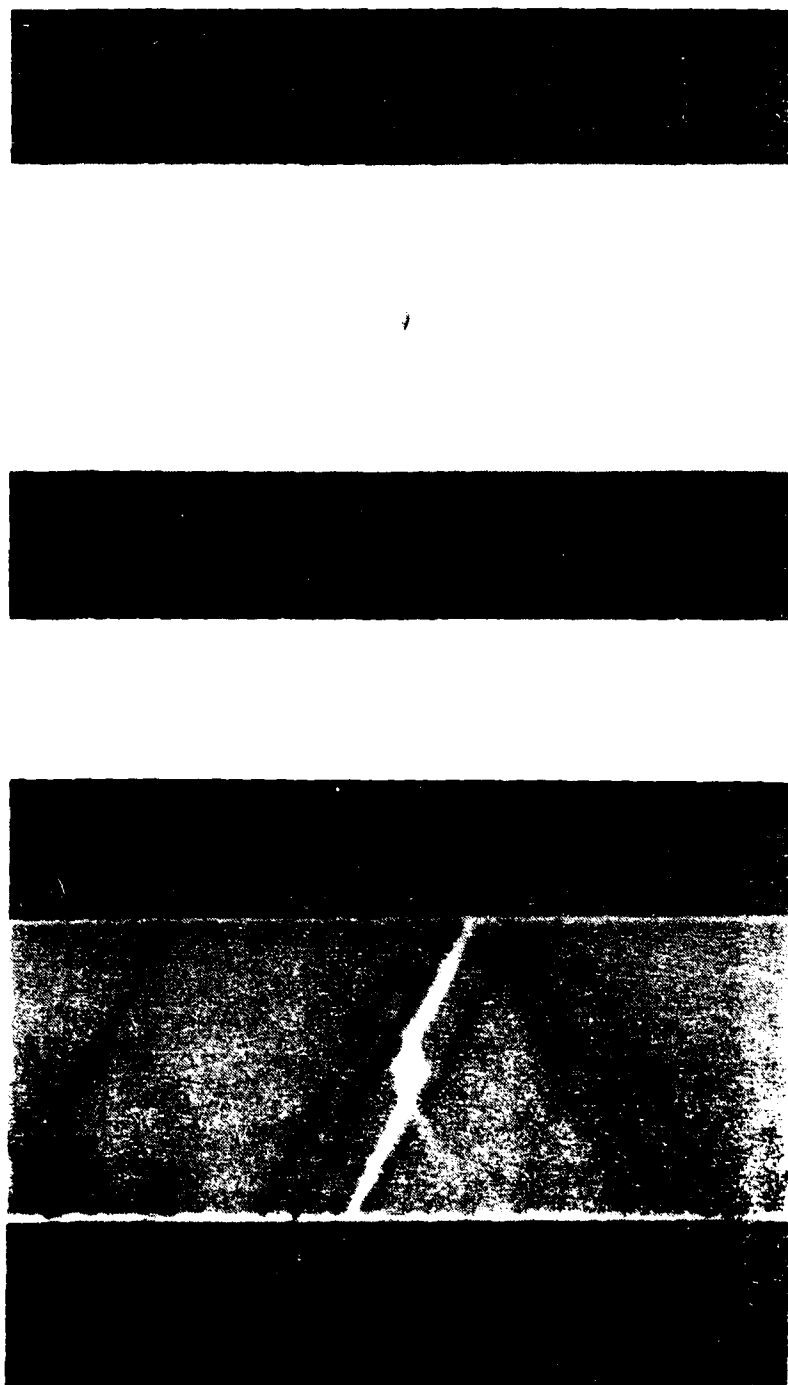


Figure 2. A 10<sup>10</sup> cm<sup>-2</sup> surface.

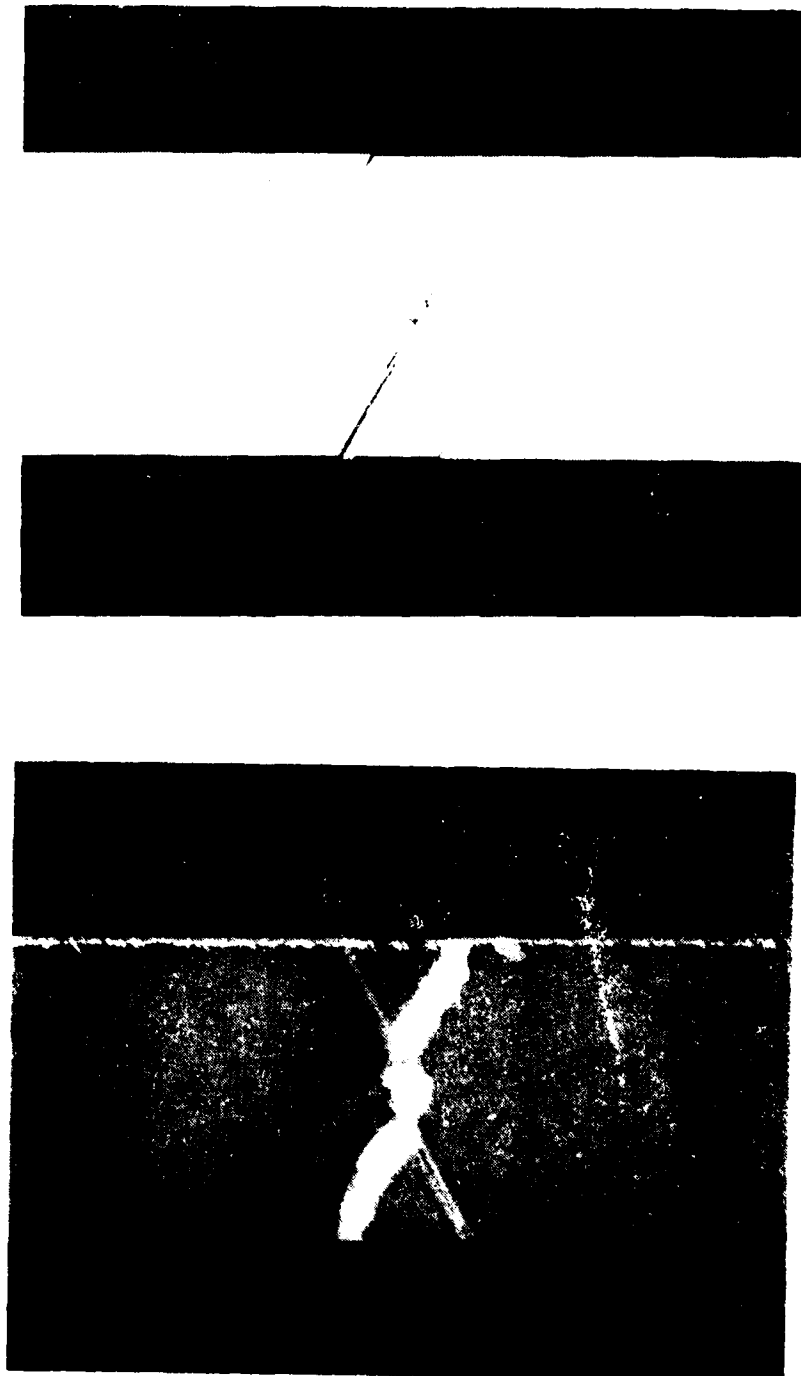


Figure D-62, (a, b, c) (continued)

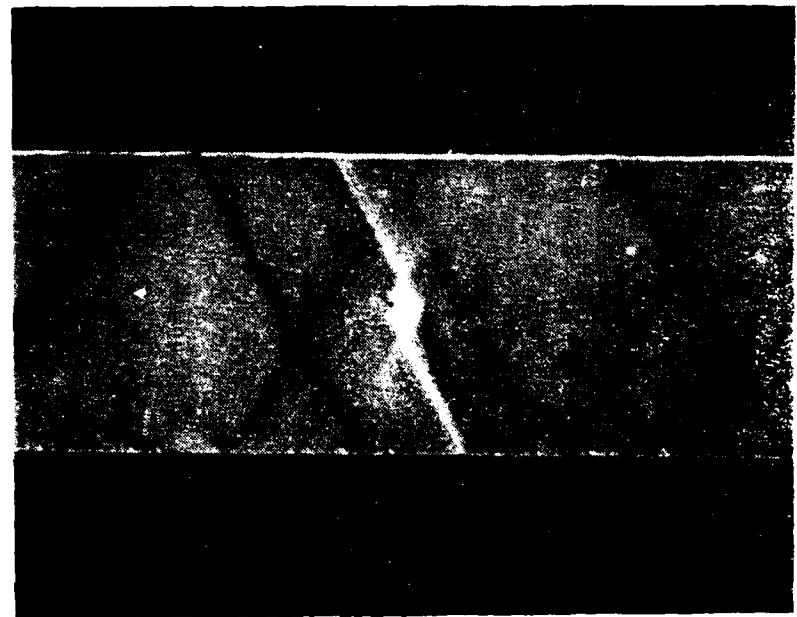
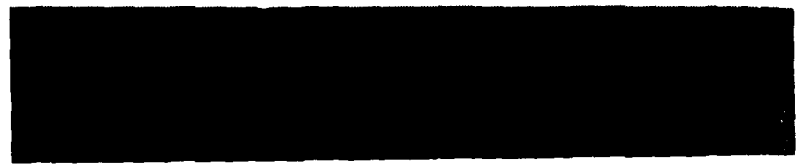


Figure 11.3.  $\mu$ CT specimen.

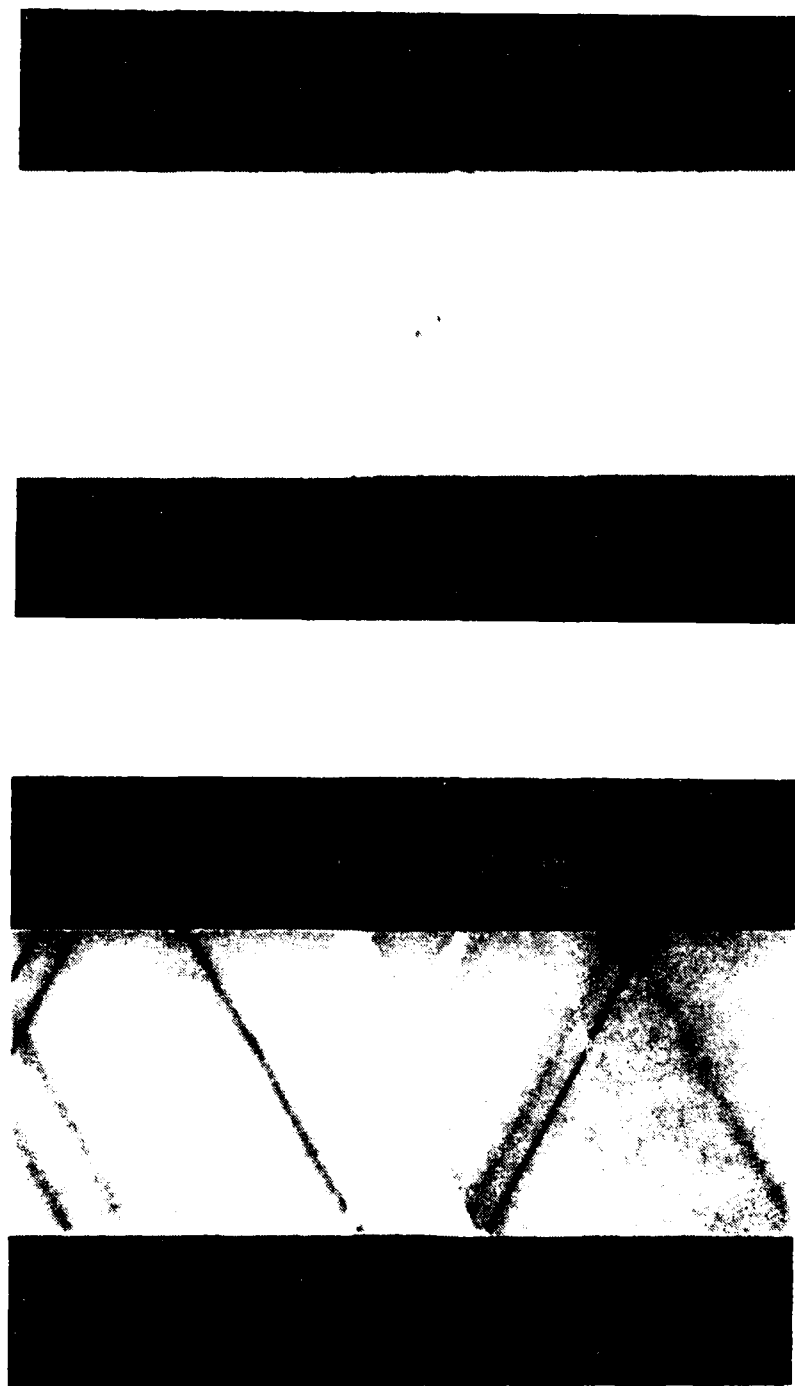


Figure D-40 - 6<sup>th</sup> F. 7 - Specimen.

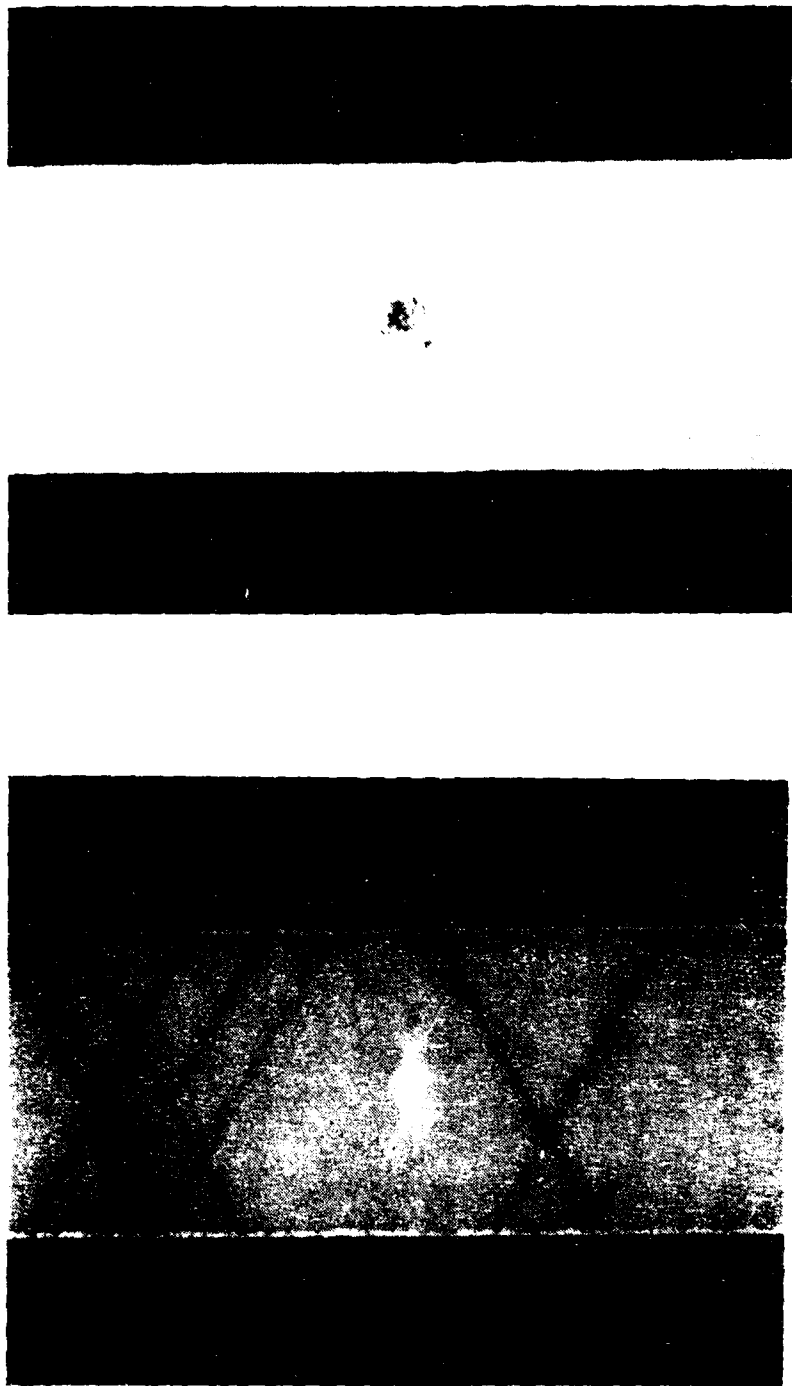


Figure D.44.  $\nu^{(2)}$  spectrum.

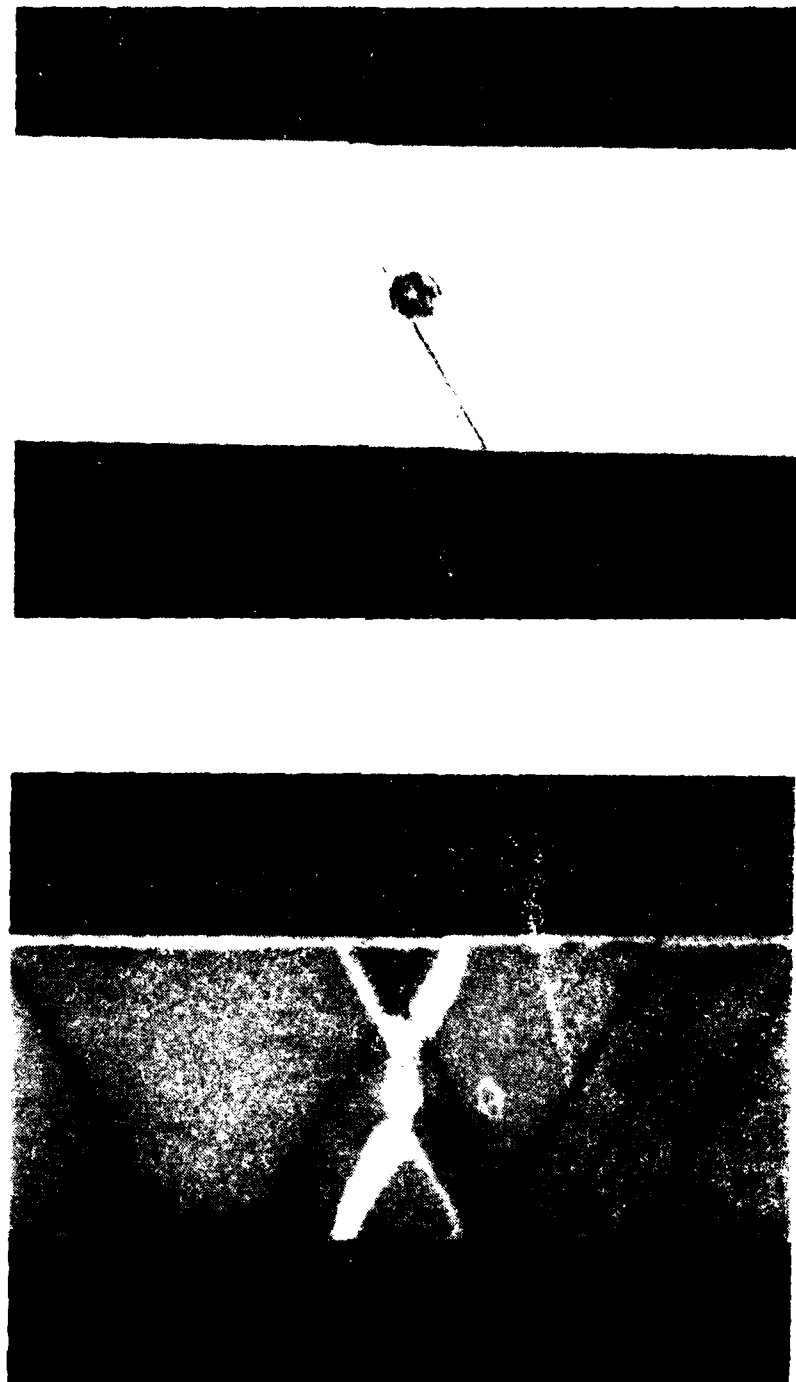


Figure D-46.  $\text{C}^{14}$   $\text{SO}_4$  specimen

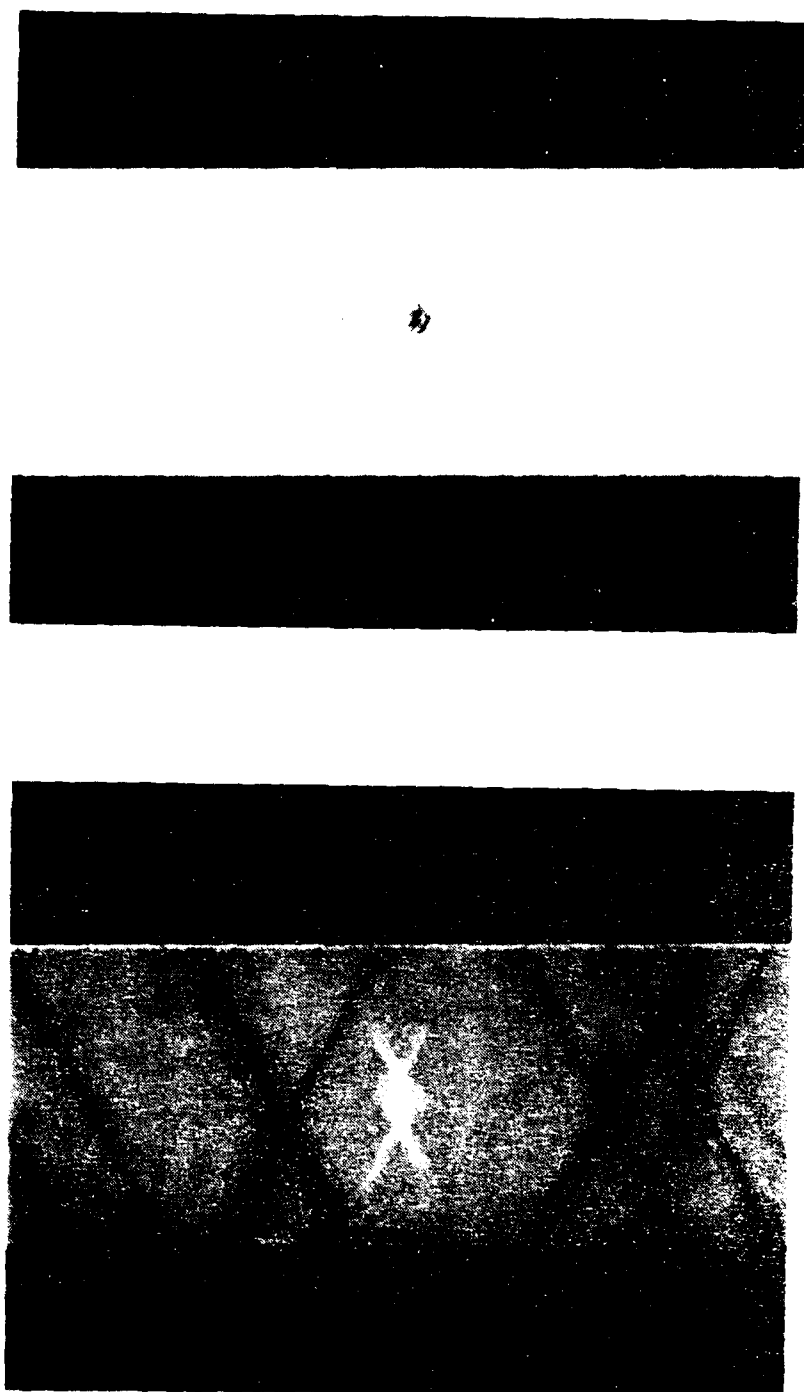


Figure 10-47 -  $10^0 \times 7$  specimen.

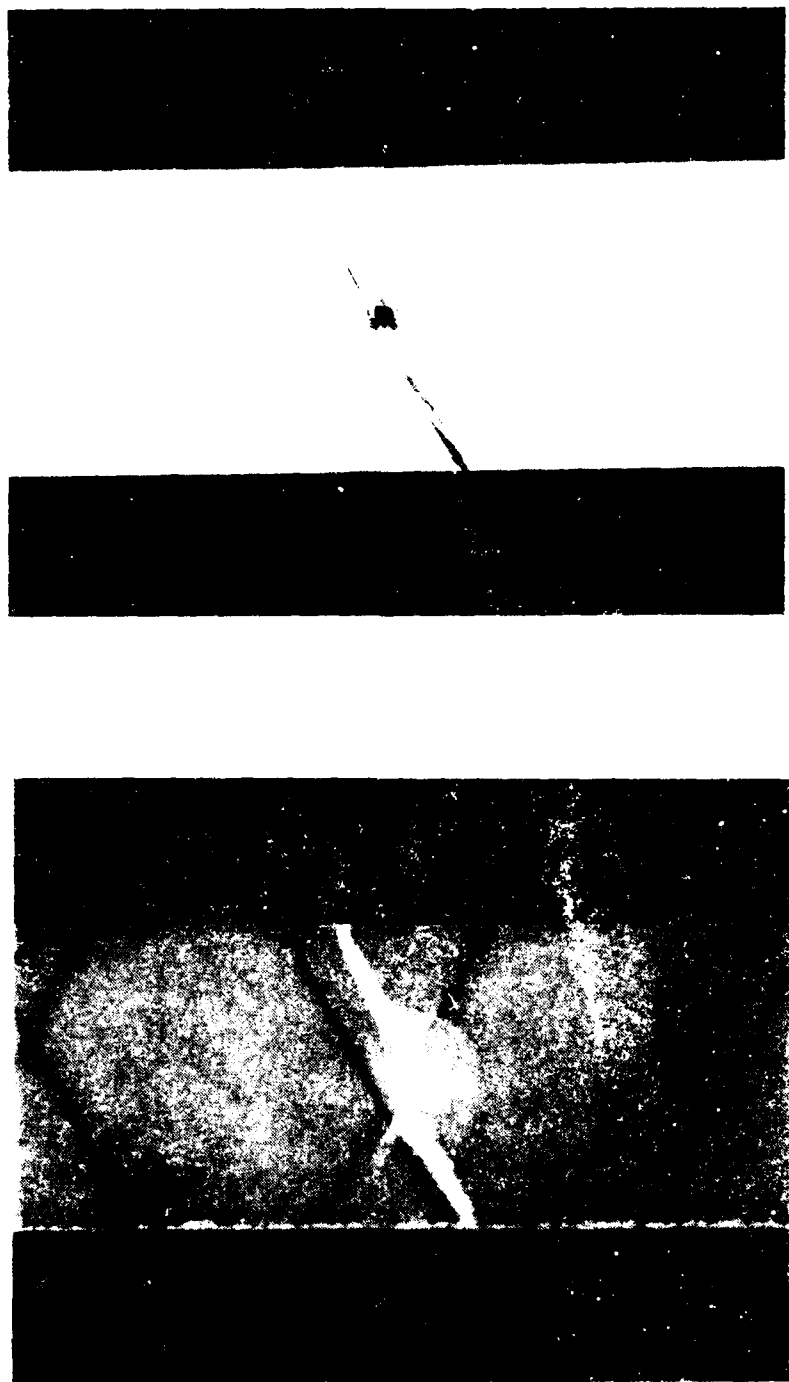


Figure D-4<sup>a</sup> to  $\delta^3$  specimen.

APPENDIX E

This appendix contains tables of  $n$  values versus  $r$  for all the laser speckle interferograms made in this report.

TABLE E-1 n VALUES VERSUS r FOR 0° SPECIMENS

SPECIMEN	r=0	r=1	r=2	r=3	r=4	r=5	r=6	r=7
1-1	5.70	5.45	5.11	4.69	4.42	4.08	3.72	3.45
1-2	4.55	4.67	4.70	4.65	4.65	4.45	4.40	4.35
1-3	4.35	4.45	4.52	4.65	4.52	4.62	4.71	4.69
1-4	4.35	4.42	4.48	4.49	4.48	4.49	4.49	4.49
2-1	7.25	6.81	6.62	6.30	5.81	5.65	5.32	4.81
2-2	6.71	6.62	6.38	6.25	5.71	5.70	5.56	5.36
2-3	6.70	6.65	6.45	6.31	6.12	5.95	5.72	5.61
2-4	6.70	6.65	6.39	6.41	6.25	6.09	5.81	5.65
3-1	4.39	4.11	3.65	3.37	3.02	2.65	2.39	2.15
3-2	4.35	4.26	3.77	3.55	3.26	2.86	2.65	2.38
3-3	3.85	3.71	3.64	3.43	3.23	3.15	2.75	2.68
3-4	3.91	3.82	3.64	3.48	3.35	3.25	2.95	2.76

TABLE E-2  $n$  VALUES VERSUS  $r$  FOR  $0^{\circ}$  SPECIMENS

SPECIMEN	$r=0$	$r=1$	$r=2$	$r=3$	$r=4$	$r=5$	$r=6$	$r=7$
4-1	6.82	6.43	5.88	5.69	5.25	4.76	4.50	4.25
4-2	6.68	6.35	5.83	5.56	5.26	4.81	4.62	4.26
4-3	6.68	6.25	5.93	5.62	5.38	5.08	4.70	4.46
4-4	6.72	6.33	5.95	5.62	5.35	4.95	4.75	4.50
5-1	6.23	5.82	5.51	5.27	4.82	4.68	4.42	4.25
5-2	6.35	6.05	5.75	5.41	5.25	4.95	4.62	4.52
5-3	6.25	6.01	5.71	5.45	5.31	5.12	4.75	4.62
5-4	6.35	6.02	5.82	5.45	5.35	5.12	4.76	4.61
6-1	4.55	4.23	3.78	3.32	3.06	2.71	2.42	1.95
6-2	3.81	3.65	3.35	3.05	2.85	2.65	2.46	2.23
6-3	3.45	3.31	3.16	2.81	2.75	2.53	2.36	2.13
6-4	3.31	2.98	2.69	2.52	2.41	2.36	2.16	1.83

TABLE E-3 n VALUES VERSUS r FOR 0° SPECIMENS

SPECIMEN	r=0	r=1	r=2	r=3	r=4	r=5	r=6	r=7
7-1	7.15	6.68	6.21	5.83	5.38	5.03	4.71	4.33
7-2	5.41	5.45	5.48	5.48	5.44	5.44	5.35	5.25
7-3	4.75	4.99	5.21	5.41	5.61	5.71	5.78	5.85
7-4	4.51	4.72	4.81	4.85	4.91	4.99	5.08	5.10
8-1	4.75	4.63	4.37	4.11	3.78	3.38	3.23	2.83
8-2	3.85	3.82	3.91	3.94	3.75	3.81	3.75	3.65
8-3	3.52	3.68	3.73	3.82	3.82	3.82	3.82	3.84
8-4	3.68	3.68	3.75	3.82	3.82	3.83	3.81	3.80
A-1	6.25	5.89	5.62	5.38	5.08	4.81	4.65	4.48
A-2	5.81	5.69	5.48	5.35	5.11	4.95	4.81	4.71
A-3	5.82	5.71	5.52	5.37	5.18	5.01	4.91	4.65
A-4	6.35	6.01	5.81	5.69	5.48	5.28	5.03	4.81

TABLE E-4  $n$  VALUES VERSUS  $r$  FOR + 15° SPECIMENS

SPECIMEN	$r=0$	$r=1$	$r=2$	$r=3$	$r=4$	$r=5$	$r=6$	$r=7$
1-1	6.95	6.65	6.35	5.95	5.61	5.30	4.80	4.69
1-2	5.65	5.70	5.75	5.70	5.65	5.65	5.75	~
1-3	4.75	5.35	5.40	5.45	5.35	5.35	5.50	~
1-4	5.40	5.55	5.35	5.35	5.35	5.25	4.85	~
2-1	5.75	5.45	4.90	4.65	4.35	3.80	3.55	3.25
2-2	6.32	5.82	5.38	4.82	4.42	3.95	3.65	3.00
2-3	6.60	5.75	5.35	4.82	4.35	3.78	3.38	~
2-4	6.95	6.30	5.65	4.85	4.35	3.95	3.35	2.95
3-1	7.35	7.10	6.52	6.35	5.80	5.35	5.30	4.85
3-2	7.25	6.75	6.55	6.31	5.98	5.69	5.33	5.25
3-3	7.25	6.75	6.55	6.35	6.10	5.75	5.52	5.35
3-4	7.35	6.77	6.65	6.35	6.10	5.70	5.41	5.35

TABLE E-5  $n$  VALUES VERSUS  $r$  FOR  $\pm 15^0$  SPECIMENS

SPECIMEN	r=0	r=1	r=2	r=3	r=4	r=5	r=6	r=7
4-1	7.30	6.85	6.68	6.45	6.35	5.85	5.69	5.45
4-2	7.32	7.10	6.81	6.72	6.38	6.11	5.88	5.68
4-3	7.35	7.08	6.75	6.69	6.45	6.22	5.82	5.71
4-4	7.36	7.07	6.83	6.63	6.38	5.98	5.82	5.70
5-1	5.16	4.65	4.28	3.79	3.47	3.24	2.97	2.48
5-2	4.65	4.35	4.32	3.82	3.68	3.49	3.31	3.08
5-3	4.36	4.26	3.99	3.85	3.69	3.65	3.51	3.38
5-4	4.25	4.19	4.08	3.99	3.71	3.68	3.62	3.58
6-1	7.06	6.75	6.55	6.23	5.71	5.39	5.08	4.69
6-2	6.65	6.48	6.32	6.19	5.81	5.69	5.52	
6-3	6.55	6.45	6.35	6.20	5.91	5.69	5.60	
6-4	6.82	6.62	6.41	6.32	6.08	5.70	5.62	

TABLE E-6  $n$  VALUES VERSUS  $r$  FOR  $\pm 15^{\circ}$  SPECIMENS

SPECIMEN	r=0	r=1	r=2	r=3	r=4	r=5	r=6	r=7
7-1	5.62	5.32	5.08	4.69	4.32	4.31	3.79	3.65
7-2	5.82	5.59	5.25	4.80	4.63	4.31	4.02	3.69
7-3	5.72	5.37	4.82	4.71	4.38	3.88	3.65	3.32
7-4	5.81	5.62	5.08	4.70	4.35	3.81	3.71	3.32
8-1	7.38	7.07	6.73	6.49	6.04	5.72	5.38	5.11
8-2	7.01	6.72	6.65	6.43	6.07	5.92	5.68	5.32
8-3	6.95	6.71	6.59	6.41	5.98	5.71	5.62	5.50
8-4	7.01	6.71	6.58	6.37	5.95	5.70	5.58	5.21
A-1	7.35	7.18	6.81	6.52	6.29	5.58	5.65	5.32
A-2	7.21	7.01	6.73	6.60	6.31	6.16	5.81	5.68
A-3	7.35	7.00	6.81	6.49	6.25	5.95	5.75	5.45
A-4	6.71	6.61	6.30	6.15	5.72	5.48	5.35	5.23

TABLE E-7  $n$  VALUES VERSUS  $r$  FOR  $\pm 20^{\circ}$  SPECIMENS

SPECIMEN	r=0	r=1	r=2	r=3	r=4	r=5	r=6	r=7
A-1	5.80	5.35	4.82	4.42	3.81	3.45	3.10	2.68
A-2	5.32	4.92	4.55	4.31	3.70	3.58	3.24	2.76
A-3	5.35	4.82	4.72	4.35	3.85	3.45	3.32	2.75
A-4	4.75	4.45	4.12	3.68	3.40	3.18	2.81	2.68
1-1	5.68	5.31	4.95	4.61	4.25	3.75	3.60	3.30
1-2	5.25	4.81	4.70	4.52	4.35	3.85	3.70	3.45
1-3	5.30	4.85	4.75	4.58	4.30	3.85	3.75	3.60
1-4	5.38	5.25	4.75	4.55	4.35	3.85	3.75	3.58
2-1	5.62	5.08	4.52	4.00	3.45	2.95	2.45	2.08
2-2	5.65	5.15	4.51	4.08	3.45	3.05	2.68	2.21
2-3	5.51	4.95	4.55	4.18	3.40	3.28	2.70	2.35
2-4	5.56	5.15	4.55	4.15	3.70	3.35	2.70	2.35

TABLE E-8  $n$  VALUES VERSUS  $r$  FOR  $\pm 20^{\circ}$  SPECIMENS

SPECIMEN	$r=0$	$r=1$	$r=2$	$r=3$	$r=4$	$r=5$	$r=6$	$r=7$
3-1	6.80	6.55	6.19	5.68	5.35	4.81	4.65	4.23
3-2	6.85	6.55	6.28	5.75	5.35	5.08	4.65	4.35
3-3	6.70	6.35	6.01	5.58	5.30	5.12	4.68	4.38
3-4	6.78	6.52	6.18	5.70	5.32	5.15	4.70	4.35
4-1	8.01	7.61	7.35	6.80	6.35	5.81	5.62	5.28
4-2	7.75	7.62	7.25	6.75	6.55	6.25	5.70	5.60
4-3	8.30	7.72	7.35	6.98	6.62	6.35	5.75	5.50
4-4	8.25	7.68	7.35	6.75	6.40	6.20	5.65	5.35
5-1	5.38	4.75	4.65	4.35	3.70	3.38	2.80	2.68
5-2	4.38	4.25	4.15	3.95	3.70	3.68	3.65	3.50
5-3	4.01	3.82	3.75	3.68	3.65	3.60	3.55	3.45
5-4	4.61	4.45	4.30	3.75	3.70	3.62	3.35	2.75

TABLE E-9 n VALUES VERSUS r FOR  $\pm 20^{\circ}$  SPECIMENS

SPECIMEN	r=0	r=1	r=2	r=3	r=4	r=5	r=6	r=7
6-1	5.76	5.48	5.25	4.70	4.50	4.30	3.70	3.65
6-2	6.30	5.70	5.35	4.75	4.50	3.78	3.70	3.45
6-3	6.75	6.30	5.62	5.00	4.45	4.01	3.35	2.68
6-4	7.35	6.38	5.70	5.01	4.65	3.70	3.01	2.45
7-1	5.35	5.12	4.72	4.57	4.25	3.70	3.65	3.35
7-2	5.82	5.65	5.35	4.75	4.35	3.80	3.65	3.35
7-3	6.70	6.25	5.45	4.82	4.38	3.82	3.45	2.78
7-4	6.35	5.65	5.20	4.55	4.20	3.65	3.20	2.35
8-1	8.30	8.01	7.65	7.35	6.80	6.35	6.32	5.80
8-2	8.35	8.20	7.75	7.40	7.30	6.82	6.65	6.35
8-3	8.20	7.75	7.50	7.30	7.20	6.70	6.50	6.35
8-4	9.05	8.45	8.30	7.65	7.35	7.18	6.65	6.40

TABLE E-10  $n$  VALUES VERSUS  $r$  FOR  $\pm 30^0$  SPECIMENS

SPECIMEN	r=0	r=1	r=2	r=3	r=4	r=5	r=6	r=7
1-1	5.55	4.80	4.55	4.05	3.65	3.26	2.70	2.42
1-2	4.75	4.40	4.30	3.90	3.75	3.45	3.28	2.85
1-3	4.28	4.25	3.85	3.68	3.60	3.40	3.25	2.85
1-4	4.68	4.45	4.35	3.98	3.70	3.55	3.20	2.70
2-1	6.68	6.20	5.70	5.65	5.20	4.70	4.30	3.85
2-2	6.75	6.40	5.95	5.70	5.25	4.75	4.40	4.05
2-3	6.70	6.25	5.70	5.35	4.95	4.60	4.20	3.70
2-4	6.85	6.45	5.95	5.40	4.95	4.50	4.25	3.75
3-1	6.50	6.05	5.65	5.20	4.75	4.35	3.75	3.45
3-2	7.30	6.70	5.82	5.45	4.75	4.35	3.80	2.95
3-3	7.40	6.70	6.05	5.55	4.95	4.35	3.75	2.95
3-4	7.35	6.70	6.00	5.45	4.85	4.25	3.70	3.10

TABLE E-11 n VALUES VERSUS r FOR  $\pm 30^\circ$  SPECIMENS

SPECIMEN	r=0	r=1	r=2	r=3	r=4	r=5	r=6	r=7
4-1	6.60	6.05	5.68	5.25	4.70	4.35	3.80	3.60
4-2	6.70	6.30	5.70	5.38	4.85	4.55	4.05	3.65
4-3	6.80	6.35	5.80	5.35	4.82	4.38	3.95	3.68
4-4	7.01	6.45	5.78	5.38	4.70	4.50	3.85	3.70
5-1	6.35	5.75	5.60	4.98	4.70	4.35	3.80	3.60
5-2	6.45	5.95	5.70	5.20	4.70	4.30	3.80	3.62
5-3	6.68	6.30	5.70	5.30	4.70	4.35	3.82	3.70
5-4	6.95	6.38	5.80	5.32	4.75	4.30	3.75	3.30
6-1	6.95	6.65	6.25	5.68	5.25	4.75	4.30	3.95
6-2	6.70	6.35	5.85	5.75	5.35	4.88	4.68	4.30
6-3	6.75	6.42	6.10	5.75	5.50	5.21	4.75	4.30
6-4	7.01	6.52	6.30	5.82	5.45	5.20	4.65	4.32

TABLE E-12 n VALUES VERSUS r FOR  $\pm 30^0$  SPECIMENS

SPECIMEN	r=0	r=1	r=2	r=3	r=4	r=5	r=6	r=7
A-1	7.01	6.70	6.35	5.80	5.60	5.25	4.75	4.45
A-2	6.06	6.30	6.05	5.75	5.70	5.30	5.25	5.05
A-3	6.50	6.25	5.95	5.70	5.60	5.35	5.20	4.75
A-4	6.30	6.00	5.75	5.60	5.35	5.10	4.70	4.60
7-1	9.10	8.70	8.25	7.75	7.25	6.60	6.35	5.75
7-2	8.50	8.30	7.95	7.75	7.35	6.75	6.65	6.40
7-3	8.15	7.82	7.65	7.35	7.25	6.75	6.55	6.45
7-4	8.35	7.95	7.70	7.25	6.75	6.55	6.40	5.75
8-1	5.25	5.00	4.75	4.45	4.10	3.75	3.60	3.25
8-2	4.75	4.65	4.55	4.45	4.05	3.80	3.60	3.50
8-3	5.30	4.95	4.70	4.30	3.95	3.70	3.35	3.10
8-4	5.40	5.10	4.75	4.45	3.85	3.50	3.25	2.75

TABLE E-13 n VALUES VERSUS r FOR + 45° SPECIMENS

SPECIMEN	r=0	r=1	r=2	r=3	r=4	r=5	r=6	r=7
1-1	8.85	8.35	7.80	7.32	6.85	6.25	5.79	5.18
1-2	8.20	7.88	7.45	7.25	6.83	6.68	6.08	5.70
1-3	8.95	8.38	7.83	7.35	6.95	6.72	6.25	5.75
1-4	9.18	8.45	7.92	7.37	6.98	6.42	5.75	5.25
2-1	9.75	8.75	7.82	7.02	6.35	5.68	5.00	4.35
2-2	9.10	8.45	7.72	6.85	6.32	5.61	4.95	4.33
2-3	9.08	8.20	7.41	6.85	6.15	5.60	4.88	4.49
2-4	8.65	7.80	7.10	6.65	5.93	5.26	4.68	4.11
3-1	9.52	8.88	8.15	7.35	6.83	6.11	5.52	4.82
3-2	8.75	8.21	7.83	7.36	6.82	6.38	5.87	5.32
3-3	8.72	8.15	7.72	7.37	6.81	6.35	5.82	5.33
3-4	8.32	7.83	7.36	6.83	6.38	5.83	5.42	4.85

TABLE E-14 n VALUES VERSUS r FOR  $\pm 45^0$  SPECIMENS

SPECIMEN	r=0	r=1	r=2	r=3	r=4	r=5	r=6	r=7
4-1	11.18	10.05	9.38	8.55	7.61	6.75	5.75	5.25
4-2	8.63	8.42	8.33	8.31	7.88	7.75	7.65	7.35
4-3	7.85	7.88	7.78	7.78	7.78	7.91	7.91	~
4-4	7.92	7.92	7.92	7.90	7.85	7.75	7.65	7.65
5-1	8.83	8.20	7.65	6.86	6.33	5.65	5.03	4.39
5-2	7.65	7.38	7.12	6.87	6.63	6.35	5.85	~
5-3	7.20	7.22	7.22	6.81	6.68	6.35	6.28	5.95
5-4	7.62	7.37	7.25	6.83	6.70	6.37	5.86	5.76
6-1	9.37	8.53	7.82	7.32	6.68	5.81	5.26	4.75
6-2	8.15	7.81	7.36	6.88	6.61	6.20	5.85	5.32
6-3	8.33	8.01	7.55	7.15	6.81	6.38	6.05	5.61
6-4	8.62	8.08	7.65	7.11	6.81	6.19	5.82	5.57

TABLE E-15  $n$  VALUES VERSUS  $r$  FOR  $\pm 45^\circ$  SPECIMENS

SPECIMEN	r=0	r=1	r=2	r=3	r=4	r=5	r=6	r=7
7-1	9.82	9.06	8.16	7.61	6.80	5.97	5.30	4.75
7-2	8.71	8.30	7.85	7.32	6.89	6.18	5.89	5.30
7-3	8.12	7.89	7.62	7.13	6.89	6.33	5.70	~
7-4	8.70	8.11	7.81	7.27	6.81	6.23	5.85	5.45
8-1	10.15	9.23	8.55	7.82	6.82	6.09	5.48	~
8-2	10.62	9.82	8.65	7.83	6.92	5.97	5.27	~
8-3	11.26	9.78	8.88	7.99	6.85	6.30	5.30	~
8-4	11.02	9.88	8.72	7.81	6.92	6.02	5.35	~
A-1	9.15	8.23	7.68	6.87	6.18	5.43	4.82	4.18
A-2	9.75	8.72	7.86	6.89	6.21	5.41	4.61	3.78
A-3	10.38	8.88	7.79	6.97	6.18	5.32	4.62	~
A-4	10.11	8.82	7.80	6.85	6.16	5.41	4.32	~

TABLE E-16 n VALUES VERSUS r FOR + 60° SPECIMENS

SPECIMEN	r=0	r=1	r=2	r=3	r=4	r=5	r=6	r=7
1-1	11.75	11.25	10.31	9.45	7.69	6.83	6.31	5.55
1-2	11.33	10.82	10.15	9.45	7.77	7.31	6.38	5.81
1-3	11.31	10.75	10.18	9.43	7.81	7.23	6.74	5.88
1-4	11.62	10.75	10.35	9.62	7.83	7.25	6.56	5.76
2-1	~	~	22.75	~	7.58	6.76	6.18	5.52
2-2	~	~	~	~	7.69	7.26	6.52	6.00
2-3	~	~	~	~	7.71	7.62	6.75	6.35
2-4	~	~	~	~	7.75	7.63	6.83	6.48
3-1	14.25	13.10	12.26	11.26	9.83	8.01	7.35	6.68
3-2	~	12.15	11.75	11.32	10.21	9.67	9.35	9.00
3-3	11.45	11.70	11.31	11.01	10.32	9.70	9.60	~
3-4	12.01	12.21	11.65	11.15	10.38	9.85	9.50	~

TABLE E-17 n VALUES VERSUS r FOR  $\pm 60^\circ$  SPECIMENS

SPECIMEN	r=0	r=1	r=2	r=3	r=4	r=5	r=6	r=7
4-1	~	~	~ TOO MANY FRINGES	~	8.68	7.70	6.90	6.25
4-2	~	~	~ EST @ 43 FRINGES	~	8.62	7.82	7.51	~
4-3	~	~	~	~	8.51	8.18	8.18	~
4-4	~	~	~	~	8.55	8.31	7.85	~
5-1	10.70	9.75	9.10	8.35	7.19	6.39	5.68	4.82
5-2	8.55	8.35	8.08	7.82	7.35	7.06	6.75	~
5-3	7.65	7.92	7.82	7.68	7.35	6.93	6.75	~
5-4	8.35	8.25	8.10	7.69	7.52	6.77	6.25	~
6-1	~	~	~	~	9.32	8.74	7.82	7.25
6-2	~	~	~	~	9.71	9.32	8.75	8.35
6-3	~	~	~	~	9.65	9.31	9.05	8.75
6-4	~	~ EST 42 FRINGES	~	~	9.52	8.75	8.55	8.01

TABLE E-13 n VALUES VERSUS r FOR  $\pm 60^{\circ}$  SPECIMENS

SPECIMEN	r=0	r=1	r=2	r=3	r=4	r=5	r=6	r=7
7-1	13.25	12.38	11.55	10.70	9.68	8.76	7.95	6.35
7-2	11.82	11.43	10.92	10.50	9.81	9.30	8.70	8.01
7-3	11.62	11.25	10.81	10.49	9.92	9.45	9.82	~
7-4	12.05	11.68	11.19	10.77	10.15	9.69	9.06	8.75
8-1	~	14.75	13.68	12.75	7.92	7.31	6.32	5.68
8-2	15.45	14.68	13.48	12.79	8.25	7.62	6.93	6.35
8-3	14.68	13.71	13.21	12.70	8.25	7.74	7.18	6.65
8-4	14.35	13.62	12.95	12.48	8.33	7.91	7.26	6.68
A-1	12.75	12.15	11.38	10.81	10.07	9.31	8.61	7.75
A-2	11.53	11.25	10.83	10.67	10.37	9.72	9.56	9.25
A-3	11.35	11.23	10.81	10.62	10.35	9.70	9.62	9.18
A-4	11.72	11.35	10.78	10.63	10.22	9.68	8.98	8.70

#### APPENDIX F

This appendix contains tables of  $\beta$  values for each interferogram used in this project.  $\beta$  was computed at  $r = 3.5$  in all cases.

TABLE F-1  $\beta$  VALUES FOR  $0^\circ$  SPECIMENS

SPECIMEN ROTATION ANGLE	SPECIMEN NUMBER								
	A	1	2	3	4	5	6	7	8
$0^\circ$	.253	.330	.332	.328	.374	.283	.365	.399	.282
$10^\circ$	.165	.041	.206	.295	.344	.268	.229	.021	.026
$20^\circ$	.165	.045	.166	.174	.310	.233	.189	.158	.038
$30^\circ$	.208	.016	.150	.163	.317	.246	.185	.077	.020

TABLE F-2  $\beta$  VALUES FOR  $\pm 15^\circ$  SPECIMENS

SPECIMEN ROTATION ANGLE	SPECIMEN NUMBER								
	A	1	2	3	4	5	6	7	8
$0^\circ$	.297	.340	.364	.363	.254	.364	.344	.287	.331
$10^\circ$	.222	.003	.461	.285	.238	.224	.199	.306	.233
$20^\circ$	.266	.045	.503	.263	.233	.140	.181	.339	.222
$30^\circ$	.232	.107	.575	.284	.246	.107	.212	.370	.253

TABLE F-3  $\beta$  VALUES FOR  $\pm 20^0$  SPECIMENS

SPECIMEN ROTATION ANGLE	A	SPECIMEN NUMBER							
		1	2	3	4	5	6	7	8
0 <sup>0</sup>	.450	.347	.514	.380	.406	.394	.318	.294	.361
10 <sup>0</sup>	.355	.248	.493	.369	.331	.128	.415	.385	.293
20 <sup>0</sup>	.357	.242	.451	.327	.390	.068	.578	.556	.258
30 <sup>0</sup>	.307	.273	.461	.352	.407	.245	.684	.538	.371

TABLE F-4  $\beta$  VALUES FOR  $\pm 30^0$  SPECIMENS

SPECIMEN ROTATION ANGLE	A	SPECIMEN NUMBER							
		1	2	3	4	5	6	7	8
0 <sup>0</sup>	.371	.436	.389	.442	.437	.393	.448	.483	.289
10 <sup>0</sup>	.174	.257	.392	.595	.435	.419	.338	.320	.198
20 <sup>0</sup>	.230	.195	.416	.614	.459	.451	.338	.250	.318
30 <sup>0</sup>	.245	.271	.446	.602	.484	.521	.379	.355	.382

TABLE F-5.  $\beta$  VALUES FOR  $\pm 45^\circ$  SPECIMENS

SPECIMEN ROTATION ANGLE	A	SPECIMEN NUMBER							
		1	2	3	4	5	6	7	8
$0^\circ$	.705	.519	.757	.670	.855	.636	.659	.734	.777
$10^\circ$	.837	.347	.687	.483	.178	.298	.397	.492	.893
$20^\circ$	.866	.437	.653	.476	.020	.192	.389	.431	.916
$30^\circ$	.888	.546	.638	.492	.045	.277	.444	.467	.903

TABLE F-6.  $\beta$  VALUES FOR  $\pm 60^\circ$  SPECIMENS

SPECIMEN ROTATION ANGLE	A	SPECIMEN NUMBER							
		1	2	3	4	5	6	7	8
$0^\circ$	.710	.955	3.173	1.141	6.880	.842	6.697	.950	1.814
$10^\circ$	.333	.845	3.094	.590	8.427	.323	6.525	.546	1.482
$20^\circ$	.319	.815	3.038	.420	8.290	.234	6.475	.483	1.306
$30^\circ$	.436	.869	3.022	.520	8.336	.406	6.588	.491	1.247

#### APPENDIX G

This appendix contains tables of the PCS (Percent Change in Strain) in the flawed regions of specimens 1 through 8 as compared to Specimen A for each of the six wrap angles.

TABLE G-1. PERCENT CHANGE IN STRAIN FOR  $0^0$  FLAWED SPECIMENS

SPECIMEN ROTATION ANGLE	SPECIMEN NUMBER							
	1	2	3	4	5	6	7	8
$0^0$	30.43	31.23	29.64	47.83	11.86	44.27	57.71	11.46
$10^0$	75.15	24.85	78.79	108.48	62.42	38.79	87.27	84.24
$20^0$	72.73	0.61	5.45	87.88	41.21	14.55	4.24	76.97
$30^0$	92.31	27.88	21.63	52.40	18.27	11.06	62.98	90.38

TABLE G-2. PERCENT CHANGE IN STRAIN FOR  $\pm 15^0$  FLAWED SPECIMENS

SPECIMEN ROTATION ANGLE	SPECIMEN NUMBER							
	1	2	3	4	5	6	7	8
$0^0$	14.48	22.56	22.22	14.48	22.56	15.82	3.37	11.45
$10^0$	98.65	107.66	28.38	7.21	0.90	10.36	37.84	4.95
$20^0$	83.08	89.10	1.13	12.41	47.37	31.95	27.44	16.54
$30^0$	53.88	147.84	22.41	6.03	53.88	8.62	59.48	9.05

TABLE G-3. PERCENT CHANGE IN STRAIN FOR  $\pm 20^\circ$  FLAWED SPECIMENS

SPECIMEN ROTATION ANGLE	SPECIMEN NUMBER							
	1	2	3	4	5	6	7	8
$0^\circ$	22.89	14.22	15.56	9.78	12.44	29.33	34.67	19.78
$10^\circ$	30.14	38.87	3.94	6.76	63.94	16.90	8.45	17.46
$20^\circ$	32.21	26.33	8.40	9.24	80.95	61.90	55.74	27.73
$30^\circ$	11.07	50.16	14.66	32.57	20.20	122.80	75.24	20.85

TABLE G-4. PERCENT CHANGE IN STRAIN FOR  $\pm 30^\circ$  FLAWED SPECIMENS

SPECIMEN ROTATION ANGLE	SPECIMEN NUMBER							
	1	2	3	4	5	6	7	8
$0^\circ$	17.52	4.85	19.14	17.79	5.93	20.75	30.19	22.10
$10^\circ$	47.70	125.29	241.95	150.00	140.80	94.25	83.91	13.79
$20^\circ$	15.22	80.87	166.96	99.57	96.09	46.96	8.70	38.26
$30^\circ$	10.61	82.04	145.71	97.55	112.65	54.69	44.90	55.92

TABLE G-5. PERCENT CHANGE IN STRAIN FOR  $\pm 45^0$  FLAWED SPECIMENS

SPECIMEN ROTATION ANGLE	SPECIMEN NUMBER							
	1	2	3	4	5	6	7	8
0 <sup>0</sup>	26.38	7.38	4.96	21.28	9.79	6.52	4.11	10.21
10 <sup>0</sup>	58.54	17.92	42.29	78.73	64.40	52.57	41.22	6.69
20 <sup>0</sup>	49.54	24.60	45.03	97.69	77.83	55.08	50.23	5.77
30 <sup>0</sup>	38.51	28.15	44.59	94.93	68.81	50.00	47.41	1.69

AVERAGE % CHANGE = 38.52%

TABLE G-6. PERCENT CHANGE IN STRAIN FOR  $\pm 60^0$  FLAWED SPECIMENS

SPECIMEN ROTATION ANGLE	SPECIMEN NUMBER							
	1	2	3	4	5	6	7	8
0 <sup>0</sup>	34.51	346.90	60.70	869.01	18.59	843.24	33.80	155.49
10 <sup>0</sup>	153.75	829.13	77.18	2430.63	3.00	1859.46	63.96	345.05
20 <sup>0</sup>	155.49	852.35	31.66	2498.75	26.65	1929.78	51.41	309.40
30 <sup>0</sup>	99.31	593.12	19.27	1811.93	6.88	1411.01	12.61	186.01

AVERAGE % CHANGE = 566.25%

#### APPENDIX H

Composite tensile specimens tested to their ultimate strength are shown in this appendix.

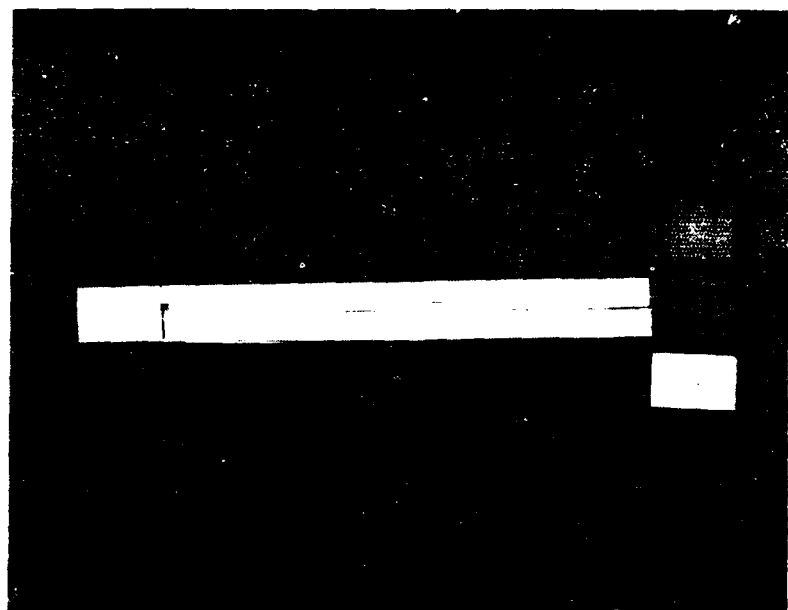


Figure H-1.  $0^0$ -1 specimen.

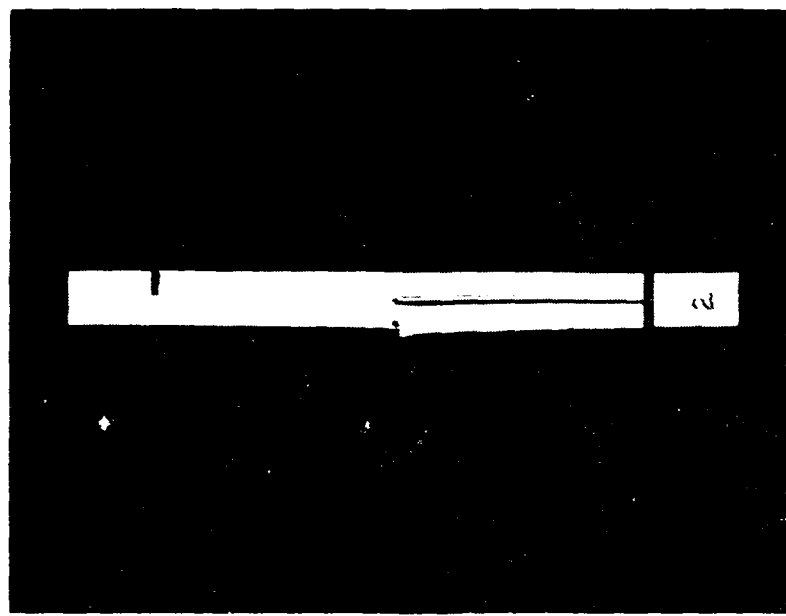


Figure H-2.  $0^0$ -2 specimen.

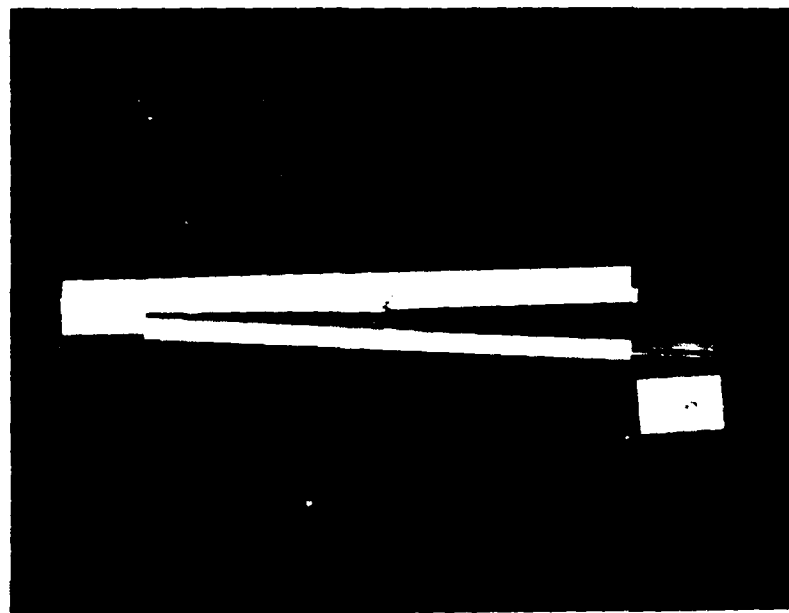


Figure H-3. 0<sup>0</sup>-3 specimen.

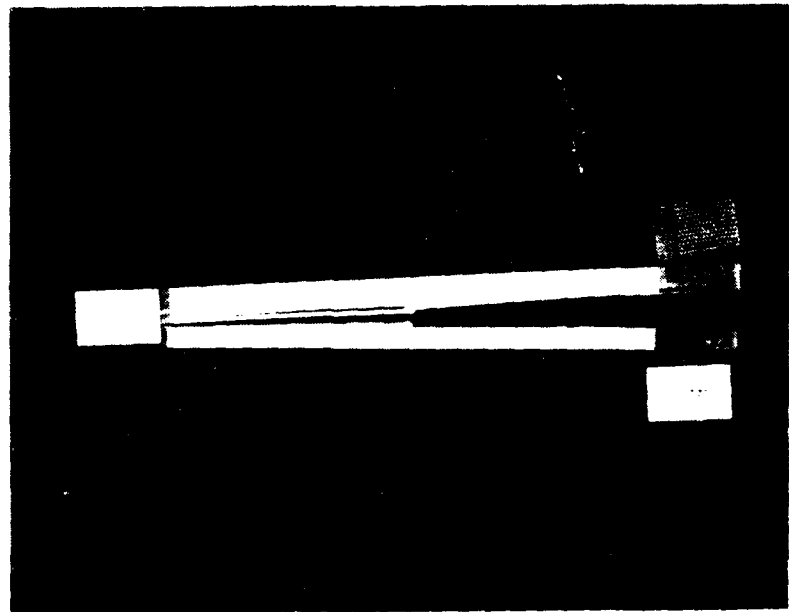


Figure H-4. 0<sup>0</sup>-5 specimen.

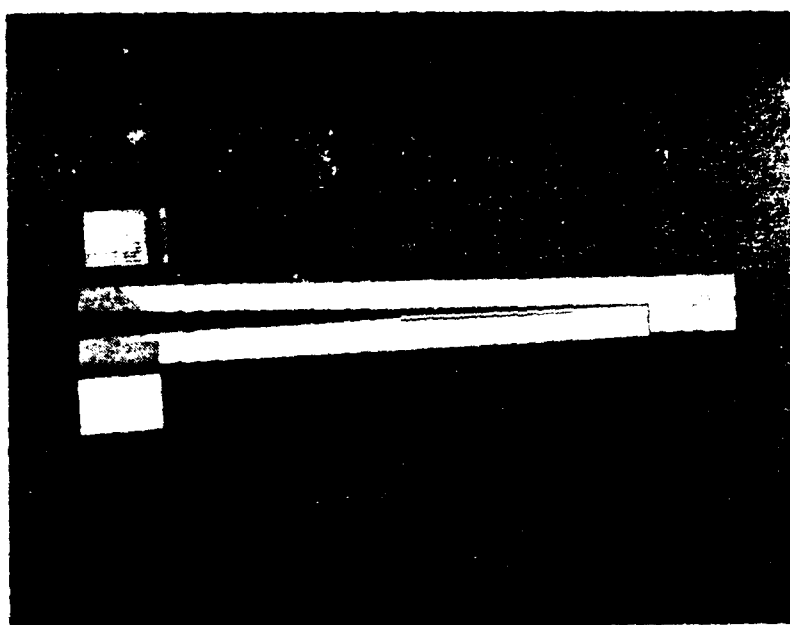


Figure H-5. H<sup>0</sup>-5 specimen.

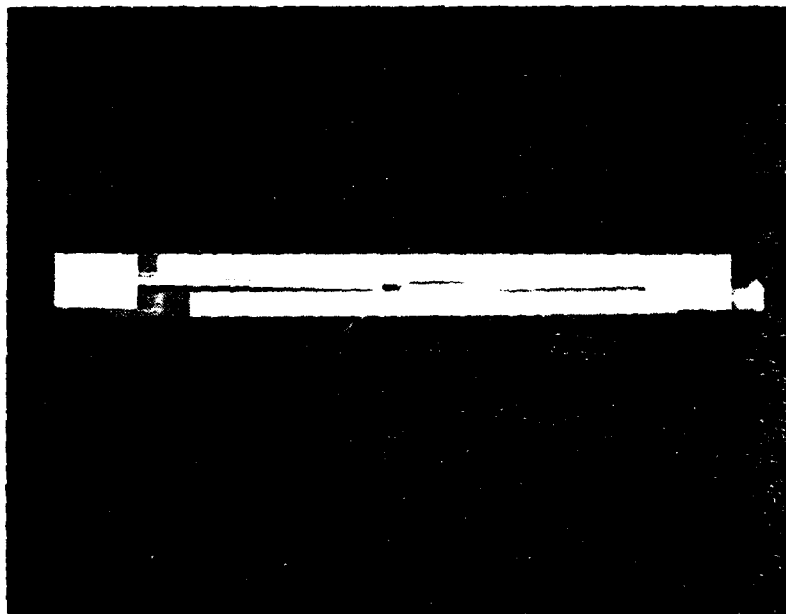


Figure H-6. H<sup>0</sup>-6 specimen.

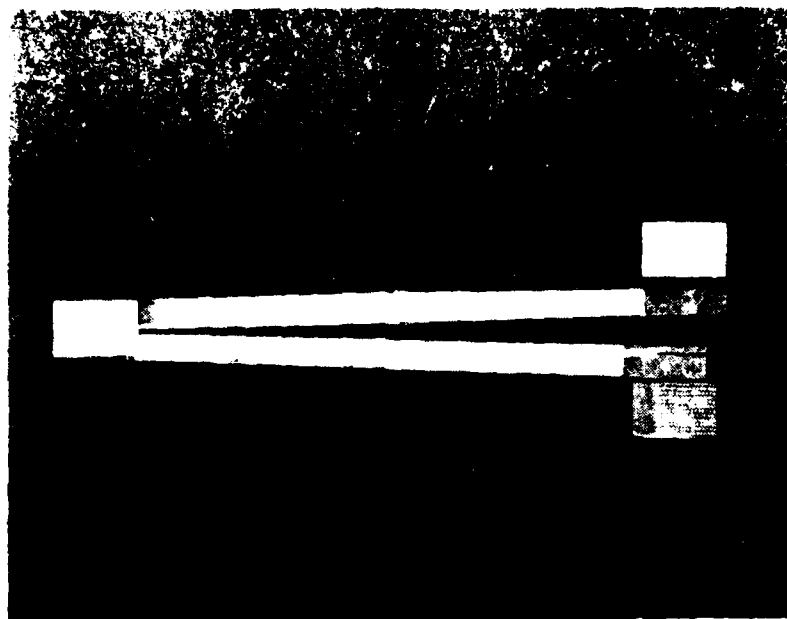


Figure H-7.  $\text{D}^0$ -7 specimen.

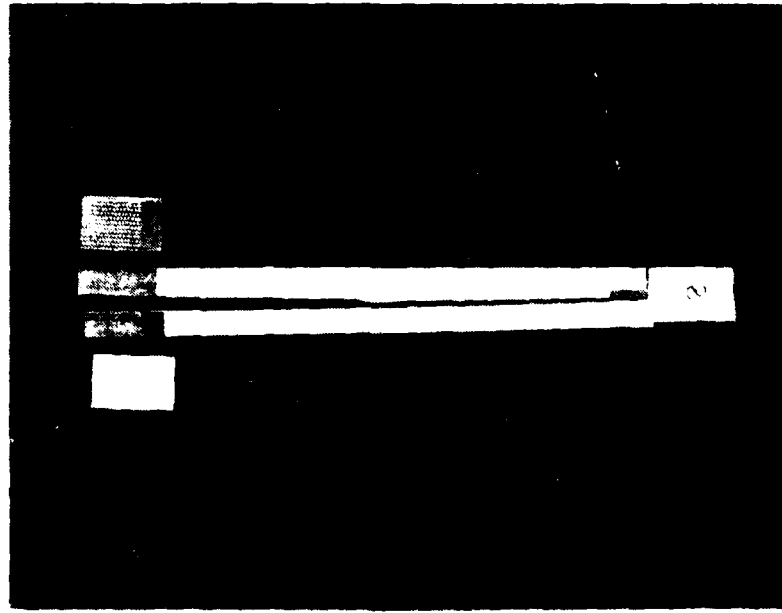


Figure H-8.  $\text{D}^0$ -8 specimen.

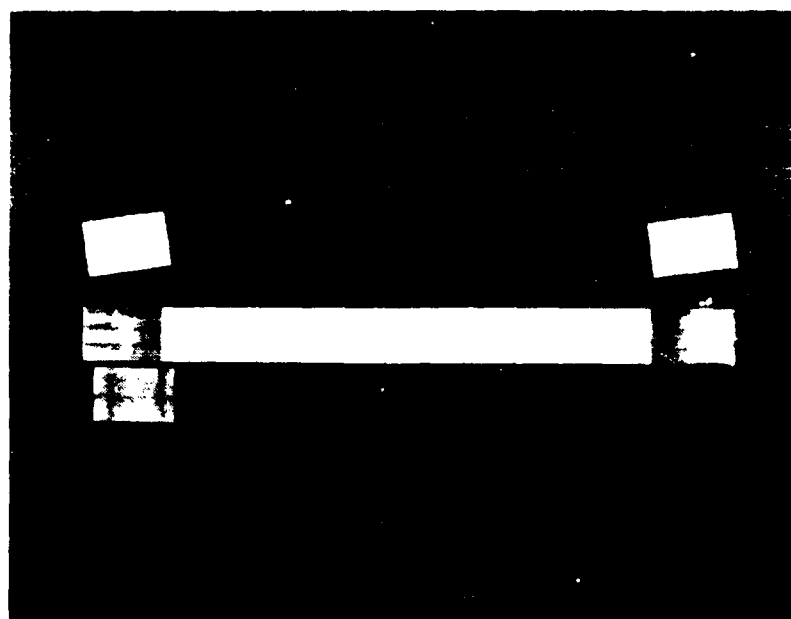


Figure H-9.  $\eta^0$ -A specimen.

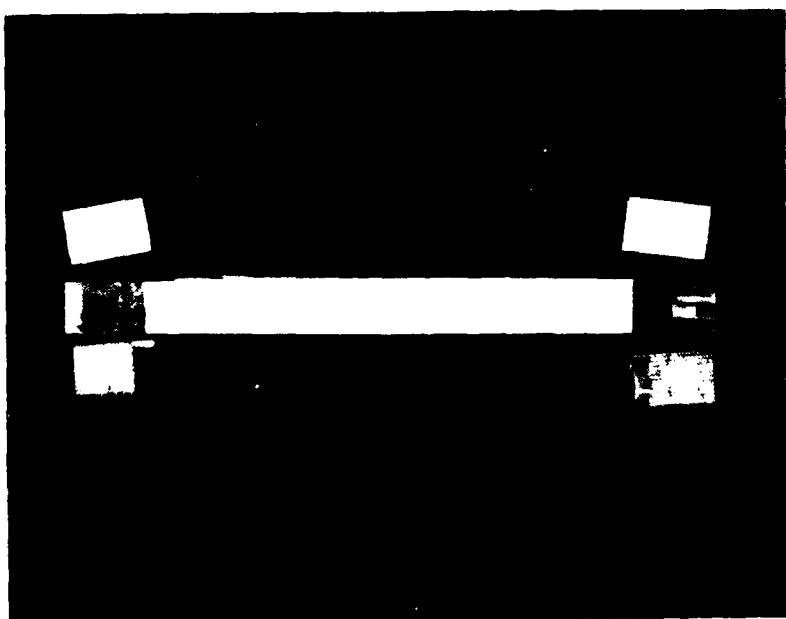


Figure H-10.  $\eta^0$ -A specimen.

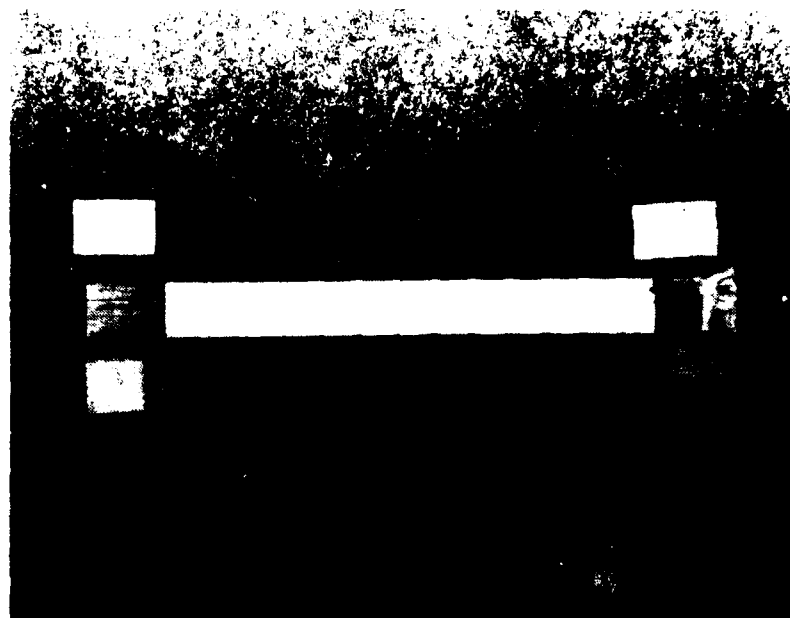


Figure H-11.  $0^0\text{-C}$  specimen.

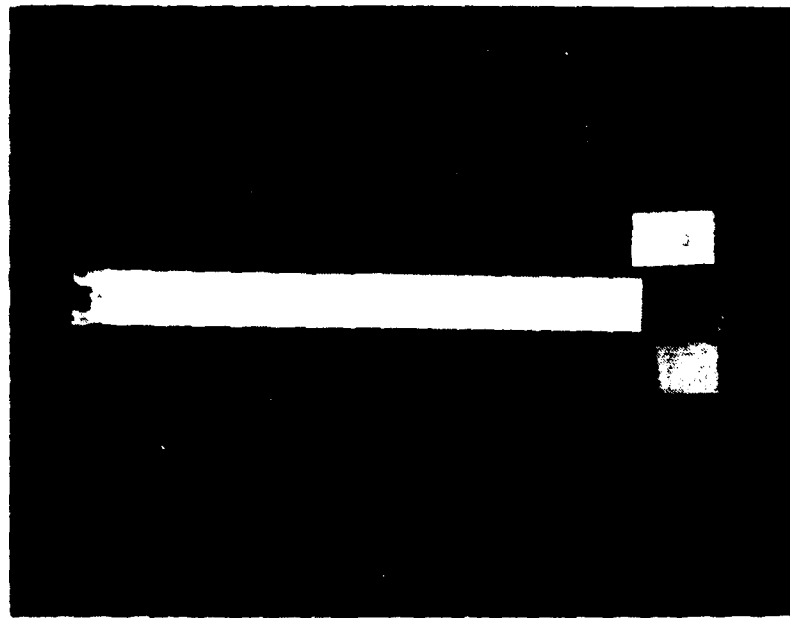


Figure H-12.  $0^0\text{-C}$  specimen.

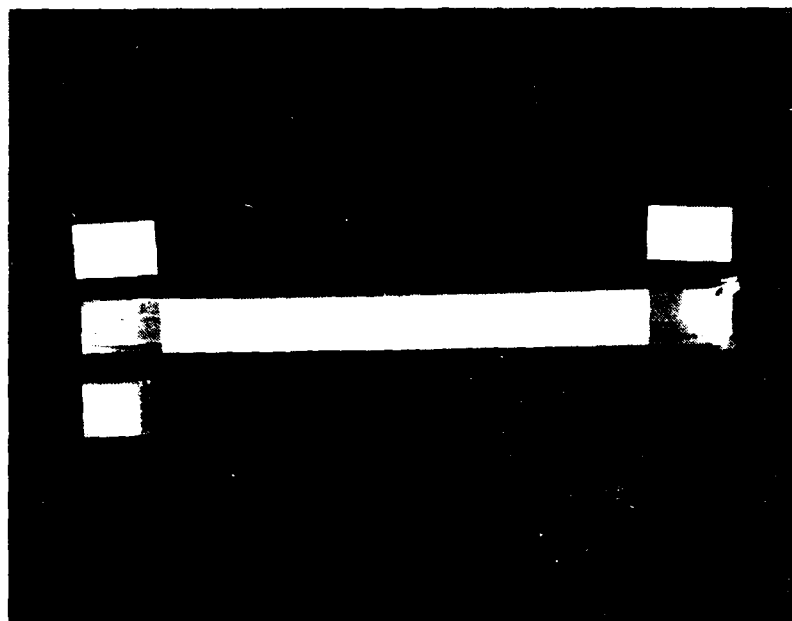


Figure H-13.  $0^0$ -E specimen.



Figure H-14 . 15<sup>0</sup>-1 specimen.

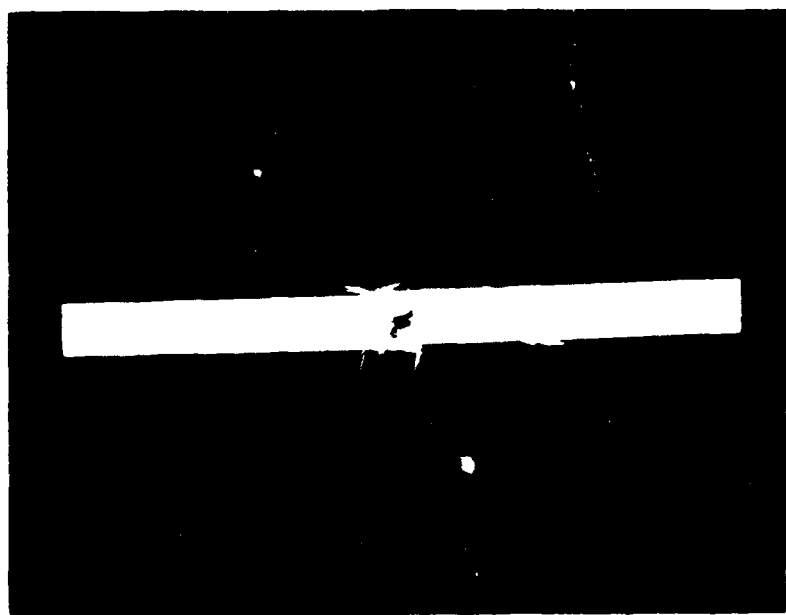


Figure H-15 . 15<sup>0</sup>-1 specimen.



Figure H-16. 15<sup>0</sup>-3 specimen.

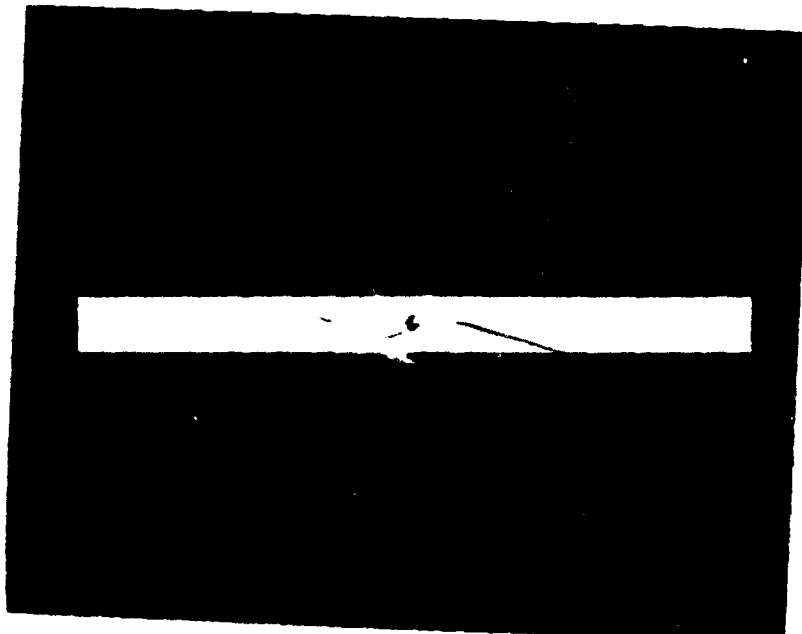


Figure H-17. 15<sup>0</sup>-4 specimen.

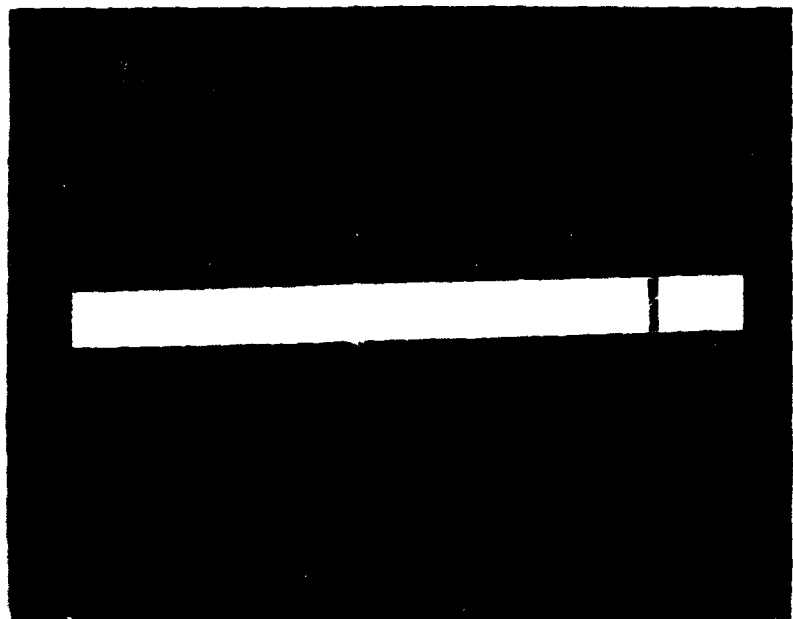


Figure H-18.  $15^0$ -5 specimen.



Figure H-19.  $15^0$ -6 specimen.

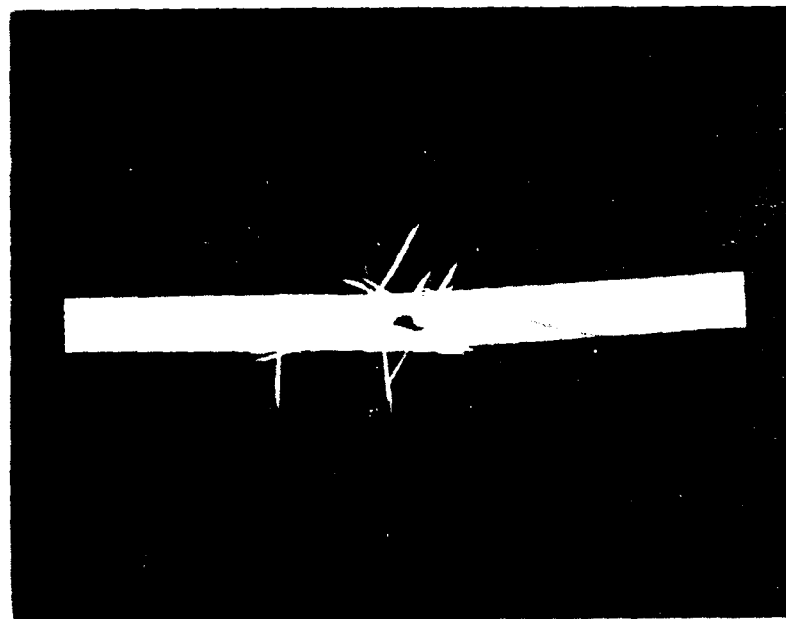


Figure H-20. 15<sup>0</sup>-7 specimen.

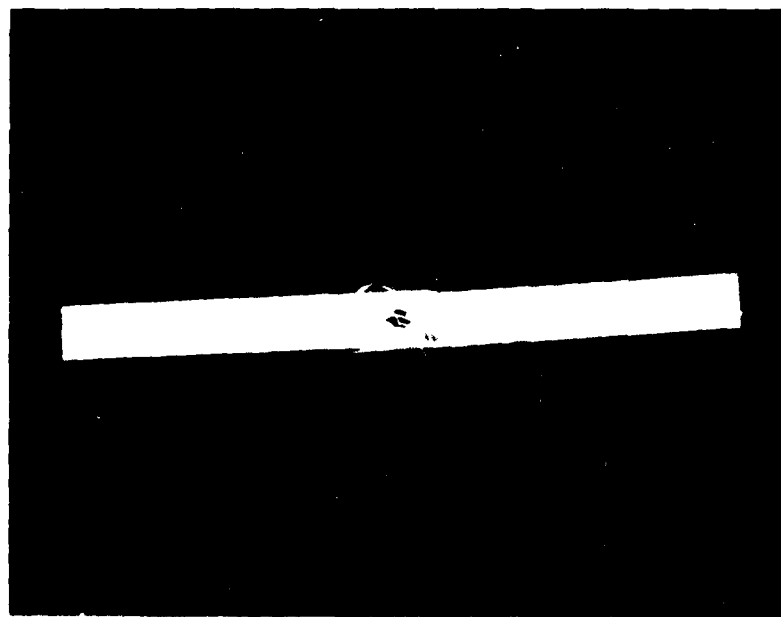


Figure H-21. 15<sup>0</sup>-8 specimen.



Figure H-22 . 15<sup>0</sup>-A specimen.

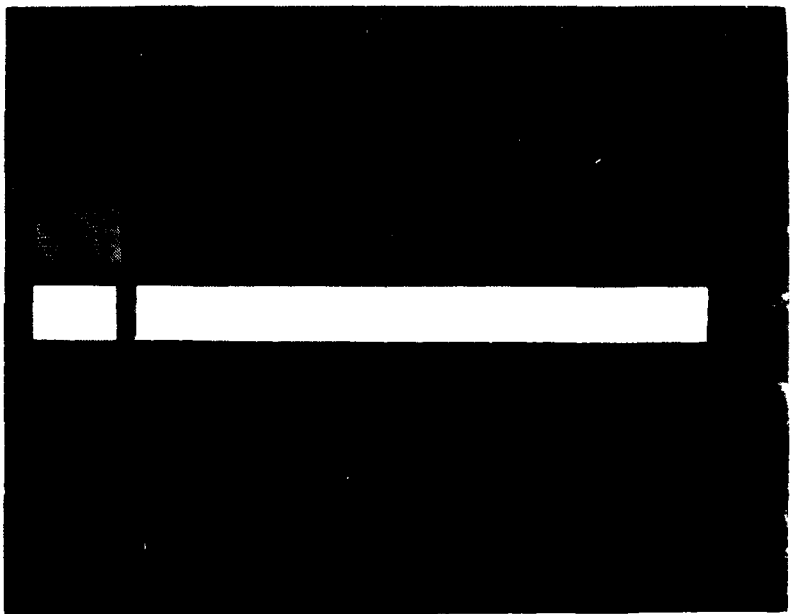


Figure H-23 . 15<sup>0</sup>-B specimen.

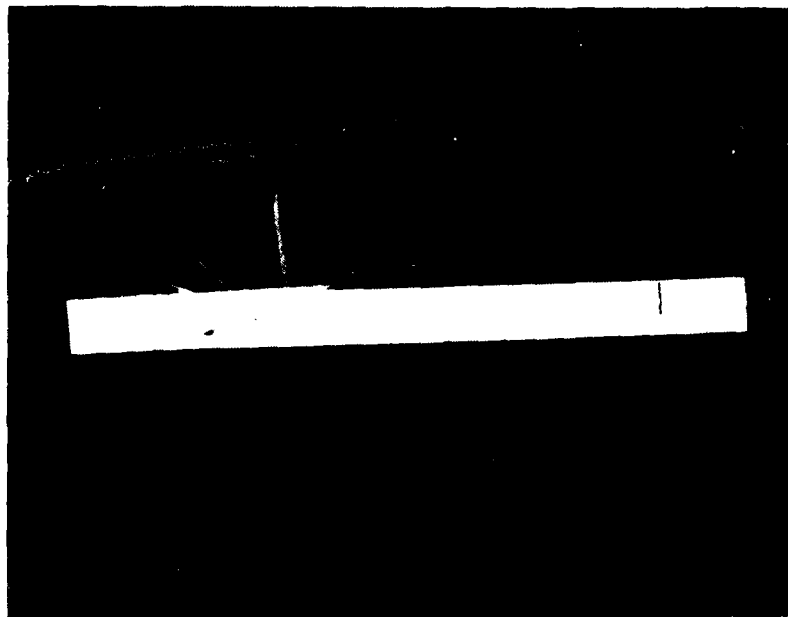


Figure H-24.  $15^0$ -C specimen.



Figure H-25.  $15^0$ -D specimen.



Figure H-26 . 15<sup>0</sup>-E specimen.

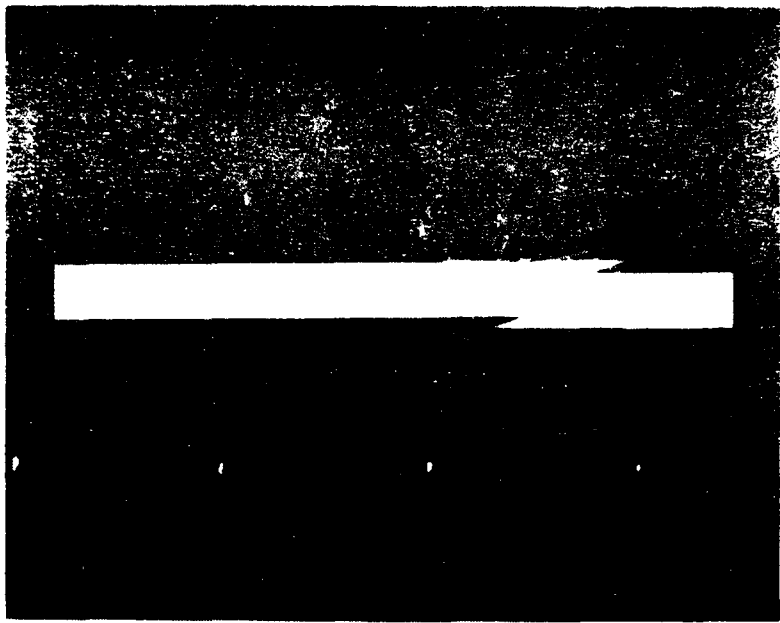


Figure H-27 . 20<sup>0</sup>-1 specimen.

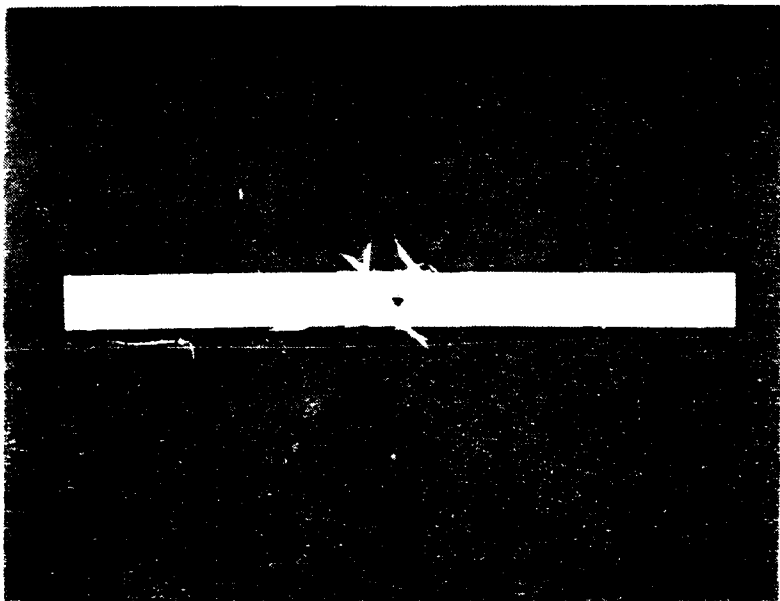


Figure H-27 . 20<sup>0</sup>-1 specimen.

[100]



Figure B-29. 2G<sup>0</sup>-3 specimen.

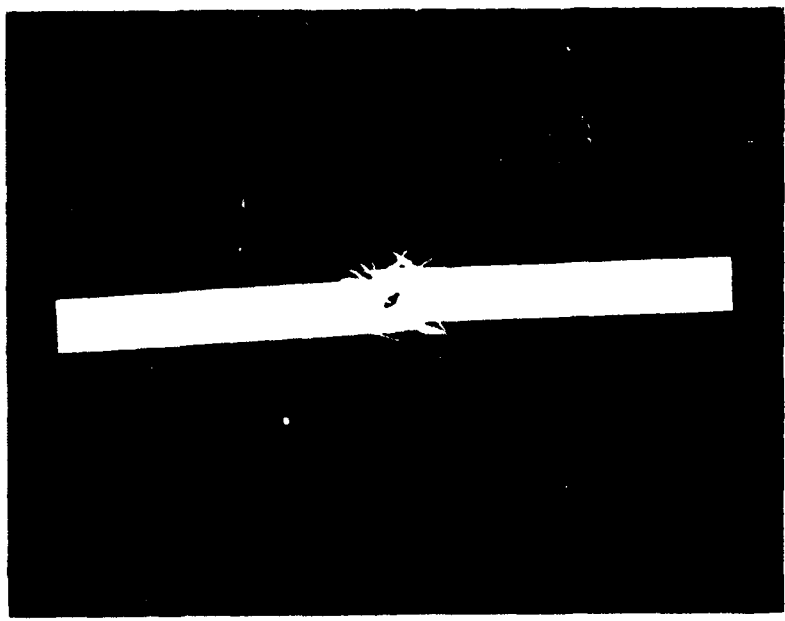


Figure B-30. 2G<sup>1</sup>-1 specimen.

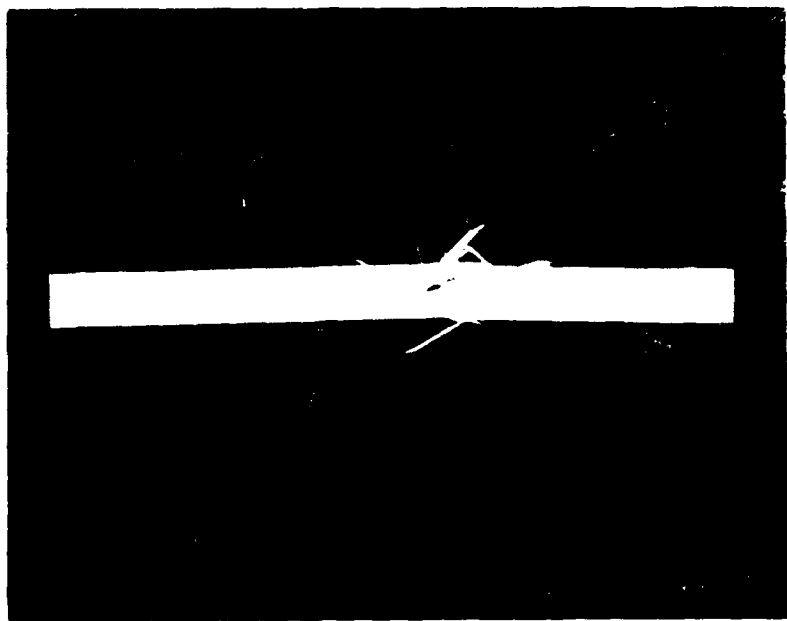


Figure H-31.  $20^0$ -5 specimen.

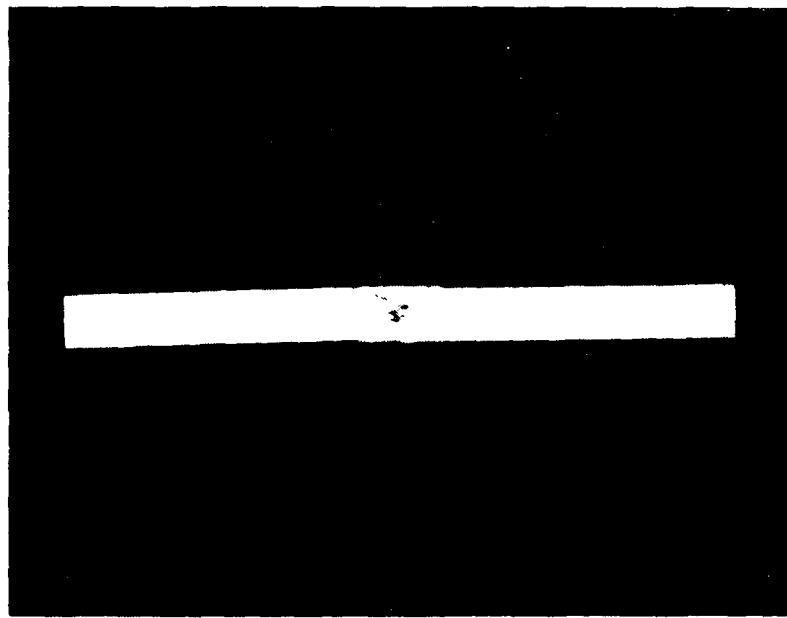


Figure H-32.  $20^0$ -6 specimen.



Figure H-33. 20<sup>0</sup>-7 specimen.

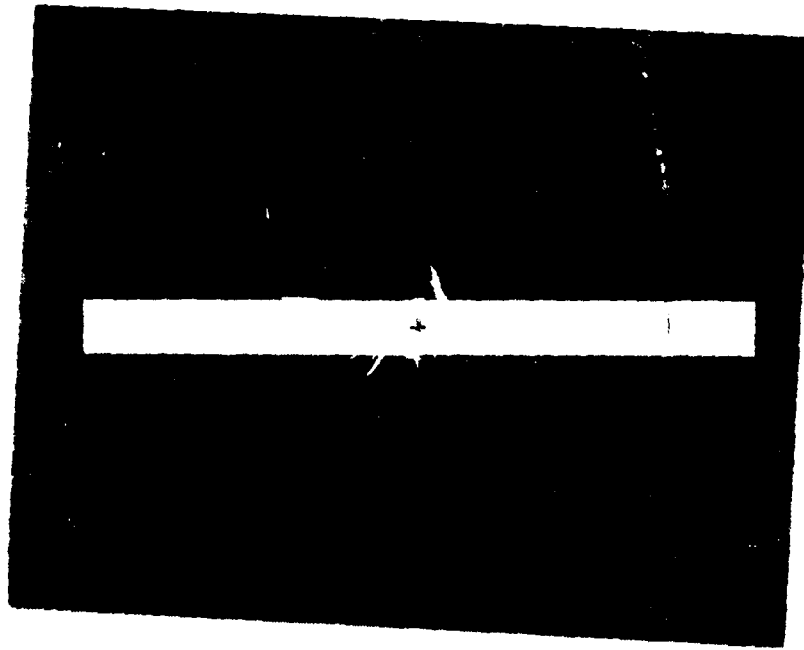


Figure H-34. 20<sup>0</sup>-7 specimen.

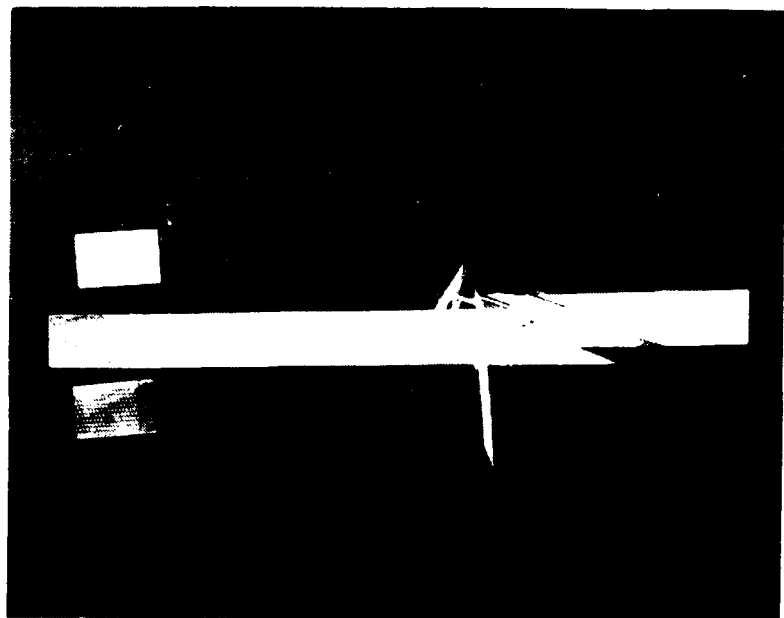


Figure H-35 . 20<sup>0</sup>-9 specimen.

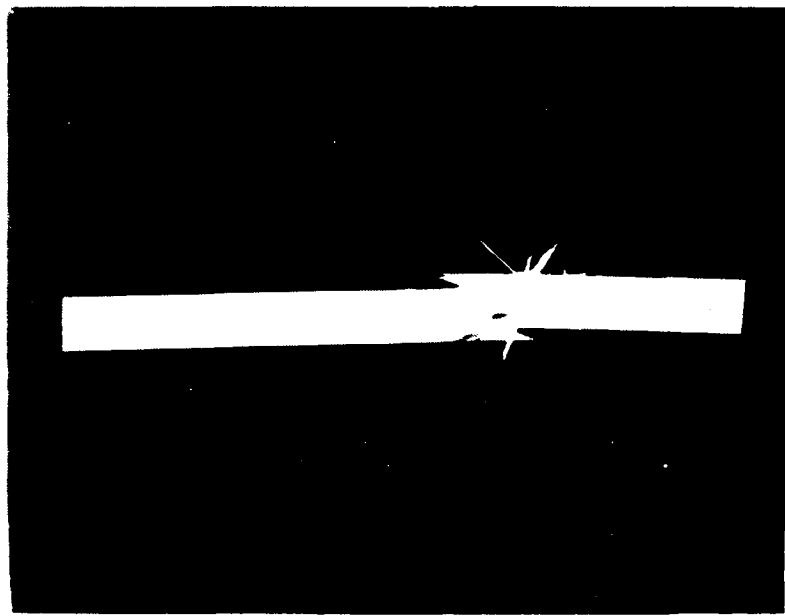


Figure H-36 . 20<sup>0</sup>-8 specimen.

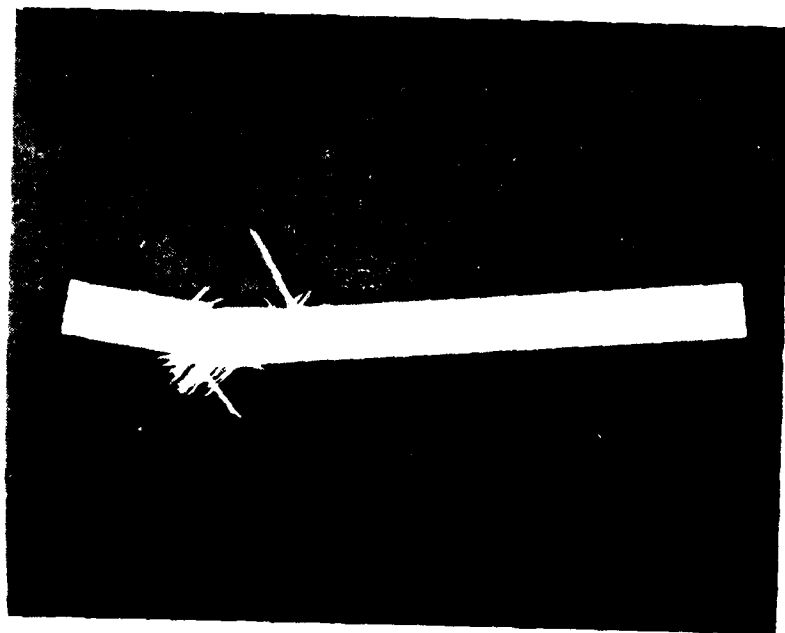


Figure H-37.  $20^0$ -C specimen.

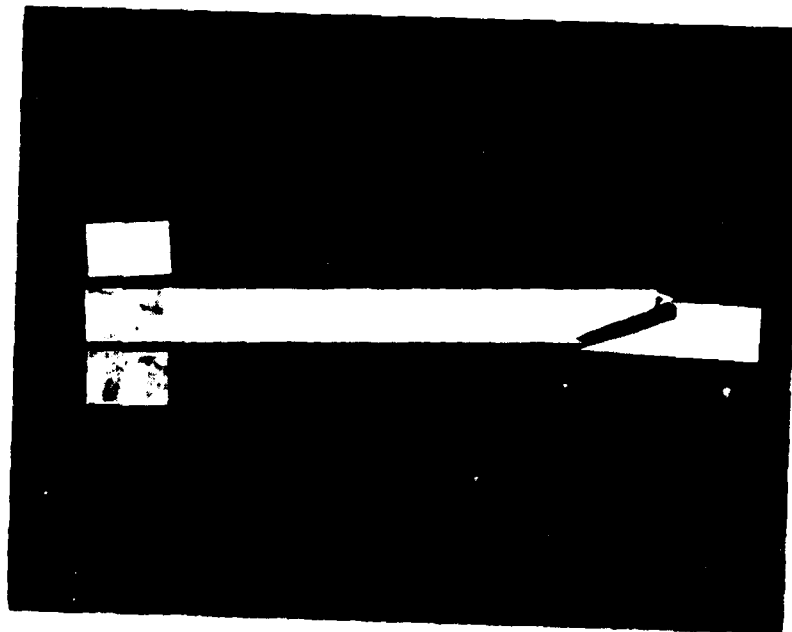


Figure H-39.  $20^0$ -D specimen.

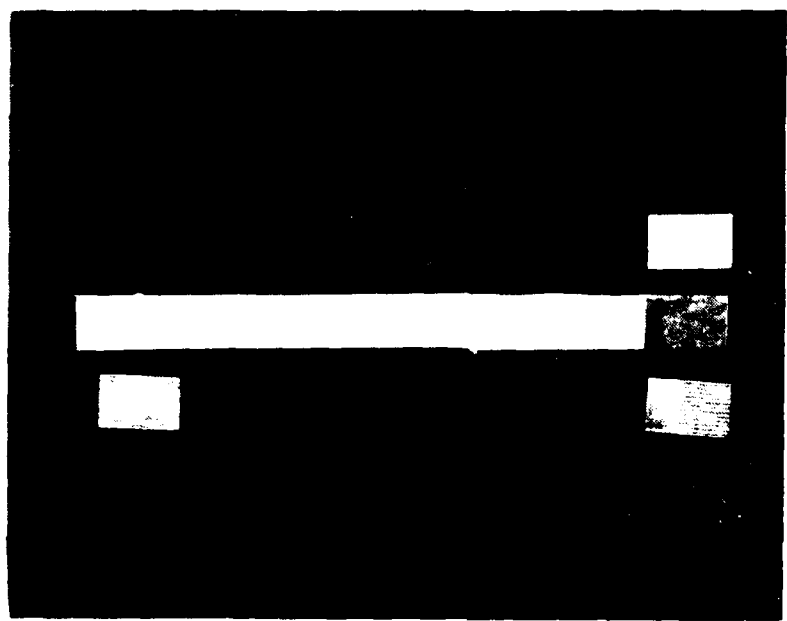


Figure H-39. 20°-E specimen.

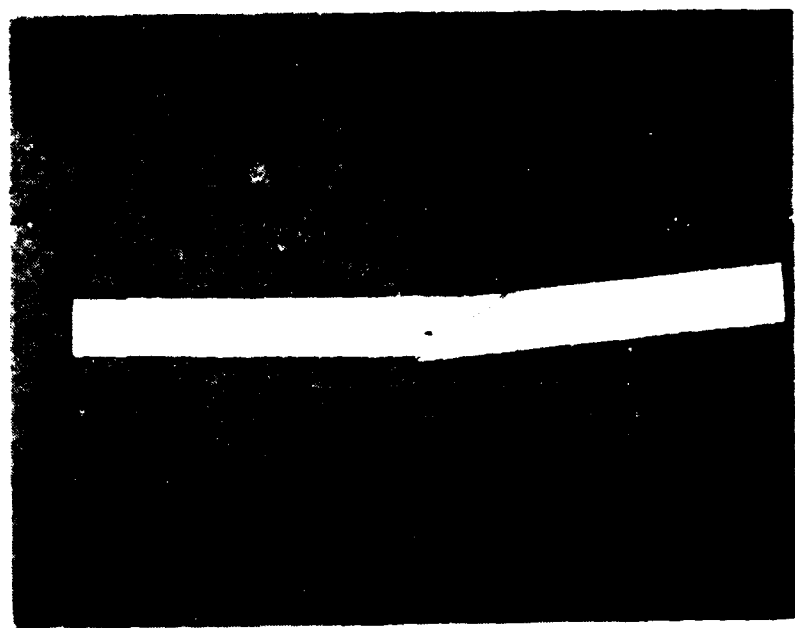


Figure H-40.  $30^0$ -1 specimen.

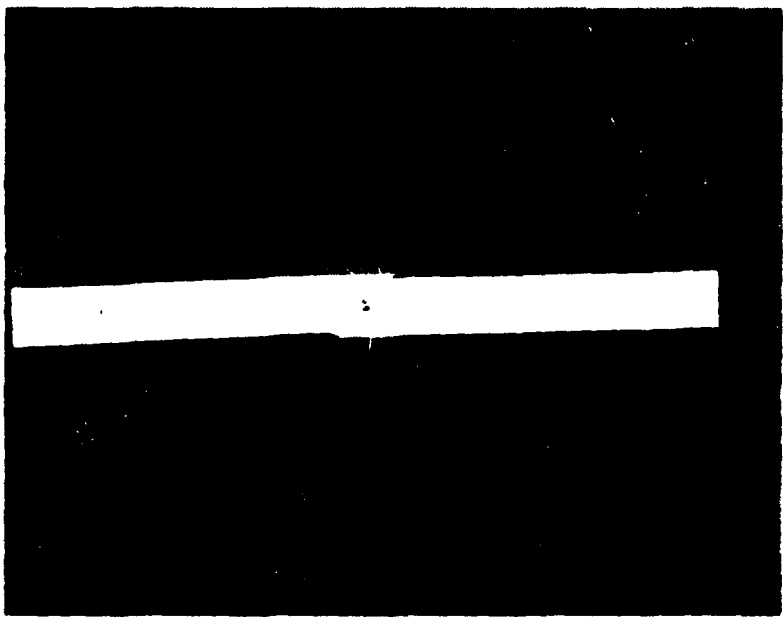


Figure H-41.  $30^0$ -2 specimen.

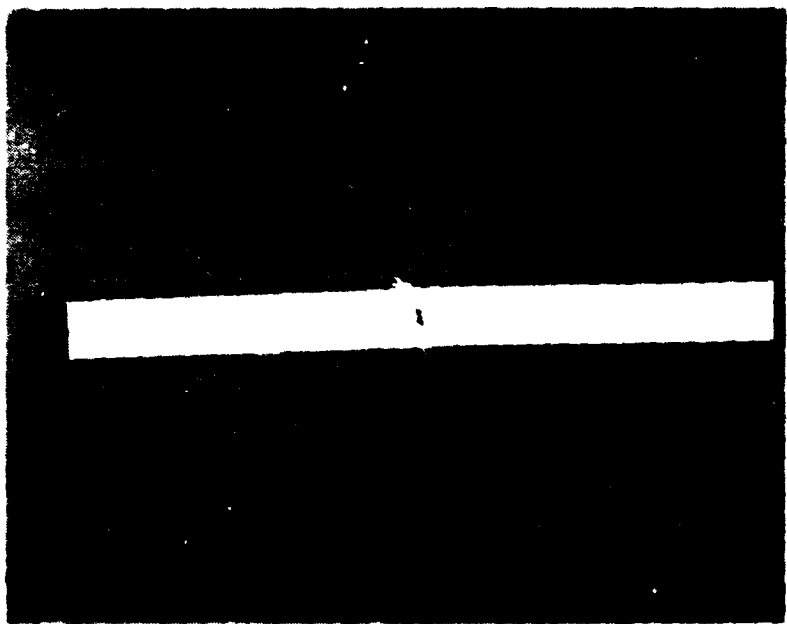


Figure H-42 . 30<sup>0</sup>-3 specimen.

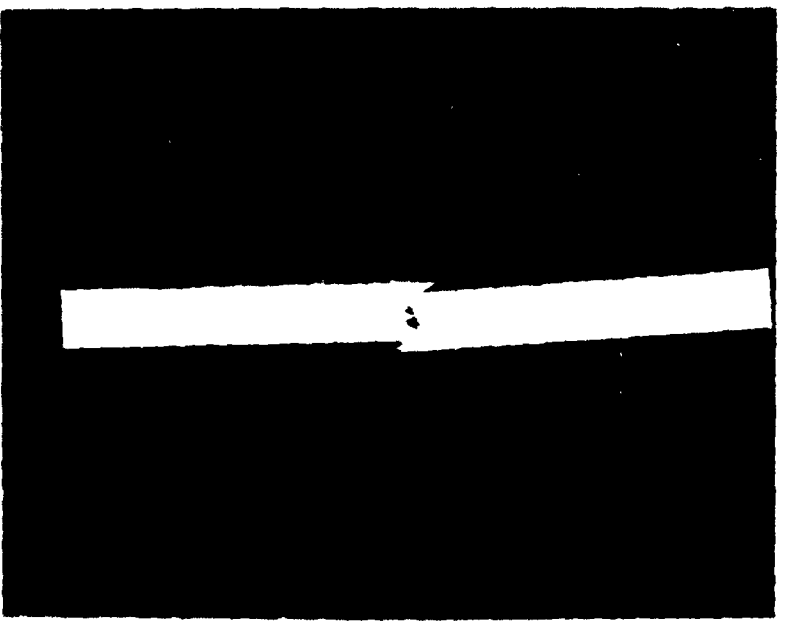


Figure H-43 . 30<sup>0</sup>-4 specimen.



Figure H-44.  $30^0$ -5 specimen.

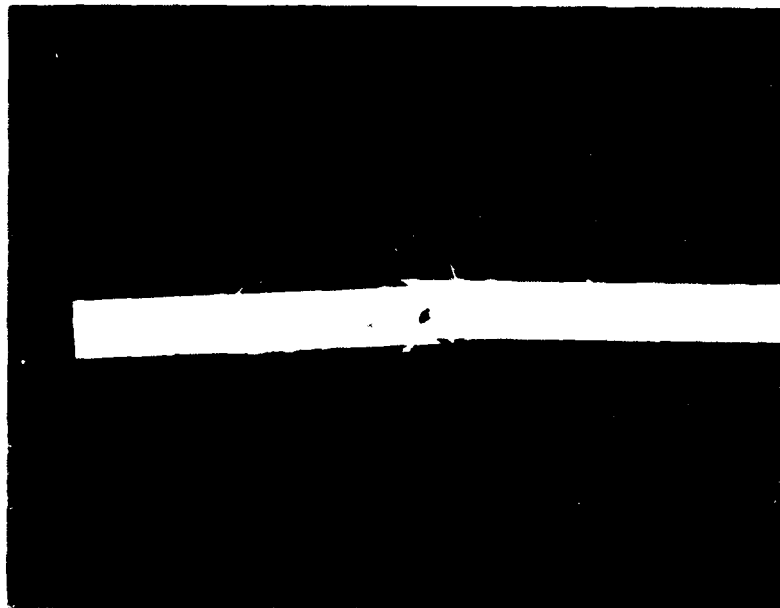


Figure H-45.  $30^0$ -6 specimen.

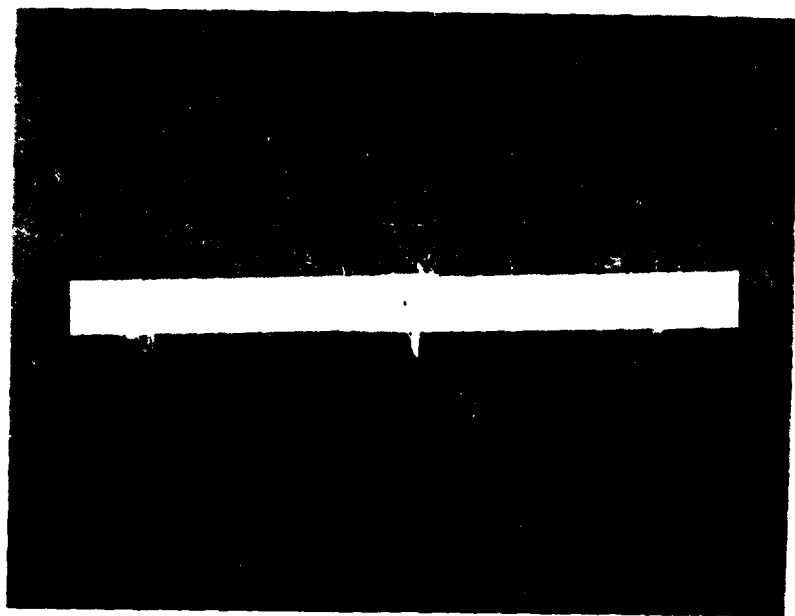


Figure H-46. 30<sup>0</sup>-7 specimen.



Figure H-47. 30<sup>0</sup>-8 specimen.



Figure H-48 . 30<sup>0</sup>-A specimen.

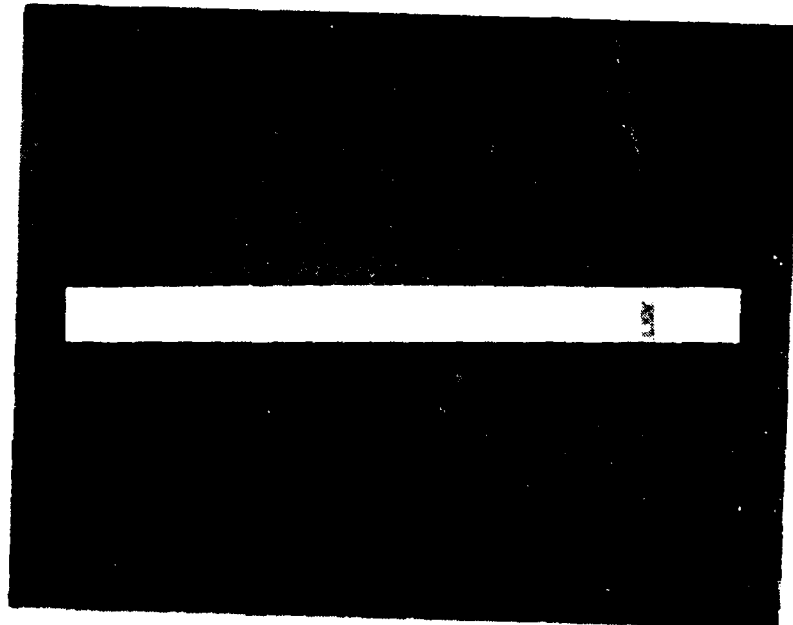


Figure H-49 . 30<sup>0</sup>-B specimen.

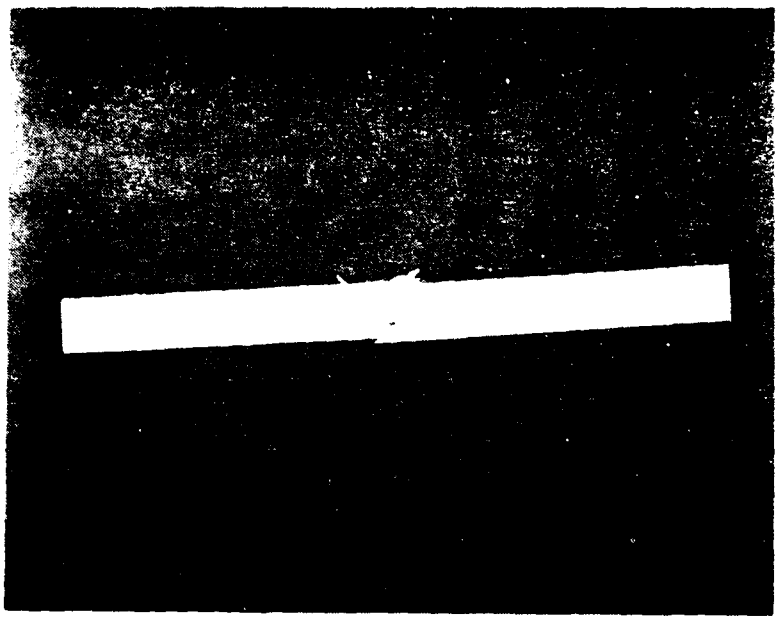


Figure H-50 . 30<sup>0</sup>-C specimen.

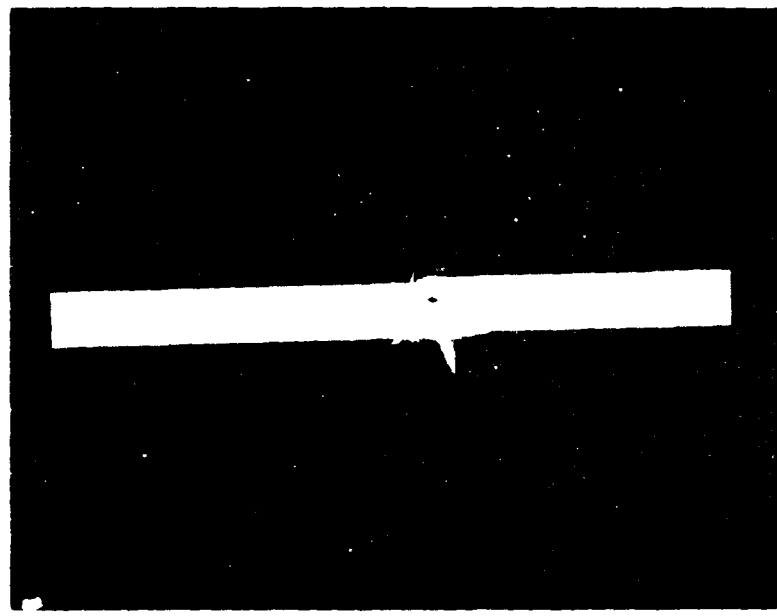


Figure H-51 . 30<sup>0</sup>-C specimen.

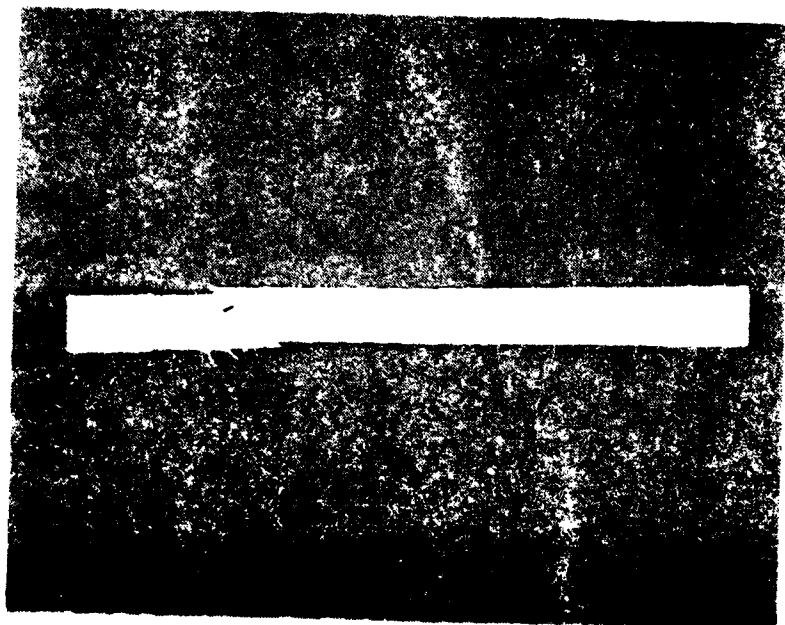


Figure H-52 . 30<sup>0</sup>-E specimen.

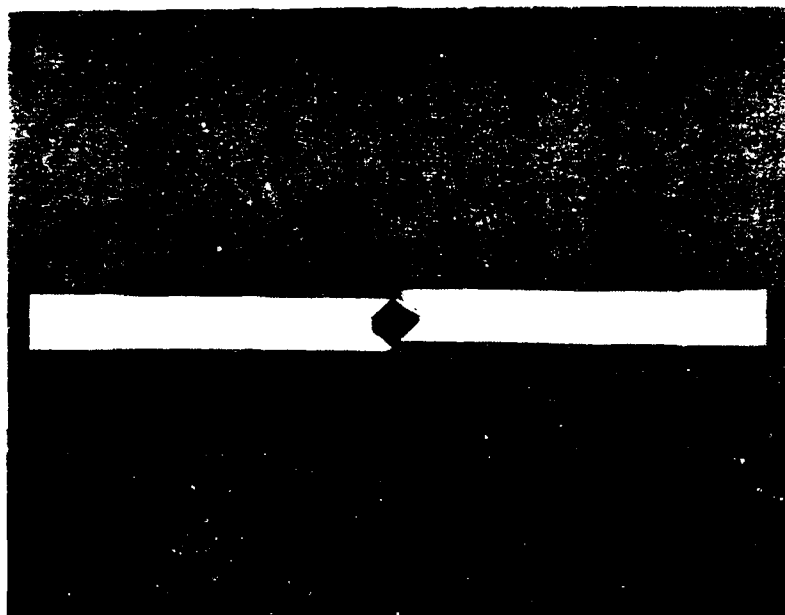


Figure H-53. 45°-1 specimen.

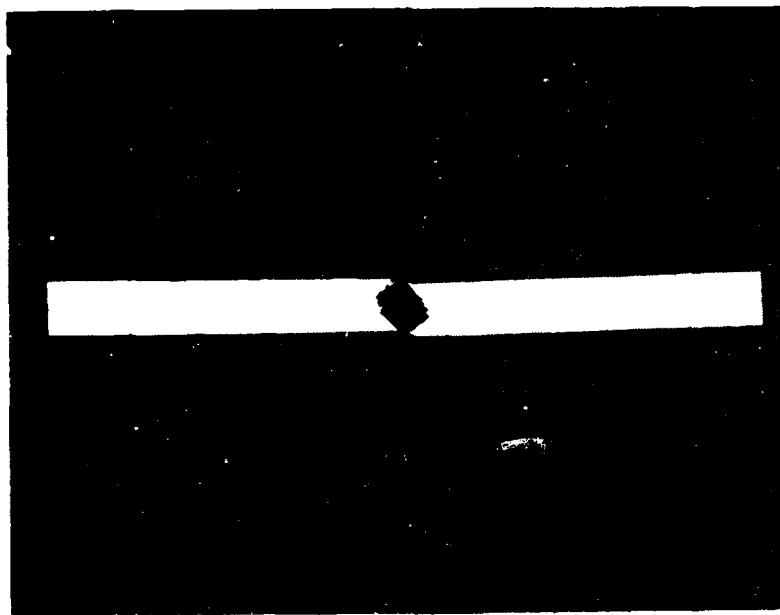


Figure H-54. 45°-1 specimen



Figure 11-55.  $\text{Al}^{10}\text{Li}$  specimen.

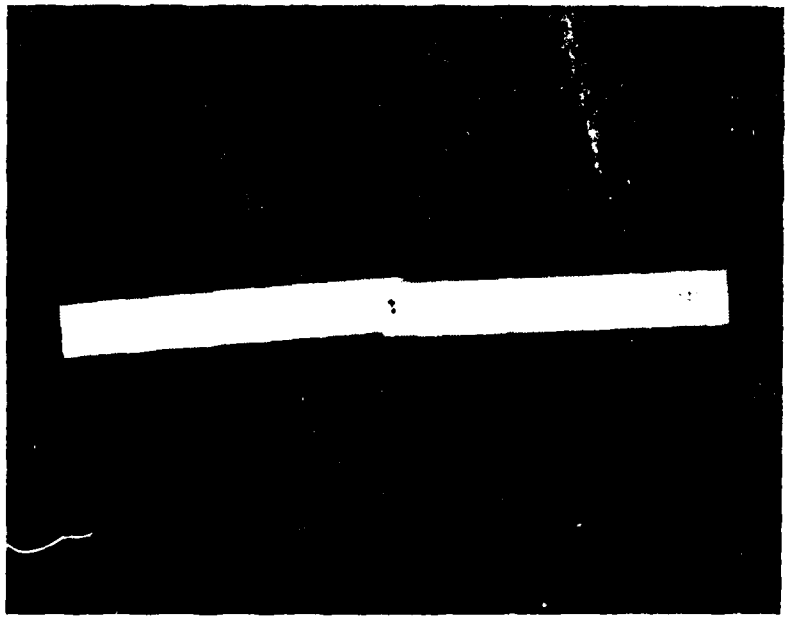


Figure 11-56.  $\text{Al}^{10}\text{Li}$  specimen.

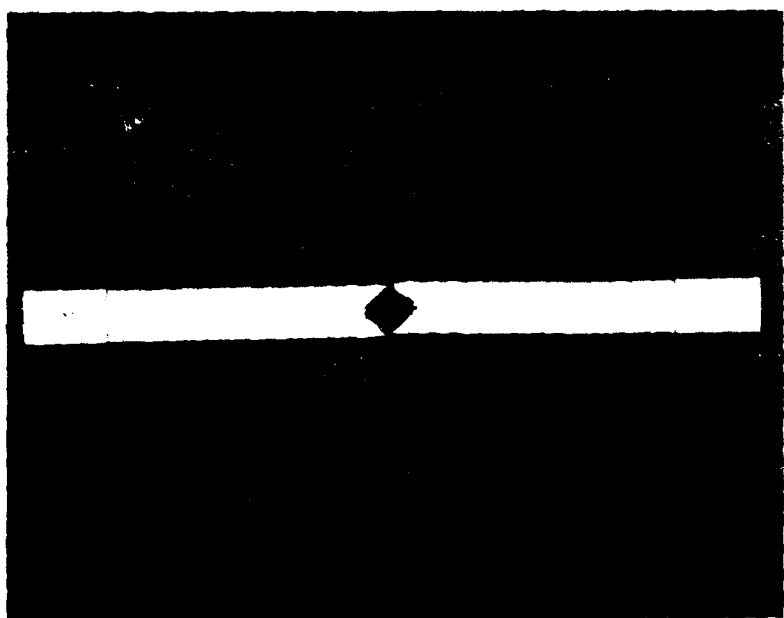


Figure H-57.  $45^0$ -5 specimen.

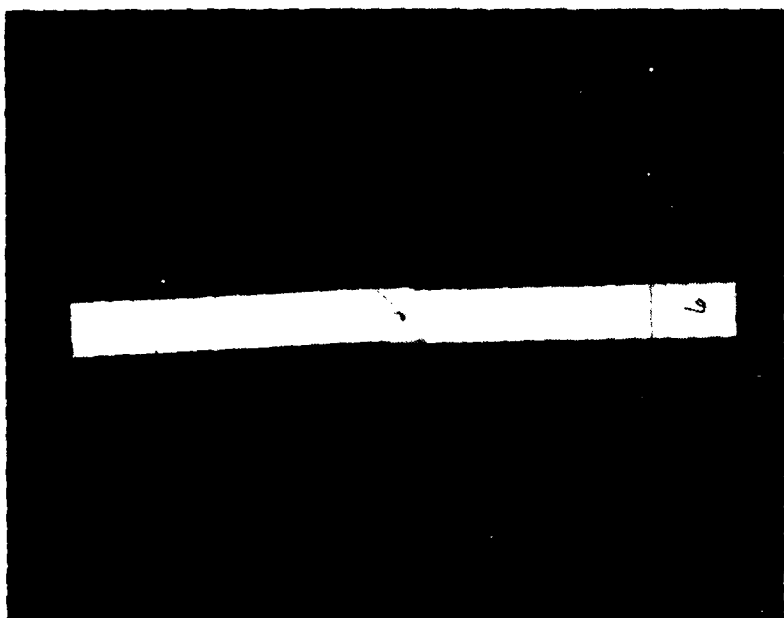


Figure H-58.  $45^0$ -6 specimen.

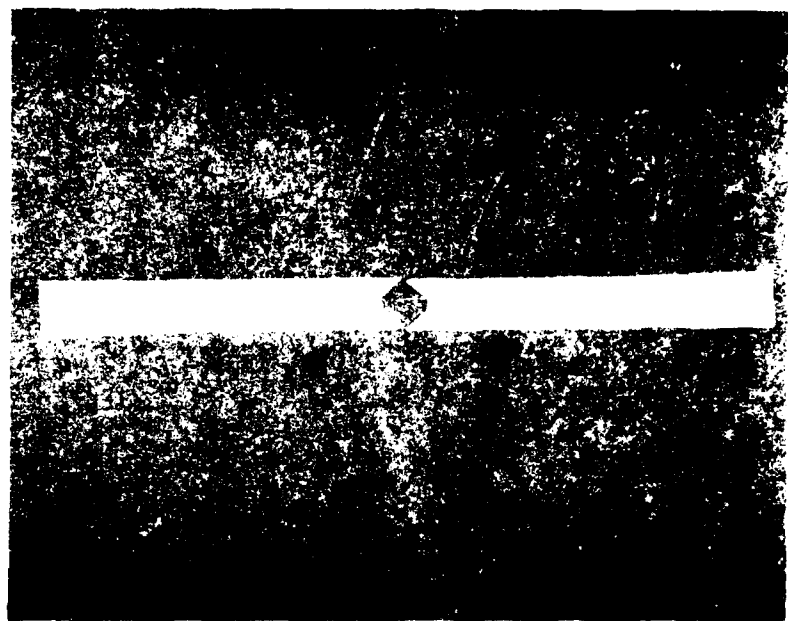


Figure H-59.  $45^0$ -7 specimen.

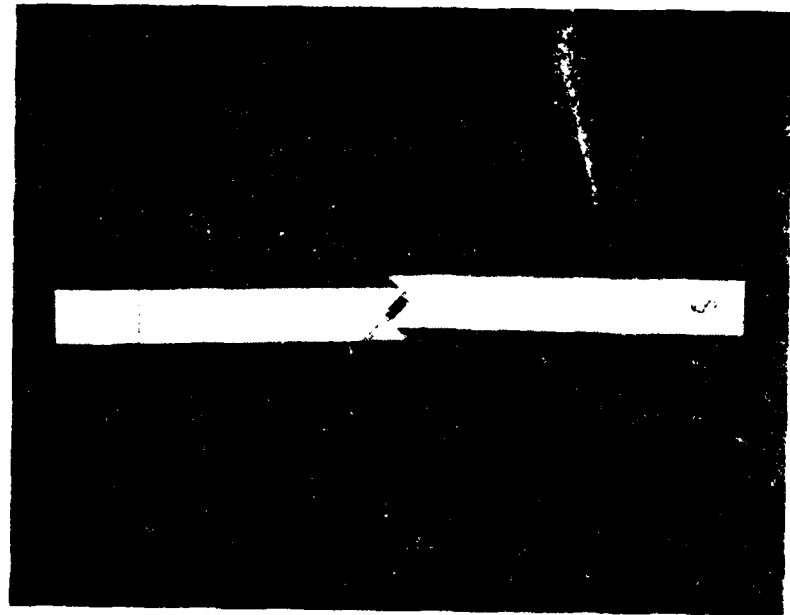


Figure H-60.  $45^0$ -7 specimen.

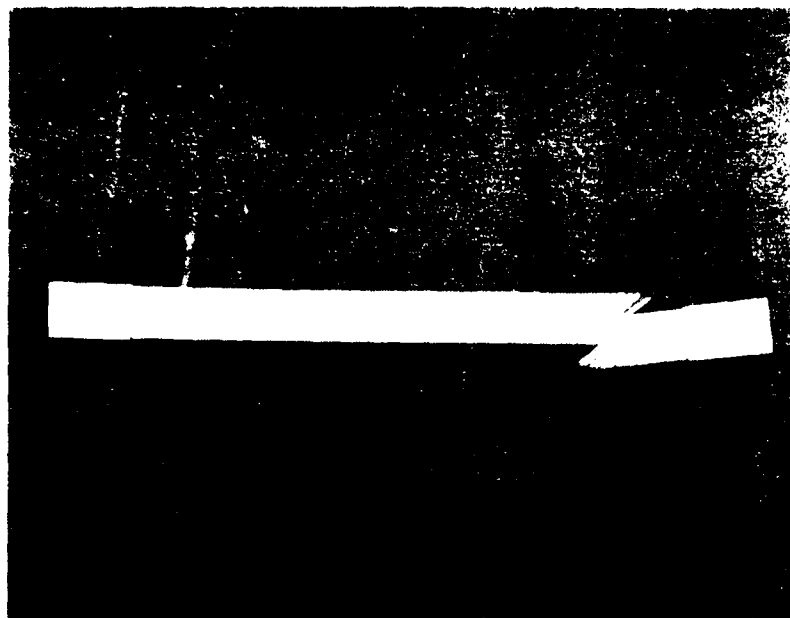


Figure H-61 . 45<sup>0</sup>-A specimen.

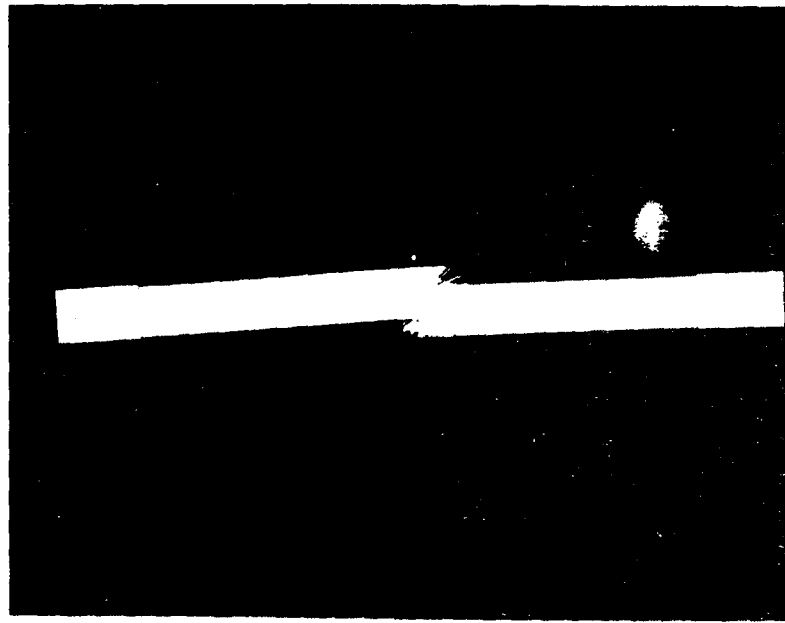


Figure H-61 . 45<sup>0</sup>-B specimen.



Figure H-63.  $45^0$ -C specimen.

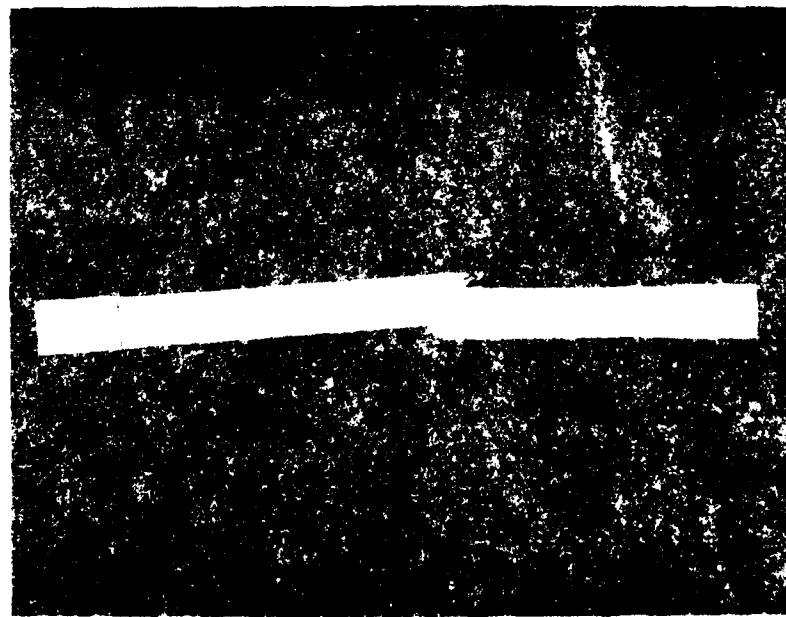


Figure H-64.  $45^0$ -C specimen.



Figure H-65. 45°-E specimen.

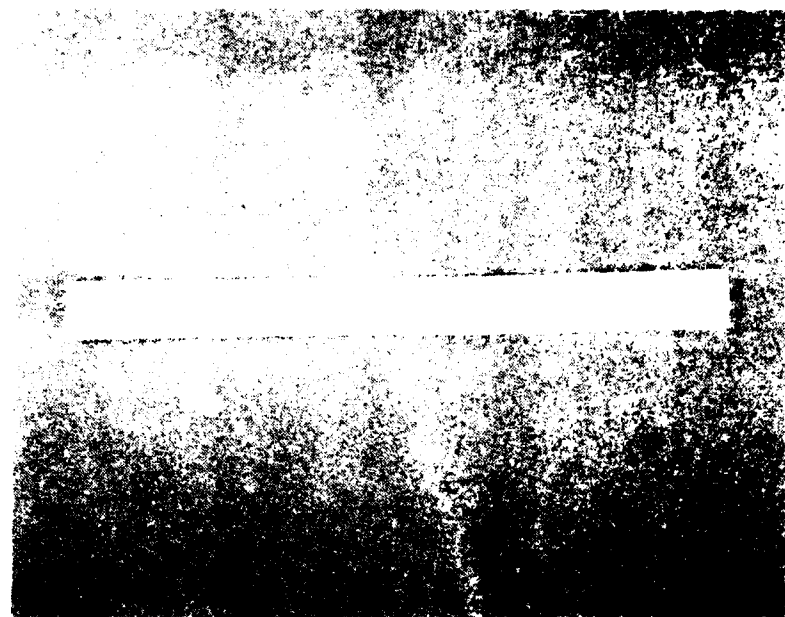


Figure H-66.  $\text{Fe}^{2+}$  specimen.

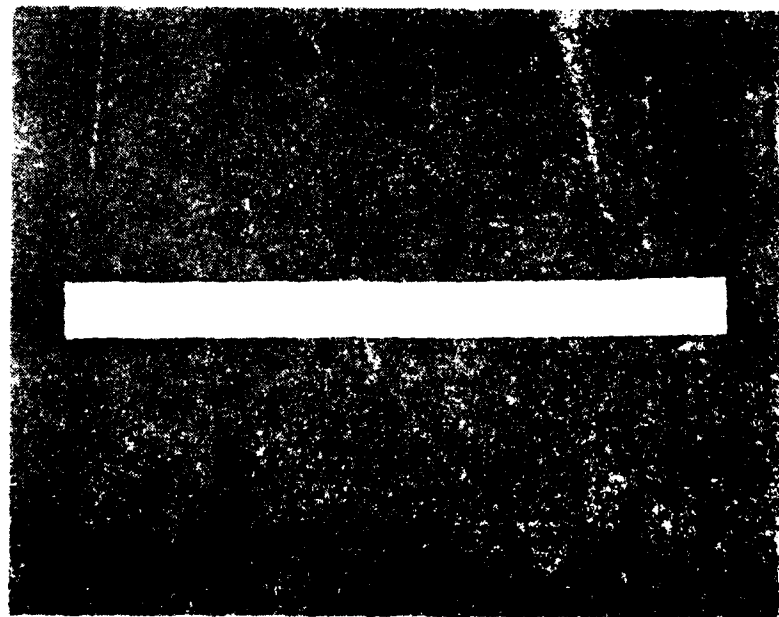


Figure H-67.  $\text{Fe}^{2+}$  specimen.

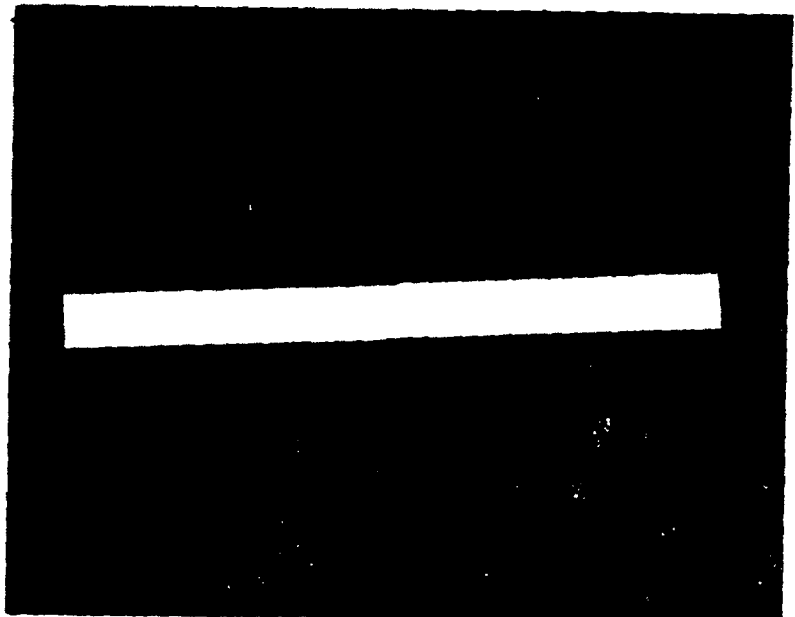


Figure H-68.  $60^0$ -3 specimen.



Figure H-69.  $60^0$ -4 specimen.

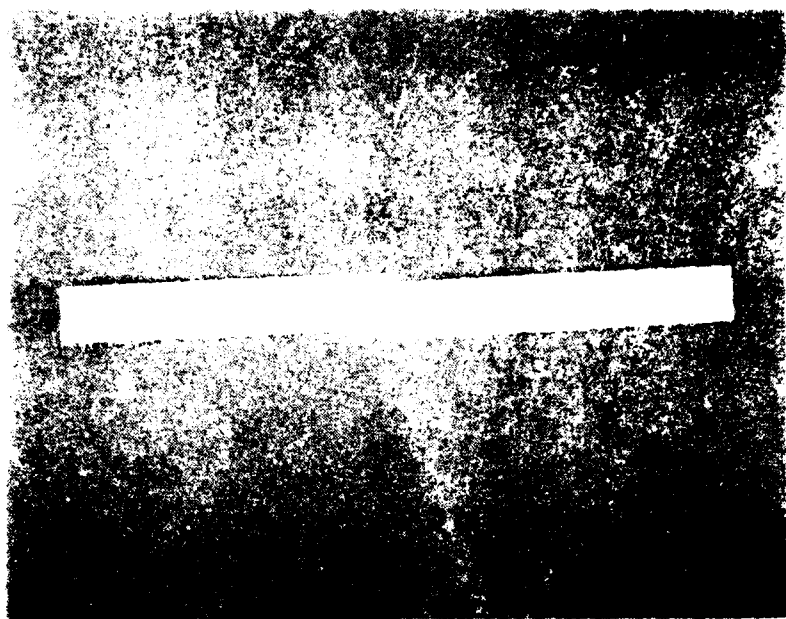


Figure H-70.  $60^0$ -5 specimen.



Figure H-71.  $60^0$ -5 specimen.

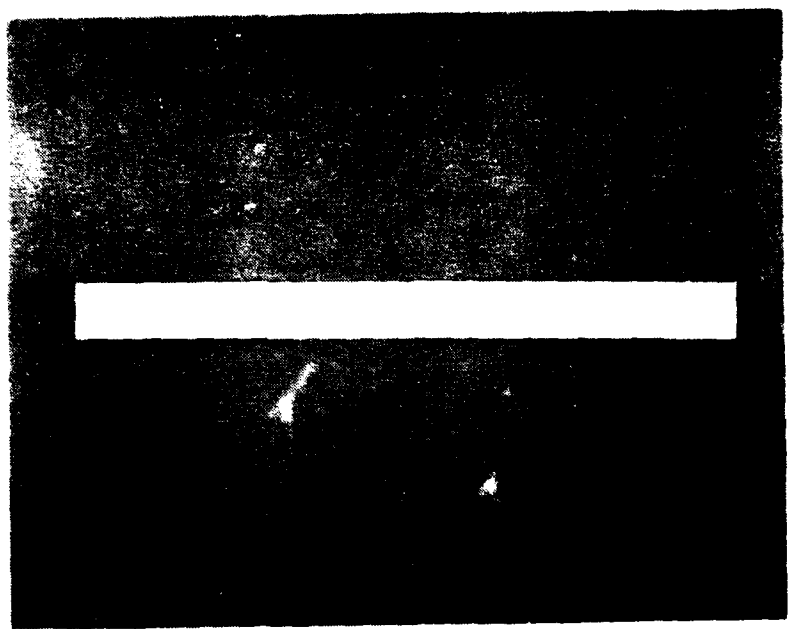


Figure H-72. 60°-7 specimen.

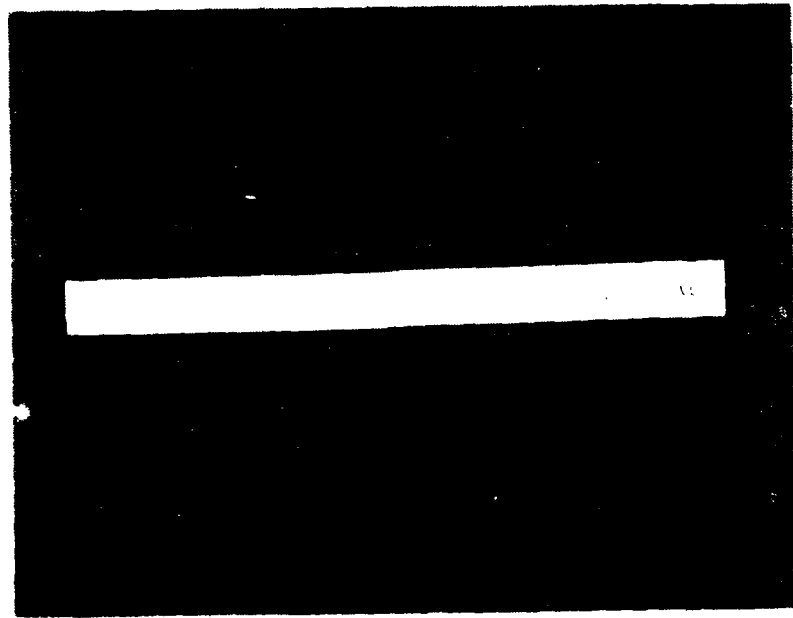


Figure H-73. 60°-3 specimen.



Figure H-74. 60<sup>0</sup>-A specimen.

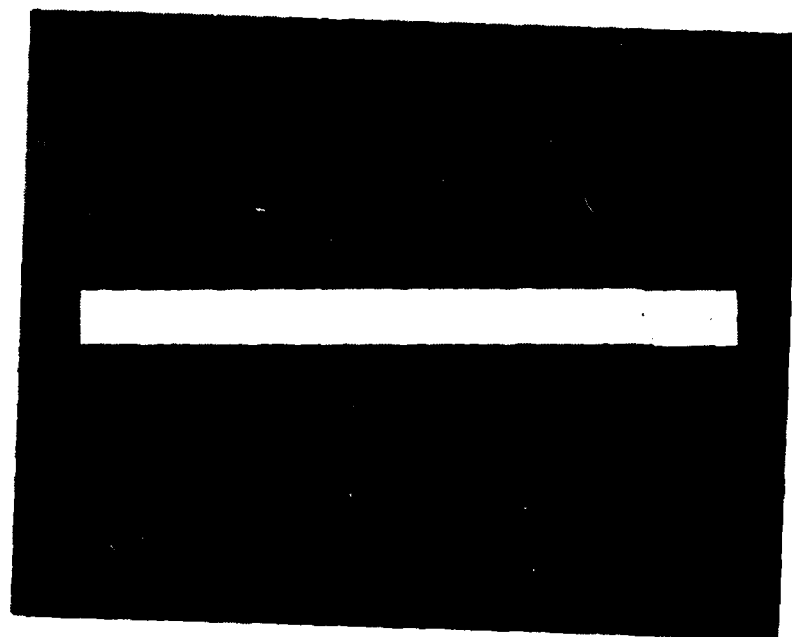


Figure H-75. 60<sup>0</sup>-B specimen.

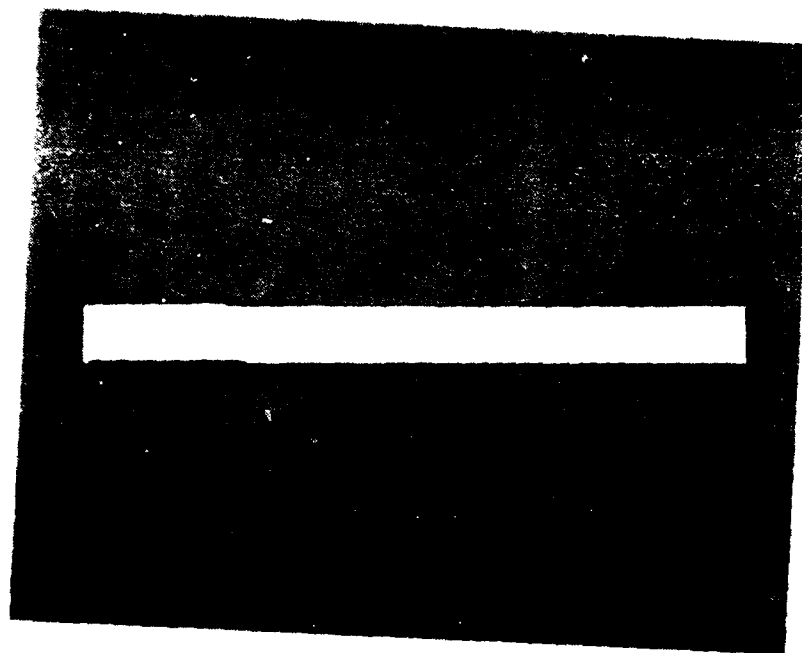


Figure H-76.  $60^0$ -C specimen.



Figure H-77.  $60^0$ -P specimen.

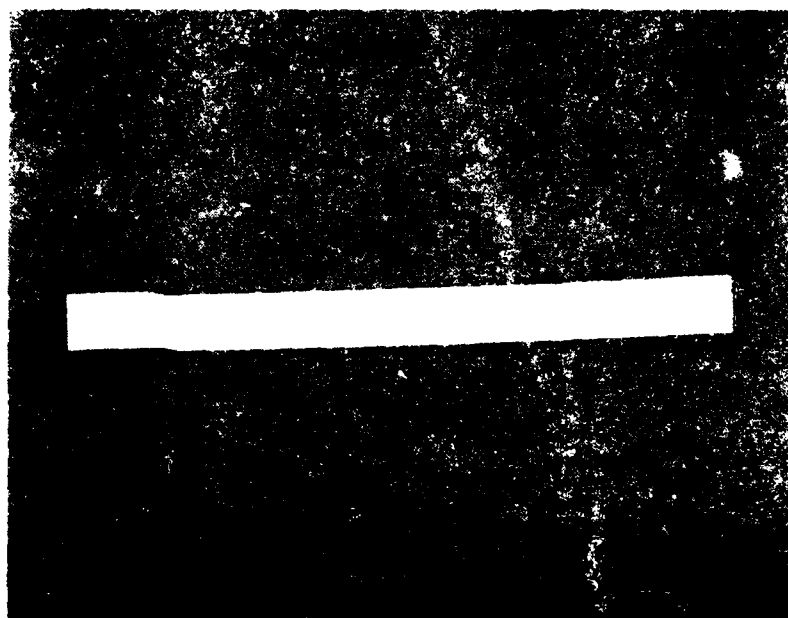


Figure H-78. 60<sup>0</sup>-F specimen.

APPENDIX I

This appendix contains the ultimate load data for each specimen obtained by testing to failure.

AD-A102 881 ARMY MISSILE COMMAND REDSTONE ARSENAL AL GROUND EQU--ETC F/G 11/4  
QUANTITATIVE ANALYSIS OF IMPACT DAMAGED COMPOSITE TENSION-TORSI--ETC(U)  
SEP 80 J A SCHAEFFEL  
DRSMI/RL-80-12-TR

UNCLASSIFIED

NL

3 of 3  
40 4  
13268

END  
DATE  
19-81  
DTIC

TABLE I-1. 0° WRAP ANGLE ULTIMATE STRENGTH TEST DATA

SPECIMEN NUMBER	ULTIMATE LOAD
1	5530 LB
2	4880 LB
3	7505 LB
4	6545 LB
5	6225 LB
6	6805 LB
7	6715 LB
8	5225 LB
A	8935 LB
B	8380 LB
C	9805 LB
D	9230 LB
E	9325 LB

AVERAGE ULTIMATE LOAD  
OF UNFLAWED SPECIMENS      = 9135 LB

MAXIMUM PERCENT DIFFERENCE  
OF UNFLAWED SPECIMENS'  
ULTIMATE LOAD      = 15.59%

TABLE I-2.  $\pm 15^\circ$  WRAP ANGLE ULTIMATE STRENGTH TEST DATA

SPECIMEN NUMBER	ULTIMATE LOAD
1	5190 LB
2	5055 LB
3	5400 LB
4	4640 LB
5	5285 LB
6	4630 LB
7	5490 LB
8	4725 LB
A	5545 LB
B	5320 LB
C	5290 LB
D	5445 LB
E	5225 LB

**AVERAGE ULTIMATE LOAD  
OF UNFLAWED SPECIMENS** = 5365 LB

**MAXIMUM PERCENT DIFFERENCE  
OF UNFLAWED SPECIMENS'  
ULTIMATE LOAD** = **5.96%**

TABLE I-3.  $\pm 20^{\circ}$  WRAP ANGLE ULTIMATE STRENGTH TEST DATA

SPECIMEN NUMBER	ULTIMATE LOAD
1	4780 LB
2	4285 LB
3	4605 LB
4	4295 LB
5	4665 LB
6	4365 LB
7	4680 LB
8	4075 LB
A	4790 LB
B	4885 LB
C	4715 LB
D	4305 LB
E	4610 LB

AVERAGE ULTIMATE LOAD  
OF UNFLAWED SPECIMENS = 4661 LB

MAXIMUM PERCENT DIFFERENCE  
OF UNFLAWED SPECIMENS'  
ULTIMATE LOAD = 5.90%

TABLE I-4 .  $\pm 30^{\circ}$  WRAP ANGLE ULTIMATE STRENGTH TEST DATA

SPECIMEN NUMBER	ULTIMATE LOAD
1	3735 LB
2	3310 LB
3	3475 LB
4	2960 LB
5	3545 LB
6	3270 LB
7	3435 LB
8	3120 LB
A	3560 LB
B	3785 LB
C	3755 LB
D	3765 LB
E	3720 LB

AVERAGE ULTIMATE LOAD  
OF UNFLAWED SPECIMENS = 3717 LB

MAXIMUM PERCENT DIFFERENCE  
OF UNFLAWED SPECIMENS'  
ULTIMATE LOAD = 6.05%

TABLE I-5 .  $\pm 45^{\circ}$  WRAP ANGLE ULTIMATE STRENGTH TEST DATA

SPECIMEN NUMBER	ULTIMATE LOAD
1	1382 LB
2	1068 LB
3	1284 LB
4	980 LB
5	1382 LB
6	958 LB
7	1382 LB
8	1095 LB
A	1538 LB
B	1616 LB
C	1635 LB
D	1566 LB
E	1570 LB

AVERAGE ULTIMATE LOAD  
OF UNFLAWED SPECIMENS      = 1585 LB

MAXIMUM PERCENT DIFFERENCE  
OF UNFLAWED SPECIMENS'  
ULTIMATE LOAD      = 6.11%

TABLE I-6.  $\pm 60^\circ$  WRAP ANGLE ULTIMATE STRENGTH TEST DATA

SPECIMEN NUMBER	ULTIMATE LOAD
1	287 LB
2	165 LB
3	340 LB
4	137 LB
5	228 LB
6	147 LB
7	378 LB
8	219 LB
A	594 LB
B	488 LB
C	593 LB
D	563 LB
E	545 LB

AVERAGE ULTIMATE LOAD  
OF UNFLAWED SPECIMENS      = 556.6 LB

MAXIMUM PERCENT DIFFERENCE  
OF UNFLAWED SPECIMENS'  
ULTIMATE LOAD      = 19.04%

TABLE I-7. 0° WRAP ANGLE PERCENT DIFFERENCES IN ULTIMATE STRENGTH TEST DATA

SPECIMEN NUMBER	% DIFFERENCE IN ULTIMATE STRENGTH FROM THE AVERAGE UNFLAWED SPECIMEN ULTIMATE LOAD	% DIFFERENCE IN ULTIMATE STRENGTH DUE TO LOADING ENERGY
1	39.46%	+ 12.48%
2	46.57%	- 12.48%
3	17.84%	+ 13.66%
4	28.35%	- 15.66%
5	31.85%	- 8.90%
6	25.50%	+ 8.90%
7	26.49%	+ 24.95%
8	42.80%	- 24.95%

TABLE 1-8. + 15° WRAP ANGLE PERCENT DIFFERENCES IN ULTIMATE STRENGTH TEST DATA

SPECIMEN NUMBER	% DIFFERENCE IN ULTIMATE STRENGTH FROM THE AVERAGE UNFLAWED SPECIMEN ULTIMATE LOAD	% DIFFERENCE IN ULTIMATE STRENGTH DUE TO LOADING ENERGY
1	3.26%	+ 2.63%
2	5.77%	- 2.63%
3	-.65%	+ 15.13%
4	13.51%	- 15.13%
5	1.49%	+ 13.21%
6	13.69%	- 13.21%
7	-2.32%	+ 14.97%
8	11.92%	- 14.97%

TABLE 1-9 . + 20<sup>0</sup> WRAP ANGLE PERCENT DIFFERENCES IN ULTIMATE STRENGTH TEST DATA

SPECIMEN NUMBER	% DIFFERENCE IN ULTIMATE STRENGTH FROM THE AVERAGE UNFLAWED SPECIMEN ULTIMATE LOAD	% DIFFERENCE IN ULTIMATE STRENGTH DUE TO LOADING ENERGY
1	-2.55%	+ 10.92%
2	8.06%	- 10.92%
3	1.20%	+ 6.96%
4	7.85%	- 6.96%
5	- .0858%	+ 6.64%
6	6.35%	- 6.64%
7	- .407%	+ 13.82%
8	12.57%	- 13.82%

TABLE I-10.  $+30^\circ$  WRAP ANGLE PERCENT DIFFERENCES IN ULTIMATE STRENGTH TEST DATA

SPECIMEN NUMBER	% DIFFERENCE IN ULTIMATE STRENGTH FROM THE AVERAGE UNFLAWED SPECIMEN ULTIMATE LOAD	% DIFFERENCE IN ULTIMATE STRENGTH DUE TO LOADING ENERGY
1	4.84%	+ 12.06%
2	10.94%	- 12.06%
3	6.51%	+ 16.00%
4	20.36%	- 16.00%
5	4.62%	+ 8.07%
6	12.02%	- 8.07%
7	7.58%	+ 9.60%
8	16.06%	- 9.60%

TABLE I-11.  $+ 45^\circ$  WRAP ANGLE PERCENT DIFFERENCES IN ULTIMATE STRENGTH TEST DATA

SPECIMEN NUMBER	% DIFFERENCE IN ULTIMATE STRENGTH FROM THE AVERAGE UNFLAWED SPECIMEN ULTIMATE LOAD	% DIFFERENCE IN ULTIMATE STRENGTH DUE TO LOADING ENERGY
1	12.80%	+ 25.63%
2	32.61%	- 25.63%
3	18.99%	+ 26.85%
4	38.17%	- 26.85%
5	12.80%	+ 36.23%
6	39.55%	- 36.23%
7	12.80%	+ 23.17%
8	30.91%	- 23.17%

TABLE I-12 . + 60° WRAP ANGLE PERCENT DIFFERENCES IN ULTIMATE STRENGTH TEST DATA

SPECIMEN NUMBER	% DIFFERENCE IN ULTIMATE STRENGTH FROM THE AVERAGE UNFLAWED SPECIMEN ULTIMATE LOAD	% DIFFERENCE IN ULTIMATE STRENGTH DUE TO LOADING ENERGY
1	48.43%	+ 53.98%
2	70.35%	- 53.98%
3	38.91%	+ 85.11%
4	75.38%	- 85.11%
5	59.03%	+ 43.20%
6	73.58%	- 43.20%
7	32.08%	+ 53.26%
8	60.65%	- 53.26%

APPENDIX J

This appendix contains a summary of the ultimate failure load  
for the test specimens.

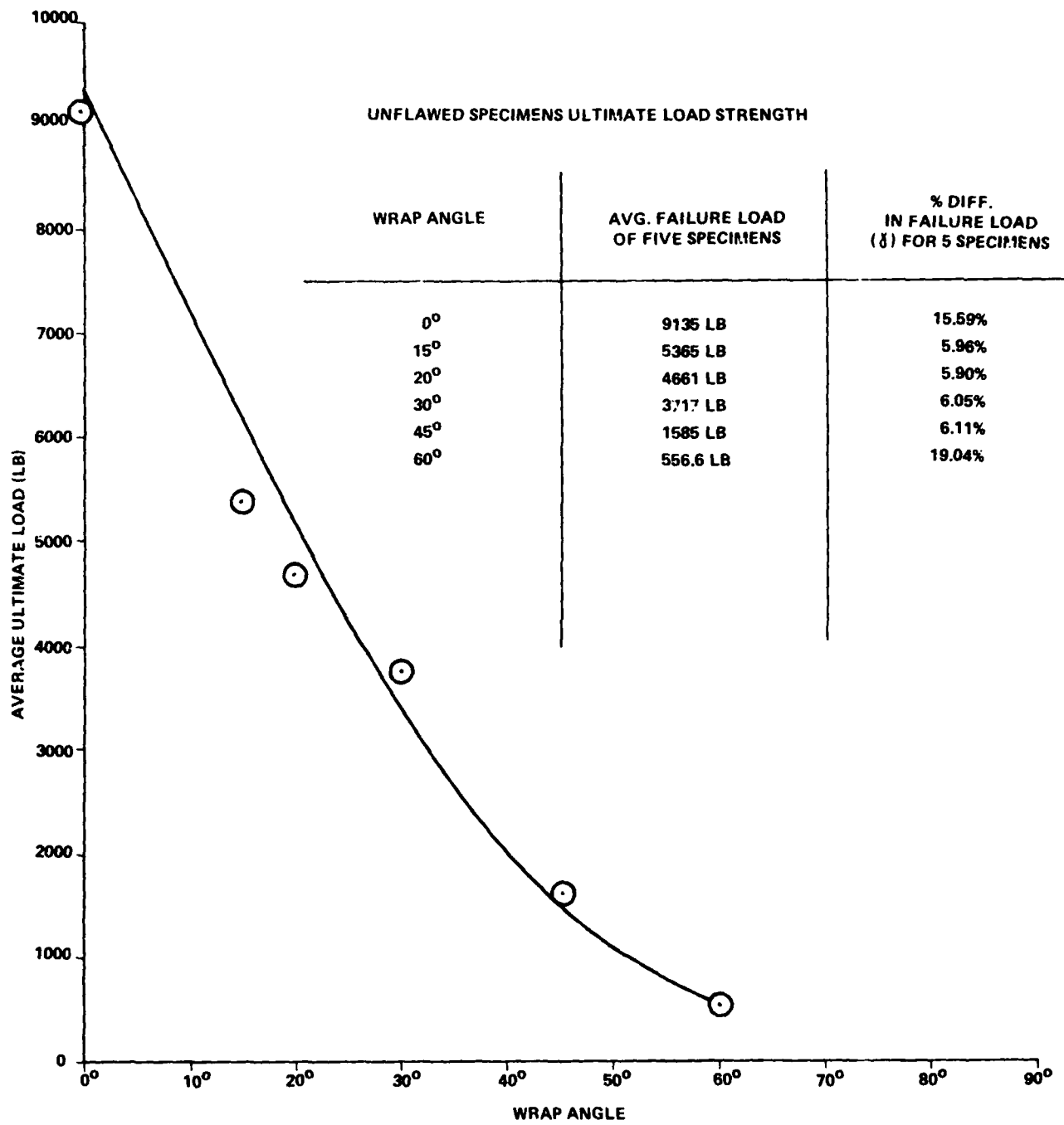


Figure J-1. Ultimate failure load versus wrap angle for unflawed tensile specimens.

TABLE J-1 . ULTIMATE FAILURE LOADS OF TENSILE SPECIMENS DYNAMICALLY IMPACTED WITH 41.184 IN-LB OF ENERGY

WRAP ANGLE	SPECIMEN NO.				UNFLAWED AVG. LOAD	8%
	1 JASJ	3	5	7		
0°	5530	7505	6225	6715	9135	15.59%
15°	5190	5400	5285	5490	5365	5.96
20°	4780	4605	4665	4680	4661	5.90
30°	3735	3475	3545	3435	3717	6.05
45°	1382	1284	1382	1382	1585	6.11
60°	287	340	228	378	556.6	14.04

TABLE J-2 . ULTIMATE FAILURE LOADS OF TENSILE SPECIMENS DYNAMICALLY IMPACTED WITH 87.264 IN-LB OF ENERGY

WRAP ANGLE	SPECIMEN NO.				UNFLAWED AVG. LOAD	8%
	1 JASJ	3	5	7		
0°	4880	6545	6805	5225	9135	15.59
15°	5055	4640	4630	4725	5365	5.96
20°	4285	4295	4365	4075	4661	5.90
30°	3310	2960	3270	3120	3717	6.05
45°	1068	980	958	1095	1585	6.11
60°	165	137	147	219	556.6	14.04

TABLE J-3 . PERCENT DECREASE IN ULTIMATE FAILURE LOAD FOR TENSILE SPECIMENS DYNAMICALLY IMPACTED WITH 41.184 IN-LB OF ENERGY

WRAP ANGLE	SPECIMEN NUMBER			
	1	3	5	7
0°	39.46	17.84	31.85	26.49
15°	3.26	-.65	1.49	-2.32
20°	-2.55	1.20	-.0858	-.407
30°	4.84	6.51	4.62	7.58
45°	12.80	18.99	12.80	12.80
60°	48.43	38.91	59.03	32.08

TABLE J-4 . PERCENT DECREASE IN ULTIMATE FAILURE LOAD FOR TENSILE SPECIMENS DYNAMICALLY IMPACTED WITH 87.264 IN-LB OF ENERGY

WRAP ANGLE	SPECIMEN NUMBER			
	2	4	6	8
0°	46.57	28.35	25.50	42.80
15°	5.77	13.51	13.69	11.92
20°	8.06	7.85	6.35	12.57
30°	10.94	20.36	12.02	16.06
45°	32.61	38.17	39.55	30.91
60°	70.35	75.38	73.58	60.65

TABLE J-5 . PERCENT DECREASE IN ULTIMATE FAILURE LOAD FOR TENSILE SPECIMENS LOADED WITH 87,264 IN-LB OF DYNAMIC IMPACT LOAD VERSUS THOSE LOADED WITH 41,184 IN-LB FOR THE SAME TYPE FLOW TYPE FLAW TYPE

WRAP ANGLE	SPECIMENS				
	1-2	3-4	5-6	7-8	
0°	12.48	13.66	- 8.90	24.95	
15°	2.63	15.13	13.21	14.97	
20°	10.92	6.96	6.64	13.82	
30°	12.06	16.00	8.07	9.60	
45°	25.63	26.85	36.23	23.17	
60°	53.98	85.11	43.20	53.26	

APPENDIX K

This appendix contains a summary of the laser speckle interferometry data.

TABLE K-1 . AVERAGE VALUES OF  $\beta$  FOR ALL THE FLANGE SPECIMEN CONDITIONS EXAMINED ( $\beta_1$ )

SPECIMEN ROTATION ANGLE	WRAP ANGLE					$60^\circ$
	$0^\circ$	$15^\circ$	$20^\circ$	$30^\circ$	$45^\circ$	
$0^\circ$	.336	.330	.376	.414	.700	2.806
$10^\circ$	.178	.243	.332	.369	.471	2.729
$20^\circ$	.164	.240	.358	.380	.439	2.632
$30^\circ$	.146	.269	.416	.430	.476	2.684
AVERAGES =	.206	.270	.370	.398	.521	2.712

TABLE K-2 . VALUES OF  $\beta$  FOR ALL THE UNFLAWED SPECIMEN CONDITIONS EXAMINED (82)

SPECIMEN ROTATION ANGLE	WRAP ANGLE					
	0°	15°	20°	30°	45°	60°
0°	.253	.297	.450	.371	.705	.710
10°	.165	.222	.355	.174	.837	.333
20°	.165	.266	.357	.230	.866	.319
30°	.208	.232	.307	.245	.888	.436
AVERAGES =	.791	.452	.367	.255	.824	.449

TABLE K-3 . AVERAGE ULTIMATE FAILURE LOADS OF SPECIMENS

WRAP ANGLE	AVERAGE FAILURE LOAD OF FLAWED SPECIMENS $L_1$ (LBS)	AVERAGE FAILURE LOAD OF UNFLAWED SPECIMENS $L_2$ (LBS)	$L_1$ $L_2$
0°	6178	9135	.676
15°	5051	5365	.941
20°	4468	4661	.958
30°	3356	3717	.902
45°	1191	1585	.751
60°	237	556	.426

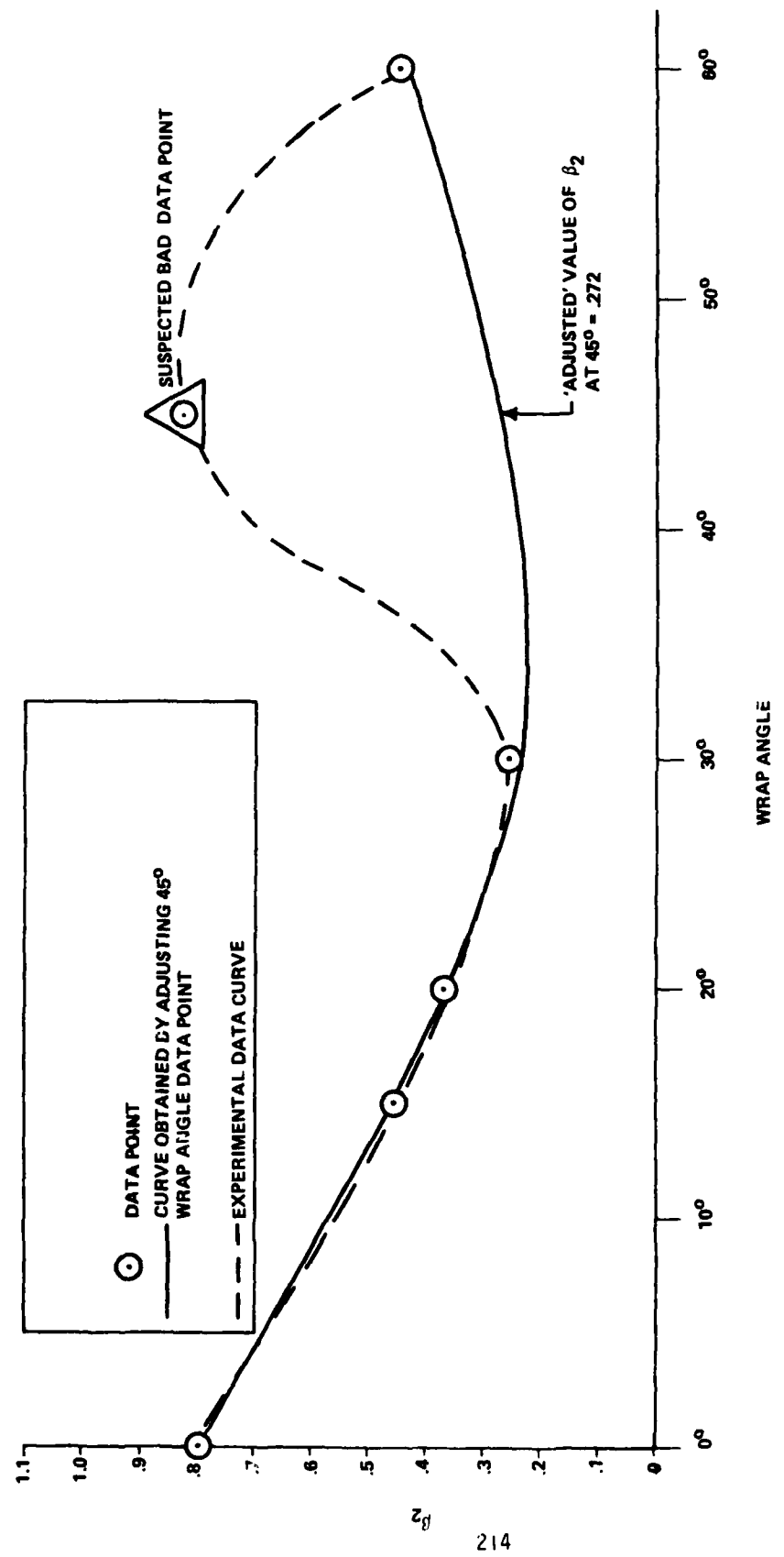


Figure K-1.  $\beta_2$  versus wrap angle.

TABLE K-4. COMPARISON OF  $\Delta B$  AND  $\Delta L$  DATA OBTAINED FROM TABLES 67 AND 68

WRAP ANGLE	$\beta_1$	$\beta_2$	$\Delta\beta = \beta_1 - \beta_2$	$L_1$	$L_2$	$\Delta L = L_1 - L_2$	$\Psi = \frac{\Delta\beta}{\Delta L}$
0°	.206	.791	.260	6178	9135	.676	.384
15°	.270	.452	.597	5051	5365	.941	.634
20°	.370	.367	1.008	4468	4661	.958	1.052
30°	.398	.255	1.560	3356	3717	.902	1.729
45°	.521	.824	.632	1191	1585	.751	.841
60°	2.712	.449	6.040	237	556	.426	14.178
ADJUSTED 45°	.521	.272	1.915	1191	1585	.751	2.549

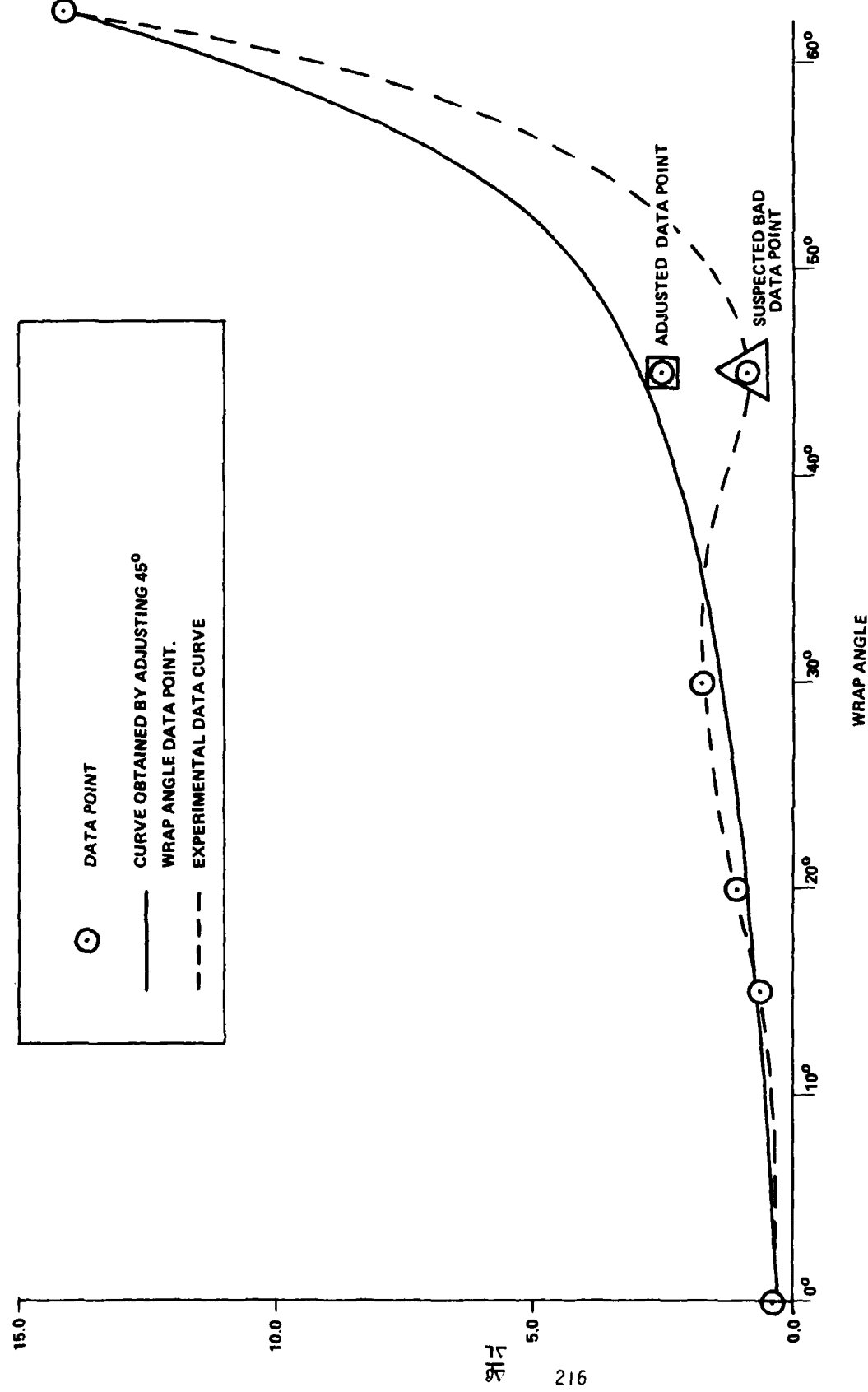


Figure K-2.  $\frac{\Delta B}{\Delta L}$  versus wrap angle.

### LIST OF SYMBOLS

<u>Symbol</u>	<u>Definition</u>
A	Cross-sectional area of tensile specimen
2d	Fringe spacing
2d <sub>H</sub>	Horizontal fringe spacing
2d <sub>V</sub>	Vertical fringe spacing
E <sub>ij</sub> <sup>C</sup>	Compressive stiffness
E <sub>ij</sub> <sup>T</sup>	Tensile stiffness
G <sub>ij</sub>	Shear stiffness
D	Analyzer screen coordinate
f	Interferogram to analyzer screen spacing
L	Specimen load
n	Fringe Order
N	Interferogram plate locations
N̄	Number of interferogram data samples
ΔP	Net gage pressure change
r	Interferogram plate location
S	Film scale factor
S <sub>ij</sub>	Ultimate shear strength
T	Tensile Load
u	Quadratic term of least squares curve fit
U <sub>θ</sub>	Displacement in the $\theta$ direction
U <sub>H</sub>	Horizontal displacement
U <sub>V</sub>	Vertical displacement
v	Linear term of least squares curve fit
w	Constant term of least squares curve fit
x	Interferogram coordinate

### SYMBOLS (Concluded)

<u>Symbol</u>	<u>Definition</u>
$x_i^c$	Compressive ultimate strength
$x_i^T$	Tensile ultimate strength
$Y$	Least squares curve fit for $\beta$
$\beta$	Interferogram fringe order gradient
$\delta$	Least squares difference
$E$	Absolute strain
$\theta$	Rotator angle
$\lambda$	Wavelength of light from laser
$\nu_{ij}^c$	Poisson's ratio in compression
$\nu_{ij}^T$	Poisson's ratio in tension

#### REFERENCES

1. Smith, D.G., Schaeffel, J. A., "Quantitative Nondestructive Evaluation", Technical Report RL-80-6, U.S. Army Missile Command, October 1979.
2. Takeda, N., Sierakowski, R. L., "Localized Impact Problems of Composite Laminates", The Shock and Vibration Digest, Volume 12, No. 8, August 1988 p. 3.
3. Schaeffel, J. A., "Acoustical Speckle Interferometry," Technical Report T-79-39, US Army Missile R&D Command, 22 March 1979.
4. Leendertz, J., "Interferometric Displacement Measurement on Scattering Surfaces Utilizing Speckle Effect," Journal on Physics E, Volume 3, 1971 p. 214.
5. Mullinix, B. R., Ranson, W. F., Swinson, W.F., and Cost, T. L., "Quantification of Flaws in Fibered Composite Structures Using Interferometric Fringe Patterns", U.S. Army Missile Command, Redstone Arsenal, Alabama, 20 April 1976, Technical Report RL-76-18.
6. Schaeffel, J. A., "Automated Laser Speckle Interferometry Displacement Contour Analyzer", Technical Report T-79-71, US Army Missile Command Redstone Arsenal, Alabama 2 July 1979.
7. Vandiver, T. L., "Flaw Detection and Evaluation of Composite Cylinders Using Laser Speckle Interferometry and Holography", Technical Report RL-80-7, US Army Missile Command, Redstone Arsenal, Alabama, 23 November 1980.
8. Smith, D. G., Huang, J. C., Post-Crating Stress Analysis of Glass-Epoxy Laminates, Tennessee Technological University, Dept. of Engineering Science and Mechanics, Cookeville, Tennessee, May 1979, Contract No. DAAK40-78-C-0165.

## DISTRIBUTION

	No. of Copies
Defense Documentation Center Cameron Station Alexandria, Virginia 22314	12
Defense Metals Information Center Battelle Memorial Institute 505 King Avenue Columbus, Ohio 43201	1
Commander US Army Foreign Science and Technology Center ATTN: DRXST-SD3 220 Seventh Street, NE Charlottesville, Virginia 22901	1
Office of Chief of Research and Development Department of the Army ATTN: DARD-ARS-P Washington, DC 20301	1
Commander US Army Electronics Command ATTN: DRSEL-PA-P -CT-DT -PP, Mr. Sulkolove Fort Monmouth, New Jersey 07703	1 1 1
Commander US Army Natick Laboratories Kansas Street ATTN: STSNLT-EQR Natick, Massachusetts 01760	1
Commander US Army Mobility Equipment Research and Development Center Fort Belvoir, Virginia 22060	1

## DISTRIBUTION

	No. of Copies
Director USA Mobility Equipment Research and Development Center Coating and Chemical Laboratory ATTN: STSFB-CL Aberdeen Proving Ground, Maryland 21005	1
Commander Edgewood Arsenal ATTN: SAREA-TS-A Aberdeen Proving Ground, Maryland 21010	1
Commander Picatinny Arsenal ATTN: SARPA-TS-S, Mr. M. Costello Dover, New Jersey 07801	1
Commander Rock Island Arsenal Research and Development ATTN: 9320 Rock Island, Illinois 61201	1
Commander Watervliet Arsenal Watervliet, New York 12189	1
Commander US Army Aviation Systems Command ATTN: DRSAV-EE -MT, Mr. Vollmer St. Louis, Missouri 63166	1 1
Commander US Army Aeronautical Depot Maintenance Center (Mail Stop) Corpus Christi, Texas 78403	1
Commander UA Army Test and Evaluation Command ATTN: DRSTE-RA Aberdeen Proving Ground, Maryland 21005	1

## DISTRIBUTION

	No. of Copies
<b>Commander</b> ATTN: STEAP-MT Aberdeen Proving Ground, Maryland 21005	1
<b>Chief</b> Bureau of Naval Weapons Department of the Navy Washington, DC 20390	1
<b>Chief</b> Bureau of Ships Department of the Navy Washington, DC 20315	1
<b>Naval Research Laboratory</b> ATTN: Dr. M.M. Krafft Code 8430 Washington, DC 20375	1
<b>Commander</b> Wright Air Development Division ATTN: ASRC Wright-Patterson AFB, Ohio 45433	1
<b>Director</b> Air Force Materiel Laboratory ATTN: AFML-DO-Library Wright-Patterson AFB, Ohio 45433	1
<b>Director</b> Army Materials and Mechanics Research Center ATTN: DRXMR-PL -MT, Mr. Farrow Watertown, Massachusetts 02172	1
<b>Commander</b> White Sands Missile Range ATTN: STEWS-AD-L White Sands Missile Range, New Mexico 88002	1

## DISTRIBUTION

	No. of Copies
<b>Jet Propulsion Laboratory</b> <b>California Institute of Technology</b> <b>ATTN: Library/Acquisitions 111-113</b> <b>4800 Oak Grove Drive</b> <b>Pasadena, California 91103</b>	1
<b>Sandia Laboratories</b> <b>ATTN: Library</b> <b>P.O. Box 969</b> <b>Livermore, California 94550</b>	1
<b>Commander</b> <b>US Army Air Defense School</b> <b>ATTN: ATSA-CD-MM</b> <b>Fort Bliss, Texas 79916</b>	1
<b>Technical Library</b> <b>Naval Ordnance Station</b> <b>Indian Head, Maryland 20640</b>	1
<b>Commander</b> <b>US Army Materiel Development and Readiness Command</b> <b>ATTN: DRCMT</b> <b>Washington, DC 20315</b>	1
<b>Headquarters</b> <b>SAC/NRI (Stinfo Library)</b> <b>Offutt Air Force Base, Nebraska 68113</b>	1
<b>Commander</b> <b>Rock Island Arsenal</b> <b>ATTN: SARRI-KLPL-Technical Library</b> <b>Rock Island, Illinois 61201</b>	1
<b>Commander (Code 233)</b> <b>Naval Weapons Center</b> <b>ATTN: Library Division</b> <b>China Lake, California 93555</b>	1
<b>Department of the Army</b> <b>US Army Research Office</b> <b>ATTN: Information Processing Office</b> <b>P.O. Box 12211</b> <b>Research Triangle Park, North Carolina 27709</b>	1

## DISTRIBUTION (Concluded)

	No. of Copies
<b>Commander</b> <b>US Army Research Office</b> ATTN: DRXRO-PW, Dr. R. Lontz P.O. Box 12211 Research Triangle Park, North Carolina 27709	2
<b>US Army Research and Standardization Group (Europe)</b> ATTN: DRXSN-E-RX, Dr. Alfred K. Nodoluha Box 65 FPO New York 09510	2
<b>Headquarters</b> <b>Department of the Army Office of the DCS for Research</b> Development and Acquisition Room 3A474, The Pentagon ATTN: DAMA-ARZ Washington, DC 20310	2
<b>US Army Materiel Systems Analysis Activity</b> ATTN: DRXSY-MP Aberdeen Proving Ground, Maryland 21005	1
<b>IIT Research Institute</b> ATTN: GACIAC 10 West 35th Street Chicago, Illinois 60616	1
<b>ADTC (DLDSL)</b> Eglin Air Force Base, Florida 32542	1
<b>University of California</b> <b>Los Alamos Scientific Laboratory</b> ATTN: Reports Library P.O. Box 1663 Los Alamos, New Mexico 87545	1
<b>Commander</b> <b>US Army Materiel Development and Readiness Command</b> ATTN: DRCRD DRCDL 5001 Eisenhower Avenue Alexandria, Virginia 22333	1 1
<b>Director</b> <b>Defense Advanced Research Projects Agency</b> 1400 Wilson Boulevard Arlington, Virginia 22209	1

DISTRIBUTION (Concluded)

	No. of Copies
DRSMI-LP, Mr. Voigt	1
-R, Dr. McCorkle	1
-RL, Mr. Comus	1
-RLA, Mr. Pettey	1
Mr. Schaeffel	50

